

**EVALUATION OF GREYWATER AND A/C CONDENSATE FOR WATER
REUSE: AN APPROACH USING ARTIFICIAL NEURAL NETWORK
MODELING**

A Dissertation

by

SHASHI KANT

Submitted to the Office of Graduate and Professional Studies of
Texas A&M University
in partial fulfillment of the requirements for the degree of

DOCTOR OF PHILOSOPHY

Chair of Committee,	Fouad Jaber
Co-Chair of Committee,	R.Karthikeyan
Committee Members,	Anish Jantrania
	Yongheng Huang
	Raul Cabrera
Head of Department,	Steve Searcy

May 2017

Major Subject: Biological and Agricultural Engineering

Copyright 2017 Shashi Kant

ABSTRACT

Alternative resources play a vital role for water-sensitive infrastructures where consistent water supply is a challenge, and freshwater resources are limited. Greywater and A/C condensate are potentially new alternatives for increasing urban water supply. An advanced physical filtration system for greywater treatment was developed named as GAC-MI-ME. It is comprised coarse filtration (CR-F) followed by microfiltration (MF), granular activated carbon (GAC), ultrafiltration (UF), ultraviolet (UV), and reverse-osmosis (RO). GAC-MI-ME effluent-quality was analyzed for greywater from laundry, shower, and wash basin. High-grade effluent equivalent to unrestricted water reuse was observed at UF and RO units. A subsequent tool (GREY-ANN) was proposed for GAC-MI-ME effluent quality predictions. Artificial Neural Network (ANN) was applied to develop 5 unit models for selected parameters including Biochemical Oxidation Demand, pH, Total Dissolved Solids, Turbidity, and Oxidation-Reduction Potential to predict effluent quality at each stage of GAC-ME-MI treatment using water quality databases (developed from a series of experiments testing greywater of varying strength). The 15 days storage potential of GAC-MI-ME treated effluents were also analyzed and showed no significant quality depletion in UF and RO effluent quality.

A hybrid modeling approach was applied to A/C condensate estimation, which included a psychrometric based “Air-Conditioner-Condensate” (ACON) model, and data-driven “Internal Load Analysis using Neural Network” (ILAN) model. The ACON model uses mass and energy balance approach for HVAC systems operating under steady state conditions. It accounts for psychrometric states of different air parcels

during the cooling and dehumidification process. The ILAN model was developed using ANN for the city of Doha to predict Internal Load at a daily time step for variable climatic conditions (temperature, relative humidity). The ACON- ILAN models were validated for a test building and applied for yearly condensate estimation for Doha. The virtual simulations of the hybrid model showed an annual condensate volume of 1370 and 3700 l/100 m³ of cooling space for 20% and 100% outdoor-ventilation. The condensate quality (for limited water quality parameters) showed values within primary and secondary drinking water standards, except for copper, which had marginally higher concentrations. Overall, the GREY-ANN and ACON-ILAN may improve greywater and A/C condensate reuse potentials.

ACKNOWLEDGEMENTS

I would like to express my gratitude to Dr. Fouad Jaber for providing me with guidance, immense support, and constant encouragement during my Ph.D. I am very thankful to him for his consistent effort and time and providing me the impetus for my current research, other than financial support during the term. I would also like to express my gratitude to Dr. R. Karthikeyan for guiding, encouraging, and providing me valuable technical advice throughout this work. These always helped me to proceed in right directions.

I am very thankful for having the committee members in my research as Dr. Hazim Qiblawey, Dr. Raul Cabrera, Dr. Yongheng Huang, and Dr. Anish Jantrania. I always got great advices and help from them during the span of my research, which I feel as an indispensable part for completion this work. I am also very thankful Mr. Ahmad and staff of the Qatar University for helping me in data collection and providing me supports during my stay at Doha. I would like to extend my gratitude to Dr. Searcy and BAEN staff for helping me in several ways during my education and research at Texas A&M University.

I would also like to express thankfulness to my family and friends for being supportive to me during my research and education.

CONTRIBUTORS AND FUNDING SOURCES

Contributors

The research work presented in the dissertation was thoroughly supervised by the committee chair Dr. Fouad Jaber, the co-chair Dr. R. Karthikeyan of Biological and Agricultural Engineering at Teas A&M University.

The data collection in section 6 was in collaboration with Qatar University under supervision of Dr. Hazim Qiblawey from department of Chemical Engineering at Qatar University.

The research work presented in the dissertation was completed by the student independently.

Funding Sources

The graduate study and research was supported by Qatar National Research Fund and Texas A&M Agrilife Extension.

NOMENCLATURE

A/C	Air Conditioning
€	Binary coefficient, m^3/m^3
µm	micro meter
ACON	A/C Condensate Tool
ANN	Artificial Neural Network
BESS	Building Energy Simulation Software
BF	Bypass Factor of Cooling Coil
BOD ₅	Biochemical Oxygen Demand
CAV	Constant Air Volume Supply
C-F	Carbon Filtration
CR-F	Coarse Filtration
cfu	Colony Forming Unit
COD	Chemical Oxidation Demand
CV	Cross Validation
CW	Constructed Wetlands
Db	Dry Bulb
DO	Dissolved Oxygen
E	Total Enthalpy, KJ/Kg
EC	Electrical Conductivity
EPA	Environmental Protection Agency

ESV	Electronic Shutoff Valve
GAC	Granular Activated Carbon
GAC-MI-ME	Granular Activated Carbon- Membrane Integrated- Multi Effluent
GCC	Gulf Cooperation Council
GFF	Generalized Feedforward (GFF),
gpm	Gallon Per Minute
GREY-ANN	Model Name
GRNN	General Regression Neural Networks
Ha	Enthalpy of Air, KJ/Kg
HFRB	Horizontal Flow Reed Bed
HVAC	Heating Ventilation And Air Conditioning
ILAN	Internal Load Analysis Using Neural-Network
LW	Laundry Water
Ma	Mass of Dry Air, Kg
MAE	Mean Absolute Error
MBR	Membrane Bioreactor
M-F	Micro-Filtration
MLP	Multilayer Preceptor
MSE	Mean Square Error
MSF	Multistage Flash Distillation
Mw	Mass Of Water, Kg

ND	Non Detectable
NF	Nano Filtration
NOM	Natural Organic Matter
NTU	Nephelometric Turbidity Unit
ORP	Oxidation Reduction Potential
Pa	Partial Pressure of Dry Air, Pa
PAC	Powered Activated Carbon
P_{atm}	Atmospheric Pressure, Pa
PCA	Principal Component Analysis
PE	Processing Element
PNN	Probabilistic Neural Network
psi	Pounds Per Square Inch
P_w	Partial Pressure of Water Vapor, Pa
P_{ws}	Partial Pressure of Water Vapor At Saturation, Pa
Q	Cooling Load, KJ
r	Correlation R
R	Specific Gas Constant,
RBC	Rotatory Biological Reactor
RBF	Radial Basis Function
RH	Relative Humidity Of Air, %
Ro	Reverse Osmosis
S	Samples

SAR	Sodium Adsorption Ration
SD	Standard Deviation
SHR	Sensible Heat Ratio
SS	Suspended Solids
SV	Conditioned Space Volume, m ³
SW:	Shower Water
T	Dry Bulb Temperature, °C
TC	Total Coliform
TCEQ	Texas Commission on Environmental Quality
T _{dew}	Dew Point Temperature. °C
TDNN	Time Delayed Neural Network
TDS	Total Dissolved Solids
TKN	Total Kjeldahl Nitrogen
TLC	Tank Level Controllers
TLRN	Time Lag Recurrent Network
TN	Total Nitrogen
TOC	Total Organic Carbon
TSS	Total Suspended Solids
TX	Texas
UD	Undetectable
UF	Ultrafiltration
UN	United Nation

UNDP	United Nation Development Program
UASB	Upflow Anaerobic Sludge Blanket
UV	Ultra Violet
V	Volume of air, m ³
VBA	Visual basic for applications
VFRB	Vertical Flow Reed Bed
W	Humidity ratio
Wb	Wet Bulb
WB	Wash-Basin water
WHO	World Health Organization
WWTP	Waste Water Treatment Plant
XOC	Xenobiotic Organic Compounds
Γ	Specific volume of air, m ³ /Kg
η	Volumetric air ratio
H	Fraction of outside air
Ω	Volumetric exchange rate, SV/hr
Φ	Relative humidity of air, %
∇	Mixed air supply coefficient, m ³ / m ³

SUBSCRIPT

Out	Outside air parcel
In	Conditioned space air parcel
Mixed	Mixed state air parcel

Supply	Supply air parcel
Return	Return air parcel
Exhaust	Exhaust air parcel
w	Water
a	Air
cond	Condensate
f	Bypass factor

TABLE OF CONTENTS

	Page
ABSTRACT	ii
ACKNOWLEDGEMENTS	iv
CONTRIBUTORS AND FUNDING SOURCES.....	v
NOMENCLATURE.....	vi
LIST OF FIGURES.....	xvi
LIST OF TABLES	xx
1 INTRODUCTION.....	1
1.1 Overview	1
1.2 Greywater	2
1.3 A/C condensate	3
1.4 Research outline	4
2 ALTERNATIVE URBAN WATER RESOURCES: A REVIEW TO 21 ST CENTURY URBAN WATER MANAGEMENT SOLUTIONS	7
2.1 Introduction	7
2.2 Drivers of alternative water sources.....	8
2.3 Primary alternative water resources and their limitations	12
2.3.1 Desalination.....	12
2.3.2 Rainwater harvesting.....	14
2.3.3 Domestic wastewater reuse and it limitations	15
2.4 Emerging alternative water resources and their limitations	17
2.4.1 Greywater reuse and limitations.....	17
2.4.2 Technological limitations in grey water treatment.....	19
2.4.3 Air-conditioning (A/C) condensate	22
2.5 Summary & conclusion.....	25
3 EVALUATION OF PORTABLE IN-HOUSE GREYWATER TREATMENT SYSTEM FOR POTENTIAL WATER-REUSE IN URBAN AREAS	26
3.1 Introduction	26
3.2 Material & methods.....	29
3.2.1 Greywater collection	29
3.2.2 GAC-MI-ME greywater treatment system description.....	29

3.2.3	Physical, chemical, and microbial evaluation of greywater	32
3.3	Results & discussions	33
3.3.1	Greywater characteristics	33
3.3.2	Permeate quality for multi-stage greywater treatment system	36
3.3.3	Water reuse potential as unrestricted water reuse	40
3.4	Conclusion.....	41
4	MACHINE LEARNING (USING ANN) FOR GREYWATER REUSE: COMPREHENSIVE APPROACH USING EFFLUENT PREDICTION MODELING AND EFFLUENT STORAGE IMPACT ON WATER QUALITY ..	42
4.1	Introduction	42
4.1.1	Background	42
4.1.2	Contemporary flaws and barriers in greywater reuse.....	42
4.1.3	Improving potentials in greywater reuse	44
4.2	Objectives.....	46
4.3	Material and methods	47
4.3.1	Greywater treatment system description	47
4.3.2	Experimental setup.....	48
4.3.3	Water quality analysis	49
4.3.4	Model development.....	51
4.3.5	ANN application in model development.....	53
4.4	Results & discussions.....	56
4.4.1	Raw and GAC-MI-ME treated effluent characteristics:.....	56
4.4.2	GREY-ANN	59
4.4.3	BOD-MP model for predicting BOD	70
4.4.4	The impact of storage on raw and “GAC-MI-ME” effluents:.....	74
4.5	Conclusion.....	80
5	AIR-CONDITIONERS (A/C) CONDENSATE MODELING USING PSYCHROMETRIC COMPUTATIONS: AN APPROACH USING MASS AND ENERGY BALANCE.....	82
5.1	Introduction	82
5.1.1	Background	82
5.1.2	Condensate	83
5.1.3	Attempts made in condensate estimation	83
5.1.4	Objective	86
5.2	Methods.....	86
5.2.1	Model logic and assumptions	86
5.2.2	Model input parameters.....	88
5.2.3	Model development.....	90
5.2.4	Condensate estimation using “condensate analysis module ”	97

5.2.5.	Determining operational duration and intensity of HVAC system using “operational HVAC module”	100
5.2.6.	Determining internal load for observed condensate data using “load analysis module”	104
5.3.	Conclusion.....	105
6	APPLICATION OF ACON MODEL SIMULATIONS IN CONDENSATE ESTIMATION USING WEATHER DATA: A CASE STUDY OF DOHA USING ANN PREDICTION TOOL	107
6.1.	Introduction	107
6.1.1.	Background of study	107
6.1.2.	A/C condensate potential	108
6.1.3.	ACON model and condensate estimation	109
6.1.4.	Internal load determination for ACON model	110
6.1.5.	Artificial intelligence in building energy generalization/prediction	111
6.1.6.	Condensate determination for Doha using ACON model.....	111
6.1.7.	Objectives.....	112
6.2.	Methods.....	112
6.2.1.	System setup and data acquisition.....	112
6.2.2.	ILAN model development using ANN	115
6.2.3.	A/C condensate water quality analysis for Doha	118
6.3.	Results and discussion.....	118
6.3.1.	ILAN model analysis.....	119
6.3.2.	ACON-ILAN model validation	123
6.4.	ILAN-ACON deployment with Doha climatic data	126
6.5.	Discussion on ILAN-ACON model development and simulation.....	131
6.5.1.	A/C condensate water quality analysis for Doha.....	132
6.6.	Conclusion.....	134
6.6.1.	ILAN model.....	134
6.6.2.	ILAN-ACON hybrid model.....	135
6.6.3.	Impact of cooling load type on condensate formation.....	135
6.6.4.	Potential of A/C condensate for the city of Doha.....	136
7	CONCLUSION AND SUMMARY	137
7.1	Future work	139
	REFERENCES	141
	APPENDIX-A1	166
	APPENDIX-A2.....	167
	APPENDIX-A3.....	169

APPENDIX-A4.....	170
APPENDIX-A5.....	171
APPENDIX-B1.....	174
APPENDIX-B2.....	176
APPENDIX-B3.....	177
APPENDIX-B4.....	178
APPENDIX C1.....	179
APPENDIX C2:.....	180
APPENDIX C3:.....	181

LIST OF FIGURES

	Page
Figure 2.1 Global water availability worldwide. (Adapted from Shiklomanov et al., 2000).....	8
Figure 2.2 Increasing water stress with growing population and declining freshwater resources in between 1985-2025 (adapted from Vorosmarty et al., 2000).....	9
Figure 2.3 Increasing water stress with growing population and declining freshwater resources in between 1995-2025. (Adapted from Rosegrant et al., 2002).....	11
Figure 2.4 Global use of desalinated water adopted from (adapted from Tsiourtis et al., 2001).....	12
Figure 3.1 Fabricated greywater filtration system with multi-stage effluent collection and pressure gauges	31
Figure 3.2 Turbidity removal along GAC-MI-ME system for different greywater samples(S)	37
Figure 3.3 Total coliform removal by GAC-MI-ME system for different in greywater samples (S).	38
Figure 3.4 BOD removal along GAC-MI-ME system for different greywater samples(S)	39
Figure 3.5 Contaminant load reduction (%) along GAC-M-MI-ME system.	40
Figure 4.1 Effluent collection scheme from the GAC-MI-ME greywater treatment system where it shows five different effluents from the raw greywater	48
Figure 4.2 Unit model flow diagram of GREY-ANN.....	52
Figure 4.3 The flowchart defining the steps applied in ANN model development.....	55
Figure 4.4 Water quality variability in raw greywater and GAC-MI-ME treated effluents.....	58
Figure 4.5 The model (Turbidity –ANN) performance in predicting the turbidity values (NTU) for CR-F (A), MF (B), and GAC (C), UF (D), and RO (E) effluents of GAC-MI-ME system.	61

Figure 4.6 The model (PH –ANN) performance in predicting the pH values (NTU) for CR-F (A), MF (B), and GAC (C), UF (D), and RO (E) effluents of GAC-MI-ME system.....	62
Figure 4.7 The model (BOD –ANN) performance in predicting the BOD5(mg/l) values (NTU) for CR-F (A), MF (B), and GAC (C), UF (D), and RO (E) effluents of GAC-MI-ME system.	64
Figure 4.8 The model (ORP –ANN) performance in predicting the ORP values (mV) for CR-F (A), MF (B), and GAC (C), UF (D), and RO (E) effluents of GAC-MI-ME system.	65
Figure 4.9 The model (TDS –ANN) performance in predicting the TDS(mg/l) values for CR-F (A), MF (B), and GAC (C), UF (D), and RO (E) effluents of GAC-MI-ME system	66
Figure 4.10 Sensitivity of GREY-ANN unit-models on UF effluents	68
Figure 4.11 Sensitivity of GREY-ANN unit models on RO effluent	69
Figure 4.12 Comparison of the model simulated and observed BOD ₅ values	70
Figure 4.13 BOD (mg/l) variation in BOD-MP model with respect the independent parameters (A) turbidity (B) TDS(C) ORP and (D) pH.....	71
Figure 4.14 Comparison of GFF, and multilinear regression predictions for observed BOD	72
Figure 4.15 BOD sensitivity in BOD –MP model.....	73
Figure 4.16 Change of TDS mg/l with storage time for raw greywater (A) and treated greywater (B,C,D,E and F) for coarse filtration (CF), microfiltration (MF), granular activated GAC), ultrafiltration (UF), and reverse osmosis (RO) respectively.	74
Figure 4.17 Change of turbidity (NTU) with storage time for raw greywater (A) and treated greywater (B,C,D,E,and F) for coarse filtration (CF), microfiltration (MF), granular activated GAC), ultrafiltration (UF), and reverse osmosis (RO), respectively.....	75
Figure 4.18 Change of pH with storage time for raw greywater (A) and treated greywater (B,C,D,E, and F) for coarse filtration (CF), microfiltration (MF), granular activated GAC), ultrafiltration (UF), and reverse osmosis (RO), respectively.	76

Figure 4.19 Change of dissolved Oxygen (DO) in mg/l with storage time (days) for raw greywater (A) and treated greywater (B, C, D, E and F) for coarse filtration (CF), micro filtration (MF), granular activated GAC), ultrafiltration (UF), and reverse osmosis (RO) r	78
Figure 5.1 Operational details of ACON model for condensate estimation during mechanical cooling and dehumidification process, assuming steady state conditioned space and considering law of conservation and mass and energy in ideal condition.	89
Figure 5.2 Psychrometric calculations considered in “ACON” model for air parcels transition.	91
Figure 5.3 The diagram depicts variable coil supply volume and mixed air volume together for total supply volume to meet the thermodynamic steady state condition of supply volume.:	105
Figure 6.1 Data acquisition and processing for hourly/daily condensate data with corresponding mean outdoor/ indoor temperature and hygrometric data	114
Figure 6.2 The ILAN (PNN) vs ACON estimated Cooling Load Index for Internal Load (ψ).....	119
Figure 6.3 The ILAN (MLP) vs ACON estimated Cooling Load Index for Internal Load (ψ).....	120
Figure 6.4 Internal Load (ψ_i) sensitivity in ILAN model for using PNN model	122
Figure 6.5 Internal Load (ψ_i) sensitivity in ILAN model for using MLP.....	123
Figure 6.6 Comparison of observed and simulated Binary Operational Coefficient for Test-Building-II.....	124
Figure 6.7 Hourly condensate simulation with ACON-ILAN for Test-Building-II	125
Figure 6.8 ILAN-ACON simulated condensate compared with the observed condensate applying A) PNN, B) MLP for Test-Building-II.....	126
Figure 6.9 Thermo-hygrometric data variation for the city of Doha.....	128
Figure 6.10 Binary Operational Coefficient with respect to outdoor energy and fixed indoor design conditions for the city of Doha.....	129
Figure 6.11 Daily condensate simulation for Doha climate at 20 and 100 % ventilation using ACON, and ILAN	130

Figure 6.12 Monthly condensate estimation by ILAN-ACON131

LIST OF TABLES

	Page
Table 2.1 Changing salt concentration from feed to reject stream in designation plants	14
Table 2.2 Characteristics of Greywater	18
Table 2.3 A/C condensate water quality analysis in different part of world.....	23
Table 3.1 Physical chemical and microbial characteristics of greywater measured in College Station, TX.....	34
Table 3.2 Treated effluent characteristics variation along the fabricated treatment system.....	36
Table 4.1 Range of water quality parameters used in GREY-ANN model development	50
Table 4.2 GREY-ANN unit models performance evaluation with best ANN architecture	60
Table 6.1 Test-Building specifications used in experimental data:	113
Table 6.2 ACON model simulation settings for case study of Doha	115
Table 6.3 ILAN Input data correlation.....	117
Table 6.4 Performance matrix for different ANN algorithms applied in ILAN model development	121

1 INTRODUCTION

A 21st-century “paradigm shift” of water demand-supply management considers alternative resources as an integral part of it (Gleick et al., 2000). Resource identification and evaluation become crucial aspects of decision making while the supply-demand ratio is volatile (Okeola et al., 2012). From an integrated water management perspective, more emphasis is given in this study towards exploring new alternatives, which can sustainably meet the needs of growing water demand (Vörösmarty et al., 2000). An efficient integrated water management tool aids decision making based on an availability of resources by its evaluation and optimal distribution for a particular need and, thereby, meeting material, cost, energy, and environmental sustainability (Makropoulos et al., 2008).

1.1 Overview

Alternative resources play a vital role for water-sensitive infrastructures where consistent water supply is a challenge and freshwater resources are limited (Lazarova et al., 2001). The depletion of fresh water resources keep continuing as the demands for irrigation, industrial and municipal water are escalating. The problem gets more complex in urban regions, where lucrative economies and high population growth together compel for more water demand (Vörösmarty et al., 2000). The limited water availability and increasing population pose a threat of a substantial decrease in per capita water availability in the near future (Pimentel et al., 2004).

This study focuses on evaluating the emerging alternative resources, including greywater and A/C condensate, regarding their variability in quality and quantity,

particularly for urban settings. To address these uncertainties and variabilities in the alternative water systems, progressive approaches are needed to improve water use potential for greywater and A/C condensate as an integrated solution for increasing urban water supply. In this study, the overall goal is to provide micro-tools for enhancing greywater and A/C condensate as potential parts of integrated water management, with the primary intent of promoting alternative resources and saving the pristine water resources.

1.2 Greywater

The importance of greywater is in its volume, which directly depends on the quantity of domestic water usage. Variability in greywater characteristics is one of the challenges for greywater application, primarily because of public health and environmental impacts (Gross et al., 2005). It shows a wide range of contamination depending on source, residents' habits, and regional/social trends and different water uses (Eriksson et al., 2009).

A number of treatment technologies (mostly biological or a combination of biological, physical, and chemical) are applied in greywater treatment (Li et al., 2009). These treatments are mostly similar to domestic wastewater treatment. With the variability in greywater characteristics, a generalized treatment method addressing greywater might not be appropriate, which needs to be identified regarding influent variability as well as its treatment reliability (Jefferson et al., 2004). Greywater needs an improvement in the existing treatment system with multi-grade effluent potential as well

as meeting the water reuse regulations. Influent/effluent variability needs to be addressed to improve the robustness of a treatment system.

This study is focused on greywater-characterization, treatment-system development for multi-grade effluent, treatment- performance evaluations, and a corresponding model development to virtually predict effluent quality with the influent variability using Artificial Neural Network (ANN).

1.3 A/C condensate

In parallel, the emerging concept of A/C condensate has substantial potential to turn the conventionally-drained condensate into a water resource in hot and humid climates (Painter et al., 2009). Although Heating Ventilation and Air Conditioning (HVAC) systems are primarily designed to meet human comfort and indoor air quality, the condensate is a result of the cooling and dehumidification process and has lately drawn attention due to increasing water scarcity issues (Guz et al., 2005). The A/C condensate may offset high-grade water uses (Guz et al., 2005). Condensate volume is an important parameter for water demand-supply management practices if condensate recovery is considered for water supply supplement. However, the condensate volumetric potential is dependent on the thermo-hygrometric data for outdoor and indoor design conditions (temperature, relative humidity), aside from factors influencing heat and moisture gain in the system through the building envelope, or human occupancy, or unknown infiltrations. In this scenario, considering the non-linearity in the cooling and humidification process with high uncertainties in the load gain information, condensate volume determination at sub-daily time steps is a very complex task.

A hybrid-modeling approach, which included a psychrometric based “Air-Conditioner-Condensate” (ACON) model, and data-driven “Internal Load Analysis using Neural Network” (ILAN) model were proposed in this study for condensate estimation, unlike the current empirical approaches (Bryant et al., 2008; Guz et al., 2005). Time-step condensate estimation was achieved considering the seasonal and operational variability.

1.4 Research outline

The thesis is presented in seven Sections. Section 1 is an introduction and statement of the problem, and corresponding conclusions and recommendations are in Section 7. Sections 2 to 6 are described below.

The Section 2 provides an overview of drivers and barriers for alternative water resources. It determines the factors affecting current water usage and future trends. Each alternative resource is discussed, addressing its quantity, quality, and current adoption and impact on the ecosystem. It also discusses the potential reform in the present trends of improving alternative resources as part of an integrated water system. Overall, it provides a rationale for use of alternative water resources for mitigating the problem of increasing water scarcity, especially in urban areas.

The Section 3 emphasizes the flaws of current greywater treatment systems, addressing biological and chemical treatments, and provides a rationale for physical treatment using UV and RO with coarse filtration, carbon filtration and micro filtration treatments as a greywater treatment system. It also presents a preliminary evaluation of in-house portable greywater treatment systems for water reuse in urban areas. The

system can be described as the Granular Activated Carbon-Membrane Integrated-Multi-grade Effluent (GAC-MI-ME) treatment. The Section also presents the preliminary results of greywater treated through GAC-MI-ME and outlines the treatment performance for each of the water quality parameters.

In the Section 4, a comprehensive analysis of greywater, treatment, and subsequent modeling, is presented and a potential decision making tool (GREY-ANN) is developed for improving greywater utilization by considering multi-grade effluent through an advanced physical filtration system and predicting its quality using Artificial Neural Network (ANN). Section 4 also shows the impact of storage time over treated and untreated greywater for 15 consecutive days. The data were analyzed for each stage of treatment to determine potential storage implications. The parameters used for the analysis are BOD, pH, ORP, TDS and turbidity

Section 5 presents the development of an A/C condensate estimation tool (ACON Model) based on psychrometric computations. Two concepts were proposed in this Section: 1) Total cooling load categorized as Ventilation Load, and cooling load other than ventilation defined as Internal Load; and 2) Cooling Load Index (ratio of coil-induced volume to the total supply volume) to determine the intensity of HVAC operation with load variability. The ACON model uses an energy-mass balance approach for HVAC systems operating under steady state conditions. It accounts for psychrometric states of different air parcels during the cooling and dehumidification process, and determines the Binary Operational Coefficient and Cooling Load Index (ventilation and internal) for condensation at hourly/daily time steps using thermo-

hygrometric data and HVAC controls (outdoor ventilation, room volume air exchange rate, cooling coil temperature and its bypass factor). The model determines the Ventilation Load and uses Internal Load as input.

In the Section 6, data-driven Internal Load Analysis Using Neural-Network ILAN model was developed. A hybrid modeling approach, using psychrometric-based ACON, and ILAN, was applied semi-empirically for condensate volume estimation for the city of Doha. The ILAN model was developed using ANN for the city of Doha (Qatar) to predict Internal Load at a daily time step for variable climatic conditions (temperature, relative humidity). The input-output database for ILAN include; 1) temperature, 2) relative humidity, 3) air enthalpy for outdoor and indoor condition and 4) Ventilation Load Index at 20 % as an independent parameter and 5) Internal Load Index as desired output. The ACON- ILAN models were validated for a test building with satisfactory model performance indicators and applied for yearly condensate estimation for Doha City.

2 ALTERNATIVE URBAN WATER RESOURCES: A REVIEW TO 21ST CENTURY URBAN WATER MANAGEMENT SOLUTIONS

2.1 Introduction

Freshwater scarcity with degrading water quality and growing water demand are critical concerns for future water availability. The municipal and industrial sectors are becoming more water demand intensive with improved economies, demographic migrations, and changing lifestyles (UN, 2014). In these conditions, conventional water supply systems, along with contemporary water management strategies, cannot meet future water demand. Improving water infrastructure may not help to completely subside the problem of increasing water stress (Gleick et al., 2000). Alternatively, management strategies are shifting either towards exploring new resources or on conserving existing resources by maximizing water utility.

Alternative water resources imply new resource exploration rather than making structural changes in conserving, storing, or diverting existing water resources (Greenlee et al., 2009). The primary alternative water resources include 1) rainwater harvesting; 2) wastewater reuse; and 3) desalination of brackish groundwater or seawater, depending on the feasibility. Other emerging alternative water resources include air conditioning (A/C) condensate and greywater, which together can substantially offset the urban water demand, especially in water deficient zones (Loveless et al., 2013; Madungwe et al., 2007).

2.2 Drivers of alternative water sources

The major drivers for the use of alternative water resources include: 1) uneven distribution of freshwater: 2) growing population; 3) increasing urbanization; and 4) anthropogenic factors impacting water quality and quantity (Scanlon et al., 2007).

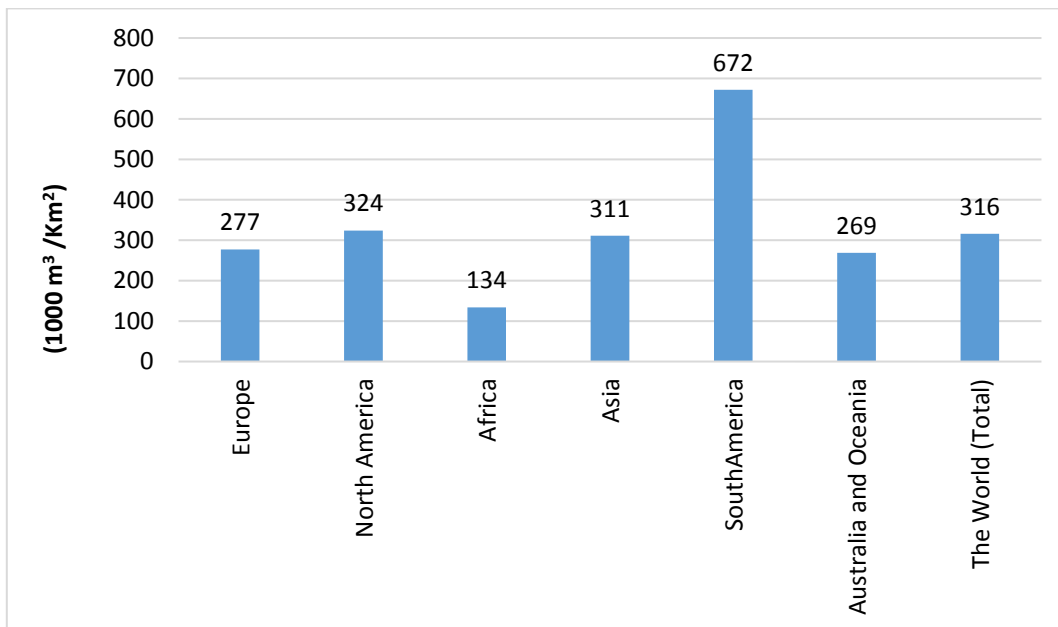


Figure 2.1 Global water availability worldwide (Adapted from Shiklomanov et al., 2000)

Freshwater availability is unevenly distributed over the globe (Al-Weshah et al., 2003). The world's annual, average, and available renewable freshwater accounts for 42,780 k m³/year (Shiklomanov et al., 2000). The majority of surface runoff (40%) is limited to water-rich countries, including India, Canada, and the United States (US). At the same time, some regions like "Arabian Peninsula, southern Europe, northern Africa,

Australia, and some parts of the southwestern United States”, suffer from acute water scarcity (Shiklomanov et al., 1998). Global freshwater availability for different regions of the world is shown in Figure 2.1.

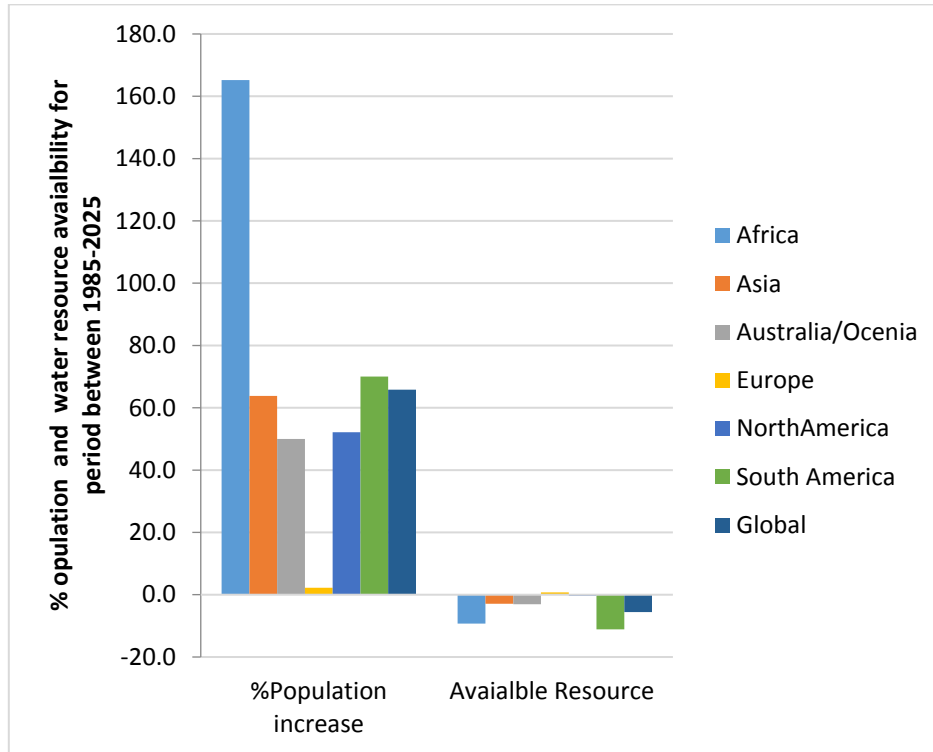


Figure 2.2 Increasing water stress with growing population and declining freshwater resources in between 1985-2025 (adapted from Vorosmarty et al., 2000)

Rapidly growing population is another major cause of water stress (Vorosmarty et al., 2000). Figure 2.2 shows the current and predicted sustainable freshwater resources and growing population between the years 1985 to 2025. It clearly shows a global population increase of 65 % between years 1985 to 2025, with declining water resource of about 5.6 % for the same period. Developing countries will be the worst

affected. Primary possible reasons for this could be less awareness of the problem and lack actions plans.

Anthropogenic factors are a major cause of water quality degradation of existing resources beyond the capability of natural resurrection by either point or non-point source pollution (Peters et al., 2000). Industrial effluent, domestic sewage with/without treatment, agricultural and urban drainage with high levels of pesticides and fertilizers, underground pipe leaking, mining and mineral exploration, and many more anthropogenic activities have adversely affected the physical, chemical, and microbial characteristics of surface and sub-surface water quality (Vitousek et al., 1997). These factors result in ecological imbalances, changes in hydrological regimes, and overall global climate change (Arnell et al., 1999).

The 21st-century water demand situation is also changing concerning the type of water use. In the current trend, agriculture accounts for a maximum water use of 66 %, followed by industrial water use for 20 %, and merely 7 % for municipal water supply (Duarte et al., 2014). However, the distribution of water use is changing with time, and the projected water demand for 2025 compared to 1995 is shown in Figure 2.3. It shows a marginal increase in irrigation water demand, whereas the trend for urban water demand (municipal and industrial) is escalating, particularly in developing countries. The non-irrigational water demand is expected to grow by 62% as compared to only 9% for irrigation by the year 2025 compared to 1995 (Rosegrant et al., 2002).

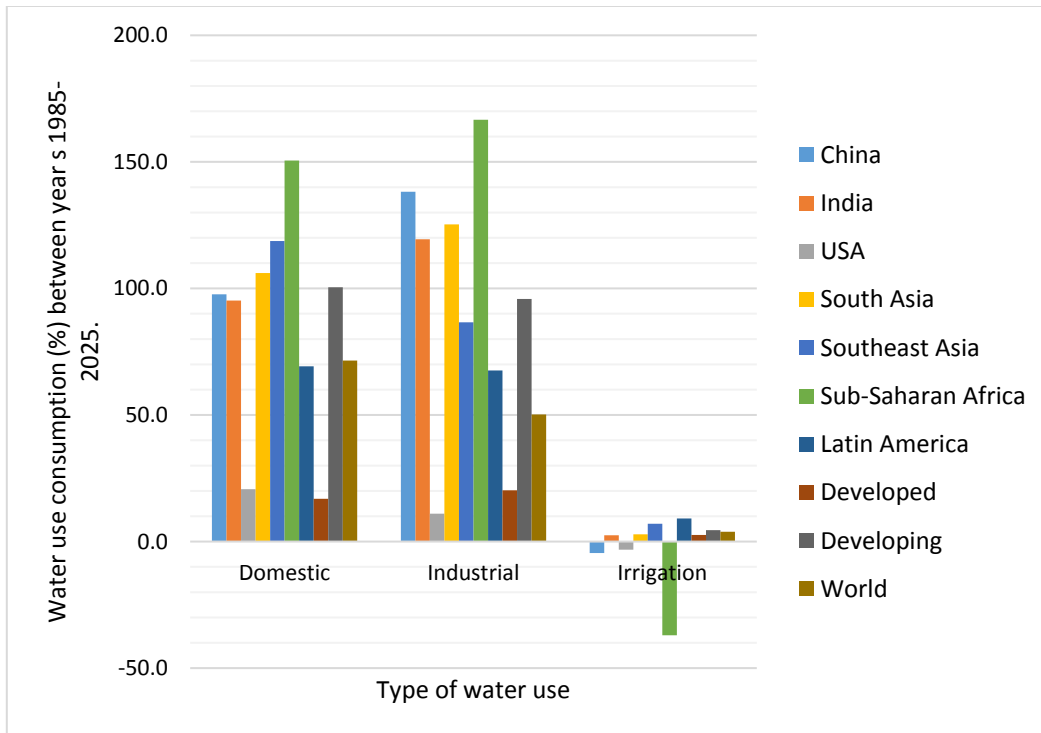


Figure 2.3 Increasing water stress with growing population and declining freshwater resources in between 1995-2025. (Adapted from Rosegrant et al., 2002)

The problem is more complex in urban regions where lucrative economies and high population growth together increase water demand (Cohen et al., 2006). Also, most new cities in the developing world will adopt a centralized water supply system, which also accounts for higher water consumption (Shiklomanov et al., 2000). For the above-mentioned reasons, the environmental sustainability concept of alternative water resources is becoming increasingly important in urban areas lacking freshwater supply (Lawrence et al., 2003).

2.3 Primary alternative water resources and their limitations

2.3.1 Desalination

Desalination is the most widely applied alternative water resource in those regions lacking freshwater supply, which are either surrounded by seawater or prevalent brackish groundwater (Einav et al., 2003). Approximately 24.5 million m³/day water is produced worldwide using seawater desalination (Lattemann et al., 2008) and is mostly used for augmenting urban water demand. Fifty % of water desalination occurs in the Gulf Cooperation Council (GCC) States, followed by North and South America, Europe, other Asian countries, and Africa, as shown in Figure 2.4 (Tsiourtis et al., 2001).

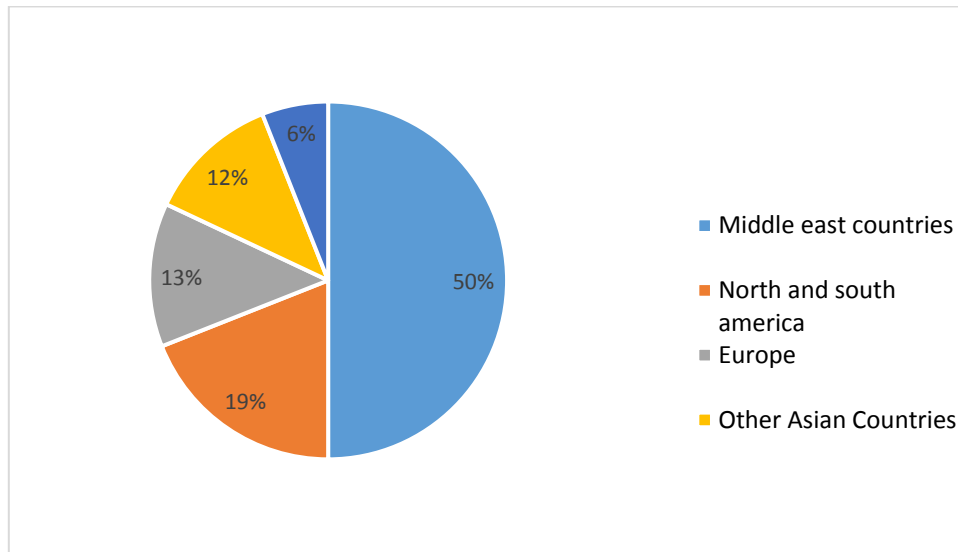


Figure 2.4 Global use of desalinated water adopted from (adapted from Tsiourtis et al., 2001)

Tsiourtis et al., (2001) also note that although desalination produces high-quality potable water, it is energy and capital intensive at the same time. With increasing water demand, the expanding desalination plants are a primary concern. According to the United Nations Development Program (UNDP, 2009), in Qatar, desalinated water increased three-fold between the years 1995 and 2008 but per capita water availability decreased during the same time-span, which shows that the increasing water demand cannot be merely met by expanding desalination plants.

Adverse environmental impacts of desalination are primary limitations in its further expansion, other than the associated capital cost of energy demand. The impacts include soil, water, air, and noise pollution (Einav et al., 2003). The reject stream makes up 30 to 40 % of feed water (Mohamed et al., 2005), which is dumped back to the sea or the environment surrounding inland desalination facilities as, for example, in El Paso, Texas. The reject stream contains concentrated brine with added toxic chemicals used in pre-processing and system maintenance, including 1) biofouling chemical (chlorine and other halogenated chemicals); 2) anti-scaling agents (polycarbonic acids, polyphosphates); 3) oxygen scavengers (sodium sulfite); and 4) anti-foaming agents (Lattemann et al., 2008; Höpner et al., 1997). Also, due to the high specific weight of the reject stream, it settles in the bottom of the sea, creating an imbalance in marine ecosystems (Einav et al., 2002). Table 2.1 shows a typical salt ion concentration comparison between feed and reject streams of three different desalination plants in Oman (Mohamed et al., 2005). According to the data, an almost three-fold higher concentrations of salt exists in the reject stream as compared to the feed stream. The

other environmental adversities also include groundwater contamination and associated greenhouse gas emission in multi-stage flash distillation (MSF) distillation processes, which are widely adopted in energy-rich countries as, for example, Qatar (UNDP, 2009).

Table 2.1 Changing salt concentration from feed to reject stream in designation plants

Desalination Unit s	Feed/Reject	Na (mg/l)	Ca(mg/l)	Mg(mg/l)	K(mg/l)	EC(dS/m)
1. Al Wagan	Feed water	741.6	146.3	112.4	28.4	5.1
	Reject water	2248.0	370.0	282.0	66.5	12.9
2. Al Qua	Feed water	451.1	162.4	103.6	27.2	4.6
	Reject water	2880.0	518.9	337.3	94.6	16.9
3. Um Al Zumool	Feed water	2481.0	456.4	194.5	110.3	14.7
	Reject water	6206.0	846.8	361.7	264.1	30.3

Source: (Mohamed et al., 2005)

2.3.2 Rainwater harvesting

The concept of rainwater harvesting consists of harnessing rainwater from the roof of a building or other impervious areas to meet local water needs (Boers et al., 1982). This is not an emerging concept and has been used since 2000 BC (Fewtrell et al., 2007). However, rainwater harvesting is being gradually considered as an alternative resource due to rising urban water demand, thus offsetting municipal demand and reducing storm-water volume in urban areas with increasing impervious land cover (Yu et al., 2014). Primarily, it has been applied to meet non-potable water use, including

lawn irrigation, washing clothes, and toilet flushing (Lye et al., 2009) and sometimes directly used for potable water supply (Fewtrell et al., 2007).

The major limitation in rainwater harvesting use includes both the variability in water quantity and water quality. The harvested rainwater quantity varies with time and geographical regions as well as frequency and intensity of precipitation (Boers et al., 1982). The type of roof and location of the facility (near industries, or densely populated urban area) and prevalent air quality significantly affect the quality of harvested rainwater. According to Förster et al., (1999), varying roof types, including zinc sheet, tar felt, pantiles, asbestos, cement, and gravel could be major sources of heavy metals like Zn, Cu, Pb, As, and Cd. Yu et al., (2014) reported the presence of fecal coliform in collected rainwater. Degrading water quality of harvested rainwater with storage time adds vulnerability to public safety and limitations to reuse (Evans et al., 2006).

An optional treatment system for the rainwater prior to its reuse may help to solve the problems of water quality, but the unreliability in water quantity during low precipitation seasons is a barrier for broadly adopting the technology. The concept may not be feasible and efficient in regions with low rainfall and high evaporation rates, primarily in arid regions of the world.

2.3.3 Domestic wastewater reuse and its limitations

The increasing volume of municipal wastewater in urban areas, especially with centralized systems (Nhapi et al., 2004), will potentially impact energy consumption, conveyance infrastructure, and treatment capacity of the wastewater treatment plant (WWTP). It will also affect the water quality of surface/sub-surface water-bodies and

therefore affect the environmental sustainability. Alternatively, the volumetric load of the wastewater can be considered as the primary postulate for water reuse perspectives; the treated wastewater can provide consistent means of supply in water-scarce regions unlike rainwater harvesting, which is season-dependent.

Treated municipal wastewater has been widely applied for irrigation, industrial applications, aquifer recharge, and other uses (Schäfer et al., 2005). The major limitations associated with treated wastewater reuse include 1) water quality; 2) capital cost associated with conveyance and treatment; 3) social acceptability, and 4) stringent water reuse regulations for treated wastewater reuse. Most of the applications are limited to low-grade non-potable uses, mainly in the irrigation sector, which is either limited to sub-surface and restricted irrigation use (Wang et al., 2006).

Tertiary treated wastewater provides a better opportunity for high-grade water quality applications but with additional energy and cost. A case study by (Fane et al., 2002) showed that secondary treated municipal effluent if followed by UV disinfection, results in 4.5 log virus removal and 2.5 log of protozoa removal. Additionally, if augmented with microfiltration, the removal rate improves to 6.5 log virus removal and 4.5 log protozoa removal. Studies also showed that for irrigation applications, the use of tertiary treated municipal wastewater compared to conventional groundwater has no additional impact on soil integrity as well as microbial contamination to plants (Pollice et al., 2004)

The added cost of treatment and rerouting the wastewater effluent sometimes conflicts with concurrent water costs and make it less effective in its implementation

(Molinos et al., 2010). Decentralized treatment units have sometimes been given priority over centralized treatment to improve the cost of wastewater reuse by minimizing piping and plumbing costs (Lens et al., 2005), but it broadens the gap of water quality and reuse limitations (Schaefer et al., 2004) in urban settings related to urban space availability, sludge disposal, and aesthetics.

Also, public perception on wastewater is not consistently favorable towards wastewater reuse. Advanced treatments using membrane filtration and RO systems applied for treating municipal wastewater is at par with drinking water regulations at a cost 40 % cheaper than desalinated water; however, there is very low public willingness to accept it for unrestricted use (Hunter et al., 2007). A public survey for a wastewater reuse case study by Kantanoleon et al., (2007) indicated that more than 80% of people do not intend to reuse wastewater in food-related water uses. However, the majority of people accept wastewater reuse for industrial applications (76%).

2.4 Emerging alternative water resources and their limitations

2.4.1 Greywater reuse and limitations

The concept of greywater is parallel to domestic wastewater reuse as it accounts up to 60-70 % of the total domestic sewage (Friedler et al., 2005), which mainly includes showers, washbasins, and laundry water (Jeppesen et al., 1996) and sometimes kitchen sinks (Birks et al., 2007). Therefore, it contains lower fecal contamination, lower BOD, less nitrogen, and lower sludge than conventional wastewater (Li et al., 2008).

Table 2.2 Characteristics of Greywater

Parameter	Source	Range		Units
Temperature		18	38	°C
Turbidly	Wash Cycle	39	296	NTU
	Rinse Cycle	14	29	NTU
	Greywater(mixed)	15.3	240	NTU
Suspended Solids	Greywater	17	330	mg/l
	conventional waste water	120	450	mg/l
Total Solids		113	2410	mg/l
(pH)		5	10	
COD		13	8000	mg/l
BOD		5	1460	mg/l
DO		0.4	5.8	mg/l
TKN	Greywater	0.6	74	mg/l
Total Phosphate	Phosphate not banned	6	24	mg/l
	Phosphate banned	4	14	mg/l
Zn	Laundry	0.09	0.34	mg/l
	Bathroom	0.2	6.3	mg/l
	others	0.01	1.8	mg/l
Ca		3.5	7.9	mg/l
K		1.5	5.2	mg/l
Mg		1.4	2.3	mg/l
Na		7.4	18	mg/l
XOC (Xenobiotic Organic Compounds)		Up to 900 compounds		mg/l
fecal coliforms	Bathroom	3×10^3	per 100 ml	per 100 ml
	Laundry	9×10^4	1.6×10^4	per 100 ml
Total Coliform	Bathroom	2.4×10^7		per 100 ml
	Laundry	56×10^5	8.9×10^5	per 100 ml
Fecal streptococci	Bathroom	7×10^4		per 100 ml
	Laundry	1×10^6	1.31×10^6	per 100 ml

Source: (Adapted from Erikson et al., 2002)

The World Health Organization (WHO, 2006) states that “Ten % of the total food production of the world relies on treated or untreated greywater”. Lawn irrigation and toilet flushing are major applications of greywater (Neal et al., 1996) compared to conventional wastewater, which is mostly limited to irrigation use. Toilet flushing and lawn irrigation with greywater could potentially alleviate 50 % of portable water demand (Maimon et al., 2010).

In general, greywater offers a better alternative to conventional wastewater reuse primarily as it has: 1) higher influent water quality; 2) lower cost of treatment; 3) lower conveyance cost if applied locally at household or community level; and 4) potentially better social acceptability as it does not include toilet/urinal flushes.

2.4.2 Technological limitations in grey water treatment

The wide variation in greywater quality is one the most challenging aspects of selecting a robust treatment system and desired goal quality. Greywater characteristics have been listed in Table 2.2 and attributed to source, type, location, regional habits, type of soap or cosmetics used, and other household activities (Erikson et al., 2002). Different types of treatments systems have been used to treat greywater for varying pollutant load and desired effluent quality, including chemical, physical, biological, or in combinations (Li et al., 2008). Coarse filtration followed by disinfection is one of the most commonly applied treatments because of its simplicity; however, high turbidity and suspended solids in the effluent deter the disinfection potential of the system (Al-Jayyousi et al., 2003; Kariuki et al., 2011). Constructed wetlands (CW) are another

option for low-cost treatment, but it may not be viable in urban areas due to lack of space, aesthetics, and variable effluent quality. Horizontal Flow Reed Beds (HFRB) and Vertical Flow Reed Beds (VFRD) (Scheumann et al., 2009) are more common in greywater treatment compared to conventional wetlands.

Different types of biological treatments can be applied for greywater treatment. However, the low nutrient content compared to carbon and nitrogen makes it unsuitable for biological treatment (Chaillou et al., 2011) unless additional nutrients are supplied to the system. At the same time, the biological treatments of greywater provide better opportunities than the basic coarse filtration regarding microbial as well as chemical contaminant removal. The Upflow Anaerobic Sludge Blanket (USAB) is a common application for biological treatment where energy cost matters, but not an attractive means to obtain high water quality (Elmitwalli et al., 2007). The Membrane Bioreactor (MBR) is being applied in most of the high-quality effluent target (Gonzalez et al., 2007). Microbial risk is still associated with MBR-treated water, which limits its applications other than being energy and cost-intensive processes; however, it is a better option at the community level or for commercial buildings with limited urban space availability (Scheumann et al., 2009).

Membrane applications for greywater treatment can provide the quality intended for unrestricted water reuse (Oron et al., 2014). Ultrafiltration can provide low turbid water with lower microbial contamination compared to MBR; however, soluble nutrients, including ammonia and phosphorus, are prevalent in the effluent (Li et al., 2008). Such effluent can be applied as high-quality irrigation water if the nutrient limits

exceed the unrestricted water reuse. At the same time, pretreated greywater augmented with an RO system provides high effluent quality water at par with drinking water standards (Onkal et al., 2011). The major limitations with membrane use are the cost, high energy consumption, and residence time of greywater in the system, which induces anaerobic decay as well as affecting membrane fouling (Ghunmi et al., 2011).

Though scientifically, greywater has been treated using advanced treatment systems, existing commercially available greywater treatment options fail to provide consistent reliability for varying load conditions, resulting in lower consumer confidence in these systems (Allen et al., 2010). Dual plumbing requirement of greywater treatment is another limitation (Prathapar et al., 2006) due to retrofitting older buildings and potentially added cost to water.

2.4.2.1 Water reuses standards for greywater

Greywater reuse has a primary limitation in the fact that reuse standards are different for different locations (Prathapar et al., 2005) and therefore in the versatility of its applications. Greywater reuse standards are limited to very few states in the U.S. (Allen et al., 2010) and lie in the same arena of wastewater reuse regulations, although their influent quality varies; nevertheless, regulations do not distinguish them differently (Maimon et al., 2010).

However, in some of the states like Texas, new regulations are being made and constantly amended to improve potential use of alternative resources. The Texas greywater reuse regulations allow influent from the source including washbasin (not used for toxic chemical disposal or food preparation), laundry water (without diaper

washing), and shower water primarily (Use of Reclaimed Water §§210.81 - 210.85-effective January 6, 2005) (TCEQ, 2005). “House Bill (HB or bill) 1902, 84th Texas Legislature (2015), amended which aims at improving greywater reuse particularly for toilet and urinal flushing (TCEQ, 2015).

2.4.2.2 Storage of greywater and public health

The public health risk is one of the major limitations to greywater reuse due to restrictions on its storage duration. Greywater quality goes under significant change with storage, especially with regard to its microbial concentrations. Robison et al., (1996) reported that the microbial count of total coliform changes significantly over a 48 hours of storage time (from 10^0 - 10^5 to $> 10^5$ per 100ml of samples). Very limited research is, however, available on the impact of storage duration on the biological and chemical quality of greywater (Liu et al., 2010).

2.4.3 Air-conditioning (A/C) condensate

A/C condensate as an alternative resource has not gained full recognition yet. This is despite hot and humid urban areas of the world relying on HVAC systems for maintaining indoor comfort; they have thereby reported significant yields /volumes of condensate. Conventionally, the A/C condensate is drained to the sewer system (Painter et al., 2009). Accordingly, the onsite collection and reuse of A/C condensate could help in partially offsetting municipal water demand, which potentially will promote green infrastructure for water-scarce regions (Wilson et al., 2008).

Determining the water quality and quantity of A/C condensate are critical steps for water management as well as public health issues. Low contamination in A/C

Table 2.3 A/C condensate water quality analysis in different part of world

Parameters		Cook et al., (2014)	Bryant et al., (2008)	Loveless et al., (2013)			
		Brisbane	Doha	Cas, Kasut	Jeddah	Makkah	Riyadh
pH		6.9	6.5	4.37-6.87	5.93-7.35	3.05-6.77	3.63-7.45
TDS	(mg/L)	-	-	-	-	-	-
DO	(mg/L)	-	7.15	-	-	-	-
Turbidity	(NTU)	-	0.7	0.041-0.15	1.62-5.5	1.63-2.47	0.89-7.89
Conductivity	μ S/cm	12	86	18-27	30.3-214	32.5-73.4	32.6-95.6
Chlorides	(mg/L)	-	1.2	-	-	-	-
Nitrates	(mg/L)	-	0.6	-	-	-	-
Total Nitrogen	(mg/L)	0.67	-	-	-	-	-
E.coli	(Count/100 ml)	1	-	-	-	-	-

condensate can be expected as it is a result of the air-moisture dehumidification process and is also “noncorrosive and non-erosive in nature” (EPA, 2007). According to Guz et al., (2005), condensate water quality can be considered better than tap water, although, the condensate quality varies with the type of air conditioners (Loveless et al., 2013) and their surrounding ambient quality. The limited studies on water quality variability do not

show a limitation towards its reuse as shown in Table 2.3. It can be directly applied for non-potable water use application, including landscape irrigation, recreation, and cooling tower toilet flushing (Painter et al., 2009), and possibly can be used as unrestricted water with a low cost of treatment (Lawrence et al., 2010; Loveless et al., 2013).

Most of the studies in condensate volumetric estimation are site and system specific (Bryant et al., 2008; Guz et al., 2005) and models are empirical in nature. The volumetric flow rate has been considered as a more conventional way to compute condensate volume. However, measuring volumetric flow rate is in itself a challenge, not only practically, but it also results in a significant error as shown in the condensate estimation (Lawrence et al., 2010).

When planning to use A/C condensate in a building, it is critical to be able to estimate condensate volume with varying load conditions, especially with seasonal variability (Cook et al., 2014). In fact, the uncertainty in condensate volume is a major barrier for its use as an alternate water resource. It can lead to two major limitations: financial obligations and water supply strategies during low production periods. The volumetric figures become important regarding determining the financial payback for the associated costs incurred on installation of condensate recovery systems, either retrofitting with existing building or with new buildings (Lawrence et al., 2009). It may not be feasible in circumstances where installation and maintenance costs exceed the financial return.

2.5 Summary & conclusion

Overall, alternative water resource adoption may vary based on 1) water quantity; 2) water quality; 3) technical feasibility in treatment and reuse; 4) capital costs and payback on piping, plumbing, storage, and type of reuse; 5) environmental sustainability, risk factors, and resilience of the system and long-term impact; 6) social acceptance; and 7) local regulatory agencies. Increasing population, diminishing water resources, changing water use patterns, adverse anthropogenic activities, and overall increasing water stress is a major driver for the reemergence of alternative water resources, which can substantially offset the escalating municipal, industrial, and agricultural water demand (Rosegrant et al., 2002). Among alternative methods, decentralized greywater and A/C condensate systems are the most promising if greywater quality can be treated to the necessary level based on potential use and if A/C condensate volume can be quantified.

3 EVALUATION OF PORTABLE IN-HOUSE GREYWATER TREATMENT SYSTEM FOR POTENTIAL WATER-REUSE IN URBAN AREAS

3.1 Introduction

Out of the total municipal water supply for household activities, 60-70% % contributes to greywater (Friedler et al., 2005). The separation and reuse of on-site greywater can reduce its volume and water treatment requirements, and thus, result in reduction in capital cost required for pipe network and pumping (Chen et al., 2009).

Treated greywater can be the best alternative for a consistent water supply in the region, where freshwater resources are limited. The physio-chemical and biological characteristics of greywater need to be evaluated before reuse for its potential impact on human health and safety (Winward et al., 2008). Uncertainty in greywater quality depends on the region and type of domestic use (Eriksson et al., 2002).

A number of attempts were made to characterize the wastewater in different parts of the world (Surendran et al., 1998, Al-Jayyousi et al., 2003, Rose et al., 1991, and Christova et al., 1996). Greywater characteristics vary with domestic uses including laundry, washbasin, shower and kitchen (Jamrah et al., 2008). Variations in water quality parameters and stringent water reuse regulations are major challenges in selecting an appropriate treatment system.

Several system design approaches have been developed to treat greywater in specific conditions (Li et al., 2008). Different types of biological reactors were also applied for treating greywater, including up-flow sludge blanket (USAB)) (Leal et al., 2007), a rotatory biological reactor (RBC) (Nolde et al., 2000) and constructed wetlands

(Gross et al., 2007). 'Membrane Bio Reactor' (MBR) is one of the most adopted means of greywater treatment at the community level because of high and stable performances (Lesjean 2006). Liu et al., (2005) used submerged MBR to treat shower water and observed greater removal of COD, BOD₅, NH₄-N, SS removal from 132-322 mg/l, 99-212 mg/l, 0.6-1 mg/l, 15-55 mg/l in influent to <40mg/l, <5 mg/l, <0.2 mg/l, ND in effluent, respectively. The MBR may provide high-efficiency treatment of greywater. However, the biological treatments are not effective in treating low nutrient (COD: N: P) greywater, especially those that originate from laundry and shower water, and need additional nutrients added to the system (Li et al., 2009).

Membrane filtration can be an attractive means of treating greywater in terms aesthetics, compatibility as decentralized water treatment system (Ramona et al., 2004). The major contamination removal through membrane filtration includes suspended solids and the associated microorganism including cyst, giardia and other bacteria (Madaeni et al., 1999). Ultrafiltration (UF) has better retention capability than microfiltration (MF), which can substantially remove viruses and organic and inorganic macromolecules (Guo et al., 1996). Nanofiltration (NF) membranes are particularly used for divalent ion removal (Crittenden et al., 2012). A 'Reverse Osmosis' (RO) system works against the osmotic potential between feed (high concentration) and permeates (low concentration) and is primarily applied for monovalent salts removal (Greenlee et al., 2009). Very few studies addressed the use of direct membrane filtration for greywater treatment (Ramona et al., 2004). Van et al., (2005) used NF to treat laundry water directly without pretreatment.

The critical limitation of membrane systems is the frequent clogging and residence time of greywater in closed conduit (Ghunmi et al., 2011) in addition to energy expenditure. This may cause a declining effluent flux over time and increase in anaerobic decay of substrate with biofilm formation over their membrane surface. The result would be an addition to the contamination level in the system, and therefore, would reduce the operational efficiency of the system (Nghiem et al., 2006).

Pre-filtration of feed for membrane RO plays a vital role in its function, which may increase the membrane life, reduce energy requirement as well as yield better effluent quality (Shannon et al., 2008). The conventional pretreatments include sedimentation flocculation, and coagulation processes (Ghunmi et al., 2011). However, activated carbon can also be applied as the pre-filtration, and it can significantly remove total organic carbon (TOC) from wastewater (Crittenden et al., 1993).

Establishing a greywater treatment system at household scale is challenging with constraints such as, (1) ease of operation with chemical free treatment either as coagulant or disinfectant, (2) portability, (3) aesthetics, (4) flexibility in doing optimal treatment based on desired goal, (5) uncertainty in greywater influent quality and (6) robustness in treatment to meet stringent water reuse standards.

This study focused on greywater characterization, treatment and reuse. The typical sources including shower, laundry and washbasins greywater were considered for analysis. The greywater treatment system was applied in the case study to provide water a reuse scheme with multi-grade effluent uses. The system was named as Granular Activated Carbon-Membrane Integrated-Multi Effluent (GAC-MI-ME), which is based

on serial filtrations conventionally applied for advanced physical filtration components, where each preceding unit works as pretreatment for the next successive level. The specific objectives of the study are as following:

- I. Characterize greywater from shower, wash basin, and laundry.
- II. Assess various commercially available water treatment components and reuse systems (GAC-MI-ME).
- III. Evaluate treatment performance of GAC-MI-ME system particularly as pre-filtration for UF and RO effluents.

3.2 Material & methods

3.2.1 Greywater collection

Greywater samples were collected from the typical sources namely, laundry, bathtub, and washbasin in College Station Texas from student housing. The laundry water was collected as an equal proportion of wash and rinse cycle of a washing machine, and also considered different types of clothes from delicate to casual. The greywater from the washbasin represented 24 hours of faucet use from student housing. The shower water was collected from bathtubs using a sump pump. At least 5 to 8 gallons of the greywater were collected in each collection-event. The collection scheme for the greywater is shown in Appendix B1.

3.2.2 GAC-MI-ME greywater treatment system description

The GAC-MI-ME treatment system is built from the components of advanced physical filtration systems connected serially. It includes coarse filtration (CR-F), microfiltration (MF), granular activated carbon filtration (C-F), ultrafiltration (UF), ultra

violet (UV), and reverse osmosis (RO). The system was fabricated by considering its compactness and potential deployment in urban settings. The GAC-MI-ME greywater treatment system is shown in Appendix B2. The system emphasizes a potential alternative solution to conventional biological and chemical processes for greywater treatment. The GAC-MI-ME system components including CR-F, MF, and GAC provide pre-filtration for UF and RO units, as well as it shields the units from shock loading and fouling. The GAC was applied with intent of organics removal (Gur-Reznik et al., 2008) which are common cause of membrane fouling (Vogel et al., 2010).

The CR-F module of GAC-MI-ME system includes serially connected polyester and polypropylene membranes with normal diameters of 50, 20, 10, and 5 μm . The MF comprises of serially connected 1, and 0.35 μm membrane modules. The customized GAC module included parallel-connected three individual GAC filter modules to increase the residence time of the water. The UF module comprises of hollow-fiber membrane with/without backwash capability. The absolute pore diameter of the UF system are 0.02 and .025 μm . The UV reactor was installed prior to RO and after UF to ensure efficient microbial disinfection. The components' details are provided in Appendix B3.

The GAC-MI-ME greywater treatment system includes two major pumps. The primary delivery pump was installed at the inlet of the system and approximately provides 1.5 gpm without head loss. The other one was a booster pump, which was installed prior to RO system for maintaining optimum pressure to efficiently utilize the

RO system. A typical flow rate observed at MF, UF and RO filtration modules were 1.2, 0.4, and 0.07 to 0.01 gpm respectively.

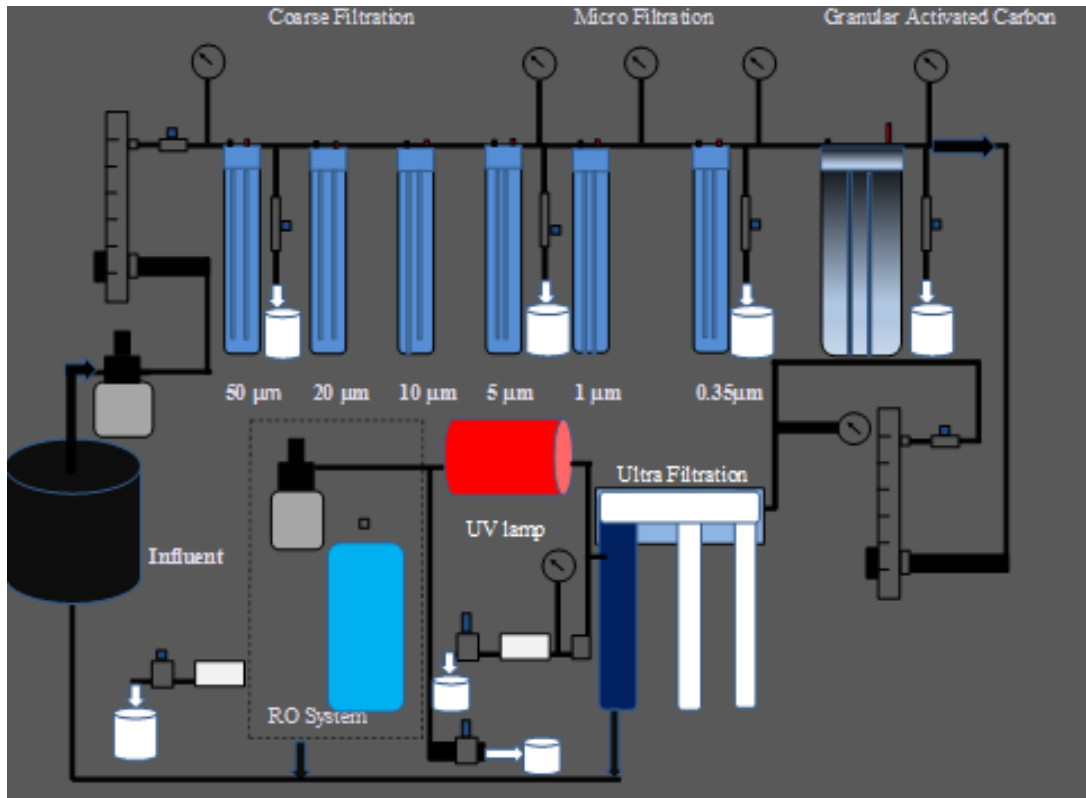


Figure 3.1 Fabricated greywater filtration system with multi-stage effluent collection and pressure gauges

The system was also installed with ‘Tank Level Controllers’ (TLC) and ‘Electronic Shutoff Valve’ (ESO series) in order to stop the system when pressure reaches 60 psi. The ESO functions to avoid membrane disruption at high contaminant load or in case of membrane clogging. The TLC shuts off the system when the storage tank is full (in case of continuous operation). Pressure gauges were installed across the

system to depict the trans-membrane pressure, and therefore an indication of membrane replacement or clogging.

The idle volume of the system was observed to be about 2.9 gallons; which means that the samples needed to be taken at least after 3 gallons of volumetric flow through the entire GAC-MI-ME system. The effluent samples were collected at each test port after CR-F, MF, GAC, UF, UV, and RO as shown in Figure 3.1.

3.2.3 Physical, chemical, and microbial evaluation of greywater

The major parameters addressed during this study were BOD₅ (Biochemical Oxidation Demand), turbidity, total dissolved solids (TDS), total coliform (TC), electrical conductivity (EC), pH, Ca, Mg, Na, K, B, HCO₃, CO₃, SO₄, Cl, NO₃-N, P, conductivity, sodium adsorption ratio (SAR), hardness, cations/anions, alkalinity, P, and Nitrate-N. The water quality analysis were conducted at Texas A&M University campus (College Station, TX). *proOBOD* sensor (YSI, Inc., Yellow Springs, OH) was used for BOD₅ measurement. *Petri-films* (3M, Sr. Paul, MN) were used for total coliform count. The samples were incubated on the petri-films for 24 hours at 35°C. YSI 6800XLM sonde was used for pH assessment. Hanna *Instruments* H3014 turbidity meter (Hanna Instruments, Inc., Ann Arbor, MI) was used to measure turbidity (NTU) of water samples. TDS probe was used to determine total dissolved solids in the samples. Concentration of ionic species was measured by inductively coupled plasma mass spectrometry (ICP-MS). The measurements accuracy for the turbidity meter, pH/ORP probe, dissolved oxygen (DO) probe and TDS-meter are shown in Appendix B4.

3.3 Results & discussions

3.3.1 Greywater characteristics

The water quality parameters for six different samples from each source of greywater are shown in Table 3.1. Physio-chemical, and microbial characteristics of the greywater showed wide variation. The primary factors that affects the quality of greywater are source of water, the type of household use, the different levels of physical, chemical, microbial addition including sanitary products, soap, detergent, bleach, food material, fibers, hairs and human contact.

Laundry water with equal proportion of wash and rinse cycle showed the highest turbidity level ranging from 277 to 432 NTU. This was a higher turbidity range as compared to a similar study (15.3-240 NTU) (Chritova-Boal et al., 1996). Lower turbidity was observed in wash-basin water (42-48 NTU) and shower water (105-126 NTU), which implied that more suspensions and colloids are associated with laundry water than the others. This implies that higher risk of clogging is associated while treating laundry water.

High variation in pH, and alkalinity were also observed in all the greywater. Laundry water showed pH values (5.09-7.5) with corresponding alkalinity (55-270) mg/l of CaCO₃. The trend was similar for shower, and wash-basin water with pH, and alkalinity values for (5.57-6.88), (162-363) mg/l of CaCO₃ and (6-6.92), (133-280) mg/l of CaCO₃ respectively. Typically, alkalinity and pH are low in shower and wash-basin water compared to laundry water (Eriksson et al., 2002).

Very low BOD₅ was observed for all three types of greywater compared to other studies (Li et al., 2009, Halalsheh et al., 2008, Eriksson et al., 2002) The maximum BOD₅ were observed as 50.4 mg/l in laundry water and lowest in wash-basin water as 8.4 mg/l.

Table 3.1 Physio-chemical and microbial characteristics of greywater measured in College Station, TX

Water Quality Parameter	WB		SW		LW	
	S1	S2	S3	S4	S5	S6
Ca-(mg/l)	9	3	6	6	2	27
Mg-(mg/l)	1	1	2	2	<1	6
Na-(mg/l)	89	159	120	183	138	298
K-(mg/l)	7	3	19	8	6	16
B-(mg/l)	0.26	0.24	15.55	0.18	0.36	1.97
(HCO ₃)	162	341	197	443	329	67
SO ₄ ⁻ -(mg/l)	33	21	216	40	10	309
Cl ⁻ -(mg/l)	37	60	1	93	40	501
NO ₃ -N(mg/l)	0.01	0.01	<0.01	0.01	<0.01	0.57
P(mg/l)	2.43	0.57	1.41	0.25	0.19	0.52
pH	6	6.92	5.57	6.88	7.5	5.09
Conductivity (µmhos/cm)	369	612	623	758	544	2110
Hardness (mg/l CaCO ₃)	27	12	22	23	8	92
ALKALINITY(mg/l CaCO ₃)	133	280	162	363	270	55
TDS -(mg/l)	341	589	578	775	526	1227
SAR -(mg/l)	7.4	19.8	11.2	16.5	21.3	13.5
BOD-(mg/l)	11.7	9.6	8.4	22.6	35.7	50.4
Turbidity -(NTU)	42	48	126	105	277	432
Total Coliform -(cfu/ml)	2.20E+03	9.25E+02	3.20E+03	3.90E+03	4.60E+03	1.00E+04

WB: Wash-Basin water SW: Shower water LW: laundry water S: Sample number

The ionic species (cations/ anions) also varied for different types of greywater. The bivalent salts (Ca, Mg) were present in lower concentration than the monovalent

species (Na, K). The highest TDS value of 1227 mg/l was observed in laundry water. High level of Na, and K can be attributed to the abundance of their salts present in surfactants/foaming agents. Significant HCO_3 was also detected in all the samples of greywater. Traces of $\text{NO}_3\text{-N}$ and P were found in all the samples, which are much lower than the typical values observed (Eriksson et al., 2002). Significant Boron (B) concentration was also observed in some of the samples up to 15 mg/l.

Total coliform counts were determined to analyze the extent of microbial contamination. The laundry water showed the highest microbial contamination up to $1.0\text{E}+04$ (cfu/ml) compared to wash-basin water ($9.25\text{E}+02$ to $2.2\text{E}+03$) cfu/ml. Although the range of contamination varied, the observed values were in close proximity with other studies (Li et al., 2009, Eriksson et al., 2002). The wash-basin water was found to be the least biologically contaminated compared to laundry and shower water.

The presence of turbidity, ionic species, coliform count, and other contaminants were observed to be the highest in laundry water and the least in wash-basin water. Similar trends were reported for greywater characterization in Oman (Halalsheh et al., 2008). This implies that the treatment of laundry water is more challenging than the treatment of shower and wash-basin water. While results may vary with the personal habits, type of soap or the cosmetics, the overall characteristics of greywater will depend on the ratio contribution of laundry, shower, and wash-basin. The results characterizing greywater may play a significant role in selection of an appropriate greywater treatment system, specific to the type of greywater.

3.3.2 Permeate quality for multi-stage greywater treatment system

Wide variability in GAC-MI-ME effluent quality were observed along multiple treatment trains, representing CR-F , M-F, C-F, UF,UV and RO. Effluent quality were monitored at all five stages of treatment. BOD and total coliform were considered for additional UV treatment. Comparative results of the treatments are presented in Table 3.2.

Table 3.2 Treated effluent characteristics variation along the fabricated treatment system

		Ca(mg/l)		Mg(mg/l)		Na(mg/l)		k(mg/l)		B(mg/l)		HCO ₃ (mg/l)		SO ₄ (mg/l)	
		Mean	SD	Mean	SD	Mean	SD	Mean	SD	Mean	SD	Mean	SD	Mean	SD
Treatment -Train	Raw	9.3	10.0	2.2	1.9	164.5	72.9	9.8	6.2	3.1	6.1	256.5	138.2	104.8	126.0
	CR-F	8.5	9.4	2.2	1.9	157.3	75.8	9.7	6.5	3.1	6.1	245.7	132.7	103.8	126.9
	M-F	5.8	4.3	1.3	0.5	119.5	37.8	8.2	5.7	2.8	6.3	243.7	134.3	56.0	79.2
	C-F	2.8	3.0	1.0	0.0	107.2	28.2	5.8	2.0	1.0	2.0	225.0	105.9	19.8	8.2
	UF	2.2	2.9	1.0	0.0	104.0	28.7	4.3	2.1	0.6	1.0	224.7	105.5	19.5	8.3
	RO	1.0	0.0	1.0	0.0	9.6	4.4	0.8	0.4	0.3	0.4	21.8	23.5	3.8	3.9
		Cl(mg/l)		NO ₃ (mg/l)		P(mg/l)		pH		Cond(umhos/cm)		Hardness (mg/l of CaCO ₃)		Alkalinity (mg/l of CaCO ₃)	
		Mean	SD	Mean	SD	Mean	SD	Mean	SD	Mean	SD	Mean	SD	Mean	SD
Treatment -Train	Raw	122.0	188.1	0.10	0.23	0.90	0.87	6.5	0.9	836.0	636.9	30.7	30.9	210.5	113.3
	CR-F	119.2	189.4	0.10	0.23	0.80	0.89	6.4	1.1	809.0	651.8	30.3	31.1	201.5	108.7
	M-F	41.0	29.8	0.01	0.00	0.54	0.52	6.7	0.9	523.8	149.3	19.8	10.8	199.8	110.0
	C-F	31.0	17.0	0.01	0.00	0.48	0.43	7.2	1.0	450.3	108.3	11.7	7.9	184.5	86.7
	UF	29.5	17.1	0.01	0.00	0.25	0.18	7.6	1.3	445.5	112.5	11.5	7.5	184.5	86.7
	RO	6.3	10.4	0.01	0.00	0.02	0.01	6.3	1.1	42.0	25.6	5.0	3.2	28.8	11.6

High turbidity reduction was observed along the treatment-train. Microfiltration showed average reduction from 171.7 NTU in raw greywater to 105.8 NTU. Although, it was significant SD removal, but potentially, could cause clogging at successive level of UF and RO. The GAC filtration (C-F) played vital role in filling the gap between nominal pore of 0.35 μm of MF to absolute pore of 0.025 μm . UF. Figure 3.2 depicts the effluent

turbidity range removal along the treatment train. The turbidity range of 0.1 to 1 NTU was mostly observed between UF and RO and a range 1-10 NTU was mostly observed between carbon and ultra-filtration.

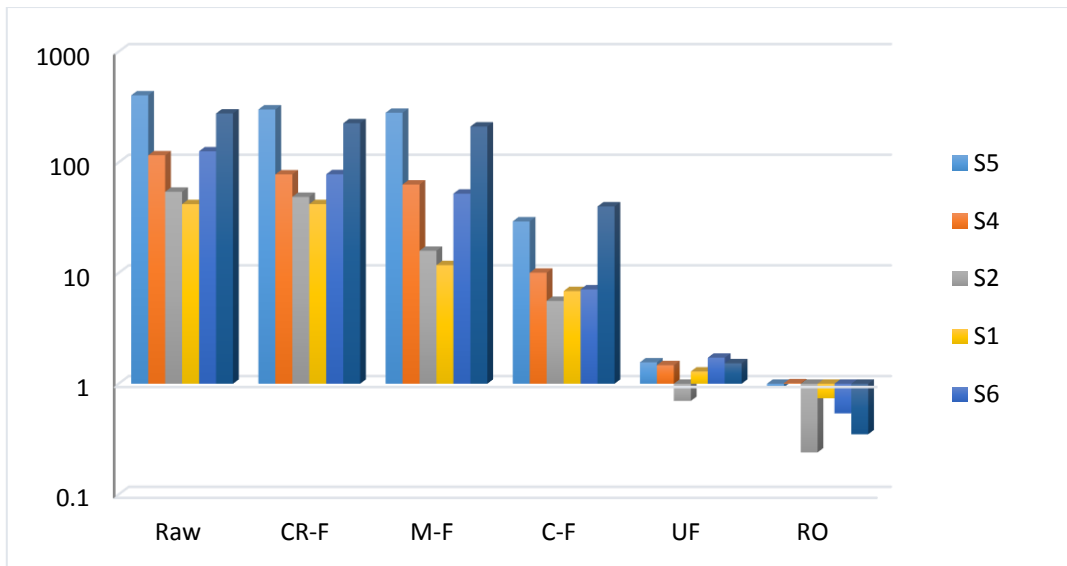


Figure 3.2 Turbidity removal along GAC-MI-ME system for different greywater samples(S)

Total coliform exhibited high level of variability in treated water. Figure 3.3 shows total coliform reduction for varying strength greywater over the treatment–train. Coarse filtration (CR-F), Microfiltration (M-F), and GAC filtration showed marginal total coliform removal over significant removal by UF, UV, and RO as 2.2, 3.2, and 3.4 (log removal) respectively. There might be possible cross-contaminations as complete removal was not achieved both at UF and UV. One reason might be short circuiting as well as mixing of water or pre-existing bacterial colonies in the system.

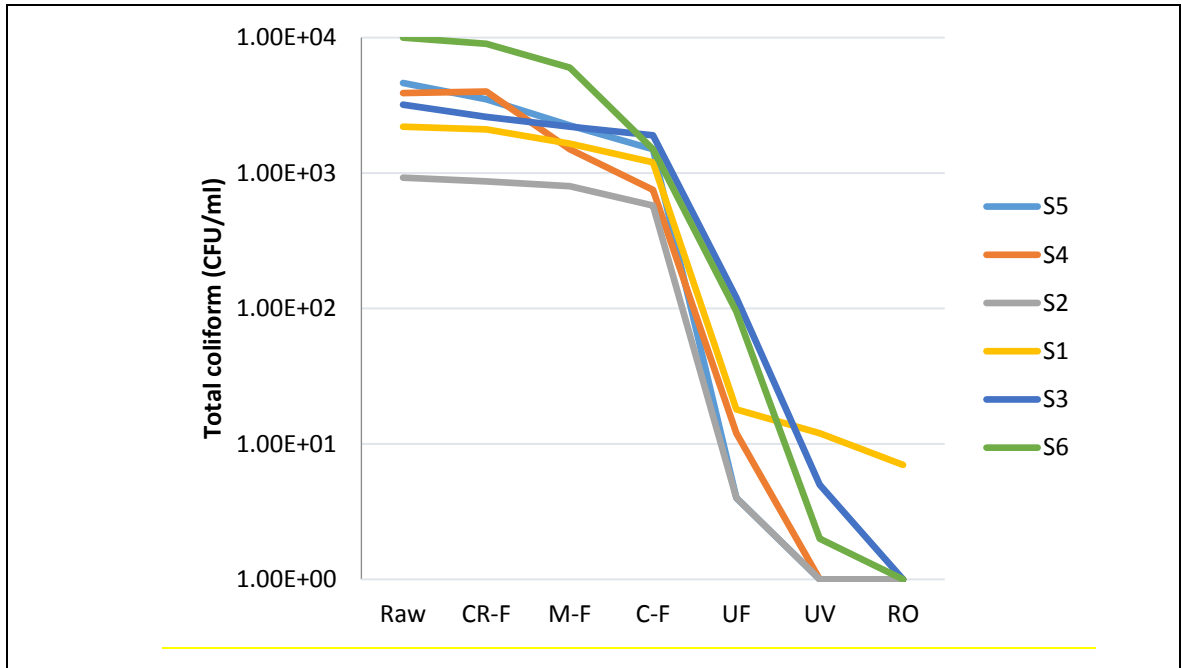


Figure 3.3 Total coliform removal by GAC-MI-ME system for different in greywater samples (S)

The BOD₅ removal for the system is shown in in Figure 3.4. It shows average reduction in BOD₅ for coarse (CR-F) and microfiltration (M-F) unit from 6 to 24.3 %. However, significant reduction (53.2%) was achieved at the GAC filtration (C-F) unit. UF and UV showed slight improvement for another 6.4 % compared to C-F. Reverse osmosis played a vital role for achieving BOD reduction up to an average of 84.8 %. The 100% BOD₅ removal was not attained by the system.

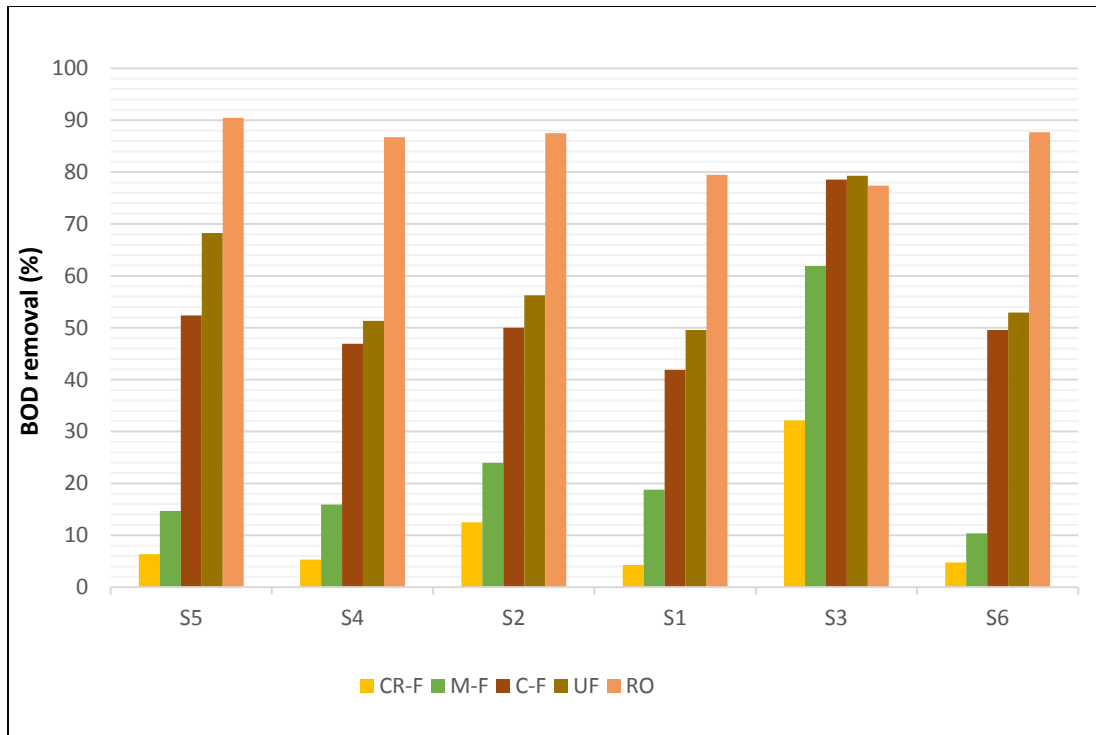


Figure 3.4 BOD removal along GAC-MI-ME system for different greywater samples(s)

Figure 3.5 can be visualized as pretreatment (CR-F, M-F, and C-F) for ultrafiltration and reverse osmosis (UF, and RO). CR-F, MF, and C-F played a vital role as pre-filtration. Significant reduction was obtained for the parameters Ca, Mg, Na, K, B, SO₄, Cl, P, and TDS by 54.5, 30.6, 24.5, 28.9, 27.7, 46.8, 34.2, 39.2 and 25.7 % respectively. C-F, and M-F showed major contribution in pre- filtration. The parameter that had low removal rates below 35% such as Mg, and NO₃-N were initially low in concentration in the influent greywater (Mg: 2.2±1.9, NO₃-N: 0.1±0.23) mg/l.

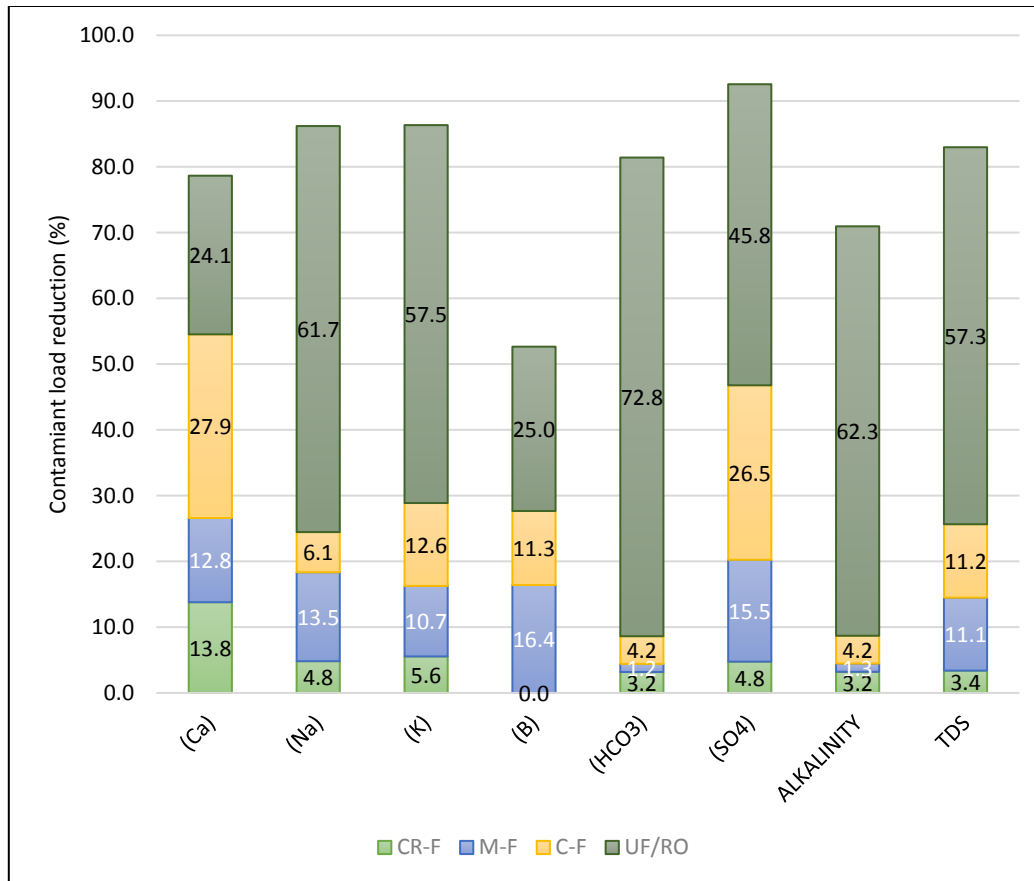


Figure 3.5 Contaminant load reduction (%) along GAC-M-MI-ME system

3.3.3 Water reuse potential as unrestricted water reuse

Multi-grade effluent can be obtained through the fabricated treatment system. There is no exhaustive list of parameters standards developed for greywater reuse but there are some restrictions on few water quality parameters. The most common are turbidity, BOD₅, total coliform count, fecal coliform count, total suspended solids, and pH depending on the environmental regulations of specific country or region. Water quality requirements or treatment goal can be attributed to such enforced standards for water reuse to determine an optimal treatment-train.

The effluents characteristics of ultrafiltration and RO are in close proximity with the unrestricted water reuse (Li et al., 2009). Standards for unrestricted water reuse (not for drinking) addresses water quality with turbidity level < 2 NTU, BOD < 100 mg/l, pH(6-9) TC form < 100 cfu/ml and fecal coliform UD (Li et al., 2009). Fecal coliform and TSS were not measured in the study. However, the observations of UF comply with turbidity level (1.4 ± 0.4 NTU) and TC count ($4.2E+ 01 \pm 5.2+01$), and in close proximity for BOD (9.3 ± 6.3 mg/l). At the same time RO water show much better quality than the desired standards for unrestricted water reuse.

3.4 Conclusion

Three different types of greywater were considered in this study including laundry, shower, and wash- basin water for evaluation of GAC-MI-ME greywater treatment system. Wash-basin water was found to be the least contaminated compared to laundry and shower water. As greywater is a mix of the all three types of water, the water quality characterization may help user in selecting influent load for the treatment system.

The treatment-train of coarse ($50- 5 \mu m$), micro and GAC filtration substantially reduced the contaminant load for UF and RO module. The effluent quality obtained at UF is in close proximity with unrestricted water standards. RO water can be categorized as extremely pure water. However, the multi-grade effluent characteristics of GAC-MI-ME system are based on limited number experiments. Further sampling and analysis is needed for potential evaluation of the GAC-MI-ME effluents with different water-reuse perspectives.

4 MACHINE LEARNING (USING ANN) FOR GREYWATER REUSE: COMPREHENSIVE APPROACH USING EFFLUENT PREDICTION MODELING AND EFFLUENT STORAGE IMPACT ON WATER QUALITY

4.1 Introduction

4.1.1 Background

The advents of alternative water resources have shown inherent possibilities in meeting world's increasing water demand (Gleick et al., 2000). Particularly greywater, which accounts for majority of domestic water usage, and therefore its acceptability as an alternative resource is increasing in urban settings (Karpiscak et al., 1990). From integrated water management perspectives, it needs information not only on quantity, depending on the need, but also on water quality for appropriately redirecting the raw/treated water for a particular reuse (Lazarova et al., 2001).

4.1.2 Contemporary flaws and barriers in greywater reuse

In the current trend, greywater is applied mostly for low-grade applications including restricted or unrestricted irrigation and toilet flushing (Li et al., 2009). Or sometimes it is contemplated for low-grade applications only (Eriksson et al., 2002), because of increasing concerns over public health and environmental safety with greywater reuse (Gulyas et al., 2007).

The primary barriers associated in greywater water reuse are the uncertainty in influent/effluent quality and the selection of an appropriate robust treatment system to meet stringent water reuse regulations (Al-Jayyousi et al., 2003). The greywater varies

in its composition with the type of households' uses, time of the day, cosmetic and toiletry products use, along with personal habits of residents (Eriksson et al., 2002; Al-Jayyousi et al., 2003). Though it is referred to either bathroom, shower, laundry, kitchen or combination of them, the individual source characteristics vary significantly (Jefferson et al., 2004). For example, the water originating from laundry, shower or wash basin have high COD: BOD ratio than the kitchen greywater (Eriksson et al., 2009). The complexity in identifying the influent variability and selection of treatment system increases, where in some cases the kitchen water is considered as greywater (Gulyas et al., 2007), whereas others include only laundry, shower and wash basin as greywater (Nolde et al, 2007).

In fact, determining the greywater treatments and reuse strategies are challenging tasks (Jefferson et al., 2000) with variability in treatment as well as reuse standards. Many treatment technologies were applied in greywater treatment (Ghunmi et al., 2011) from a rudimentary low-cost (coarse filtration and chlorination) to an amalgamated membrane bioreactor. The most of the applied treatments and reuses are analogous to the domestic wastewater (Al-Jayyousi et al., 2003). It may be a probable reason for the greywater reuse standards being equivalent to conventional wastewater reuse scheme, which again intermittently vary with and within political boundaries (Gulyas et al., 2007; Pidou et al., 2007). Therefore, opting a generalized treatment plan may not be a feasible approach for greywater reuse.

There is a need to identify and opt for a treatment system unique to the influent type, which also needs to be guaranteed for its robustness in effluent quality.

Determining the robustness in treatment would play vital role, which should be addressed to direct the reclaimed water for a specific applications (Butler et al., 2005). It may further bridge the gap between the stringency of regulatory standards and greywater reuse with the overall impact on increasing acceptability in greywater reuse.

4.1.3 Improving potentials in greywater reuse

4.1.3.1 Greywater treatment system improvement

The fate of reclaimed water either as restricted or unrestricted uses depend on its characteristics (Jefferson et al., 2004). With technological and scientific advancements in water treatment processes, water quality can be enhanced to the desired quality. An advanced physical filtration system has high-quality effluent attainability (Ghunmi, et al., 2011), and therefore it may help in resolving the current limitations of greywater reuse. At the same time, multi-grade effluents are attainable by varying the extent of treatment for the same influent (De Koning, et al., 2008). So, the concept of multi-grade water reuse can be applied in meeting different type of water demands depending on user intention, which is either governed by the cost-quality optimizations, water reuse regulations or aesthetics.

4.1.3.2 Improvement in reliability of greywater treatment system

The major thrust to improve greywater reuse potential is to ensure that the water quality parameters of treated effluents are within an acceptable range. Water quality modeling is one of the widely applied approaches in virtual assessment of real-time process using deterministic, stochastic or data-driven approaches. However, the system evaluation becomes complex with conventional methods like deterministic or stochastic

approaches (Jain et al., 2007) due to non-linearity in water treatment processes (Lee et al., 2002). Also, consistent operational data acquisition for system evaluation is an expensive and time-consuming process.

Alternatively, a black box modeling approach like Artificial Neural Network (ANN) requires no description of the governing processes (Lewin et al., 2004). ANNs are adaptive, and non-linear programs (Obaidat et al, 1998). It relies on the pattern recognition from a set of the input and output data (Rodriguez et al, 1999). This is why, a data driven machine learning approach, like ANN, is widely applied in wastewater engineering to analyze the complex system behavior by prediction, forecasting, and process control (Gontarski et al., 2000). Hamed et al., (2004) developed ANN-based models for predicting Biochemical Oxidation Demand (BOD) and Suspended Solids (SS) for treated wastewater at Cairo, Egypt. Lee et al., (2011) also applied ANN models in predicting Biochemical Oxidation Demand (BOD), Chemical Oxygen Demand (COD), Total Nitrogen (TN), and Suspended Solids (SS) from a wastewater treatment plant effluent.

4.1.3.3 Addressing degradability of raw and treated greywater

Along with the mentioned barriers in greywater reuse, there is information lag on greywater quality transitions with storage time (Dixon et al., 2000) Though the storage is a critical aspect with changing demand/supply, most of the studies are limited to storage of raw greywater only (Liu et al., 2010). The degradability of treated water remains unidentified, and therefore an informative study on treated greywater-storage-potentials may provide its wider reuse possibilities.

4.2 Objectives

The case study demonstrates a comprehensive approach in improving greywater potential using a case study of an advanced greywater filtration system (GAC-MIME). The system is comprised of a continuous matrix of treatment units based on serial filtration. Water quality analysis for raw and GAC-MI-ME treated greywater and a subsequent water quality prediction modeling tool are presented in this study. A decision support tool (GREY-ANN) was also proposed for optimal treatment selection by providing robustness and reliability in greywater treatment. It also addressed fate of raw/treated greywater with storage time. The water quality parameters including turbidity, pH, BOD, and TDS considered as treatment performance indicators. The specific objectives of this Section are:

- I. Water quality evaluations for “GAC-MI-ME” effluents for the parameters including BOD, pH, ORP, TDS and turbidity.
- II. Develop modules for “GREY-ANN”, a tool for determining appropriate “GAC-MI-ME” treatment train for effluent quality parameters including; pH, ORP, TDS, turbidity, and BOD.
- III. Develop BOD₅ prediction model (BOD-ANN) using ANN for raw and GAC-MI-ME treated effluent from known water quality parameters including pH, ORP, TDS, and Turbidity on BOD.
- IV. Sensitivity analysis for GREY-ANN for potential improvement of GAC-MI-ME treatment system.

- V. Sensitivity analysis for BOD-MP model for the understanding of the parameters affecting BOD in raw and GAC-MI-ME treated greywater.
- VI. Analyze the impact of storage on raw and GAC-MI-ME treated greywater for water quality parameters including TDS, turbidity, pH, and DO.

4.3 Material and methods

4.3.1 Greywater treatment system description

The GAC-MI-ME, a greywater treatment system produces multi-grade effluent. The five different treatment stages of the GAC-MI-ME were considered for the system analysis including effluents at coarse filtration (CR-F), microfiltration (M-F), granular activated carbon (CF), ultrafiltration (UF), and at reverse osmosis (RO) as shown in Figure 4.1. The influent greywater was referred as *RAW*.

The matrix of treatments in GAC-MI-ME were subdivided in five different units corresponding to the effluent, where each stage of treatment considered as an independent unit. The Treatment-Train A represents CR-F effluent, which follows the filtration modules of 50, 20, 10, and five μm . The Treatment Train B represents M-F effluent, which includes filtration modules of 50, 20, 10, 5, 1, and 0.35 μm . The Treatment Train C represents CF effluent, which includes filtration modules of 50, 20, 10, 5, 1, 0.35 μm , and GAC. The Treatment Train D represents UF effluent, which includes filtration modules of 50, 20, 10, 5, 1, 0.35 μm , GAC, and UF (0.025 μm). The Treatment Train E represents RO effluent, which includes filtration modules of 50, 20, 10, 5, 1, 0.35 μm , GAC, and UF (0.025 μm) and RO unit.

4.3.2 Experimental setup

4.3.2.1 Greywater formulation, and GAC-MI-ME effluent sampling

Varying strength greywater was considered during the experiment with turbidity as a benchmark for strength determination. Over 130 batches of influent greywater were formulated using laundry shower wash basin and in some instance a synthetic greywater. The synthetic greywater was formulated to be similar to the chemical combination excluding the septic content as proposed by Hourlier et al., (2010), and is shown in

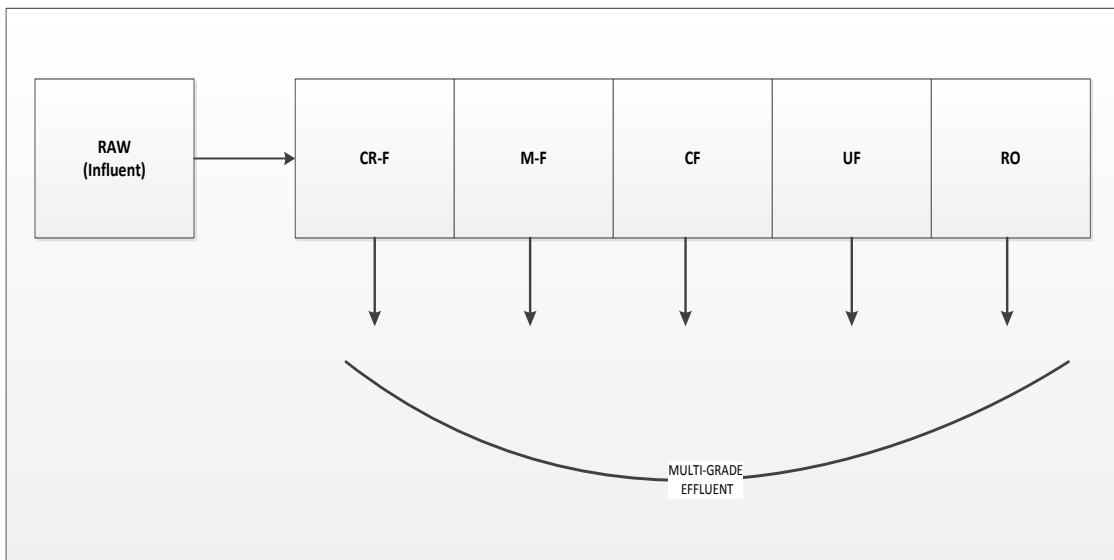


Figure 4.1 Effluent collection scheme from the GAC-MI-ME greywater treatment system where it shows five different effluents from the raw greywater

Appendix A.1. A random combination of the listed sources was used to create the multiple strength greywater with turbidity approximately ranging from 9 to 432 NTU.

Table 4.1 shows water quality variability measured in the experiments.

Batch experiments were conducted for each individually formulated greywater samples, and the corresponding effluent was collected at the five stages of GAC-MI-ME system (the concept proposed as the multi-grade effluent system). Figure 4.1 shows the sampling scheme for raw and GAC-MI-ME effluents.

4.3.3 Water quality analysis

The parameters addressed during the study for effluent quality characterization and system performance indicators were BOD₅ (Biochemical Oxidation Demand), turbidity, total dissolved solids (TDS), pH, and ORP, and dissolved oxygen (DO). *YSI proOBOD* sensor was used for DO and BOD₅ measurement. *YSI 6800XLM sonde* was used for pH assessment. Hanna Instruments *H3014* turbidity meter was used to measure turbidity (NTU) of the water samples. TDS probe (*HM Digital SP2*) was used to determine total dissolved solids in the samples. The experiments were conducted, and water quality data were analyzed at the Texas A&M University campus. The measurements accuracy for each of the instruments including turbidity-meter, pH/ORP probe, dissolved oxygen (DO) probe and TDS-meter are shown in Appendix B4.

The water quality database was developed for GAC-MI-ME effluents using the experimental results. All the data were set with outliers to avoid excessively high sample reading and to minimize over-fitting and erroneous prediction. The data outliers for pH, TDS, turbidity, ORP, DO, and BOD were (5-11), (1500) mg/l, (1500) NTU, (-500 TO + 500) mV, (15) mg/l, and (1500) mg/l respectively.

Table 4.1 Range of water quality parameters used in GREY-ANN model development

	Range of raw and GAC-ME-MI treated effluent used for GREY-ANN modeling					
Parameters	RAW	CR-F	MF	CF	UF	RO
Turbidity (NTU)	9.1 - 423	3 - 409	2.6 - 369	0.3-204	0.1 -5.3	0.1 -1.3
BIOD (mg/l)	8.4-259	5.1 - 236	1.4-185	0 -87	0 -34.2	0 -3.6
ORP (mV)	(-484) - (298)	(-407.2) - 256.5	(-414.85) - 315.3	(-381) - 312.7	(-290) - 355.2	(-151.2) -363.3
pH	5.9 - 9.2	5.92-9.93	6.05 -8.95	6.31- 9.17	6.53 - 9.02	6.37 - 8.74
TDS (mg/l)	112 - 995	78 -902	71 -878	65 -800	65-707	10 -112

4.3.3.1 Experiments on storage impact on raw and treated greywater

The storage tests were conducted for eight sets of GAC-MI-ME effluents, where each set represented the different stages as Raw, CR-F, MF, C-F, UF, and RO water.

All the samples were stored in clean plastic bottles and kept at room temperature (21 to 23° C). The impact on storage was determined for the following water quality parameters: turbidity, pH, DO, and TDS. The water quality transitions in raw and

treated greywater samples were logged at intervals of 1st, 2nd, 4th, 9th, 12th, and 15th days.

4.3.4 Model development

The decision support tool GREY-ANN is proposed in the study with the objective of determining optimal greywater treatments required to meet desired effluent standards for its reuse. Artificial Neural Network (ANN) was applied as black box modeling tool in effluent quality prediction and verified with experimental data. The GREY-ANN is comprised of five unit models, which are 1) BOD-ANN, 2) TDS-ANN, 3) TURBIDITY-ANN, 4) PH-ANN, and 5) ORP-ANN, where each unit acts as a prediction tool for the corresponding water quality parameters. The unit models were further sub-divided into five sub-models; each represents the five stages of treatment train as Treatment Train A, Treatment Train B, Treatment Train C, Treatment Train D, and Treatment Train E.

Figure 4.2 shows the flow diagram of the unit model as an element of the GREY-ANN. It represents a decision support tool for selection of appropriate treatment train for achieving a user-defined treatment goal. A total of 25 sub-models were developed, and each functions independently for a given greywater influent quality.

A multi-parameter BOD-MP model was also developed as a supportive tool for GREY-ANN. The model predicts BOD₅ values from known values of TDS, turbidity, pH, and ORP. The water quality database from the batch experiments were used

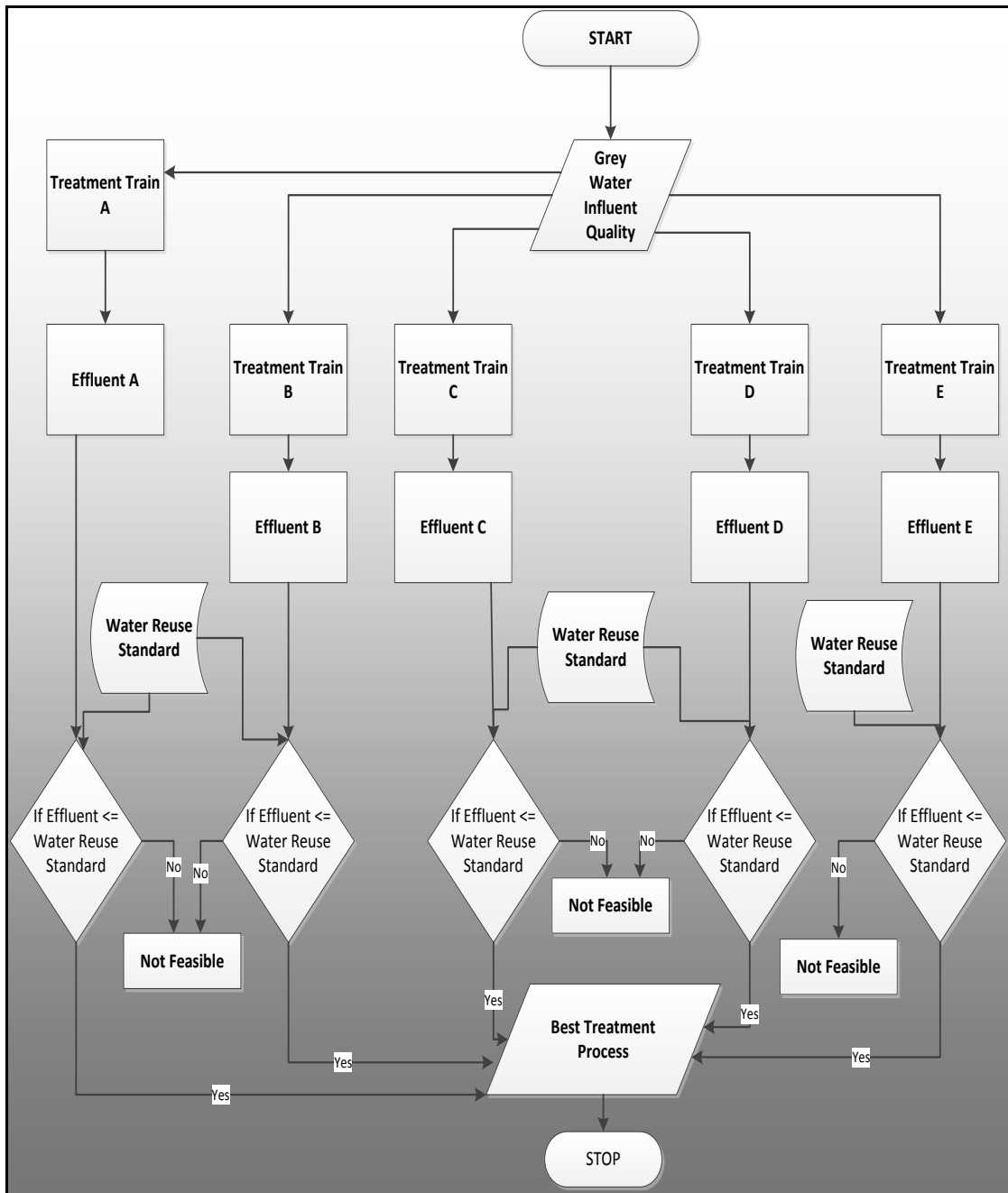


Figure 4.2 Unit model flow diagram of GREY-ANN

for the model development, where a data-driven approach using ANN was applied in water quality prediction modeling.

4.3.5 ANN application in model development

The concept of the artificial neural network was applied in developing the water quality prediction models using Neuro Solutions 6 (2008) platform. The model development flowchart is shown in Figure 4.3. The data were preprocessed before building the prediction models. All the data rows were randomized to adapt variability in observations rather than capturing a consistent pattern. Missing data points were substituted with the mean values, and erratic data (beyond the data outliers) were replaced either with the minimum and maximum value depending on its proximity to either of the values.

The ANN model development consisted of partitioning the observed data into training, cross-validation (CV) and testing data sets. The datasets were partitioned for ANN model development with 70 % of the data for training, 15% data for validation, and 15% data for testing. However, several other combinations of training, CV, and testing data with the ratio of 65:15:20, 60:20:20, and 60:25:15 were also evaluated.

Several ANN architectures were trained cross-validated and tested in the process of model development, which included probabilistic neural network (PNN), generalized feedforward (GFF), multilayer preceptor (MLP), time-delayed neural network (TDNN), and radial biased function (RBF). The training determines model architecture based on the observed input/output relation. The networks were trained and cross-validated with several epochs to minimize the error in predicted and observed values. The cross-

validation determines the accuracy of the trained network using CV data, and the training stops at a minimum validation error. Several optimized ANN architectures were applied to the test data (which were not used for training and cross-validation). Their performance was evaluated in terms of MSE, MAE, and correlation r for given input and model predicted output. The optimized ANN model architectures with the highest performance *i.e.* least MAE values were considered as the final models.

The performance parameters MSE and MAE are defined in Equations 4.1 and 4.2 respectively. The Mean square is defined as the average of the square of the errors (both positive and the negative error), and the mean absolute error (MAE) is defined as the average of the errors (both positive and negative error).

$$\text{MSE} = 1/n \sum_{i=0}^n |p_i - y_i|^2 \quad (4.1)$$

$$\text{MAE} = 1/n \sum_{i=0}^n |p_i - y_i| \quad (4.2)$$

Where: p_i is the model predicted value

And, y_i is the observed value

The procedures were applied to both the GREY-ANN unit models as well as the BOD-MP model development. The models presented in the study correspond to the best

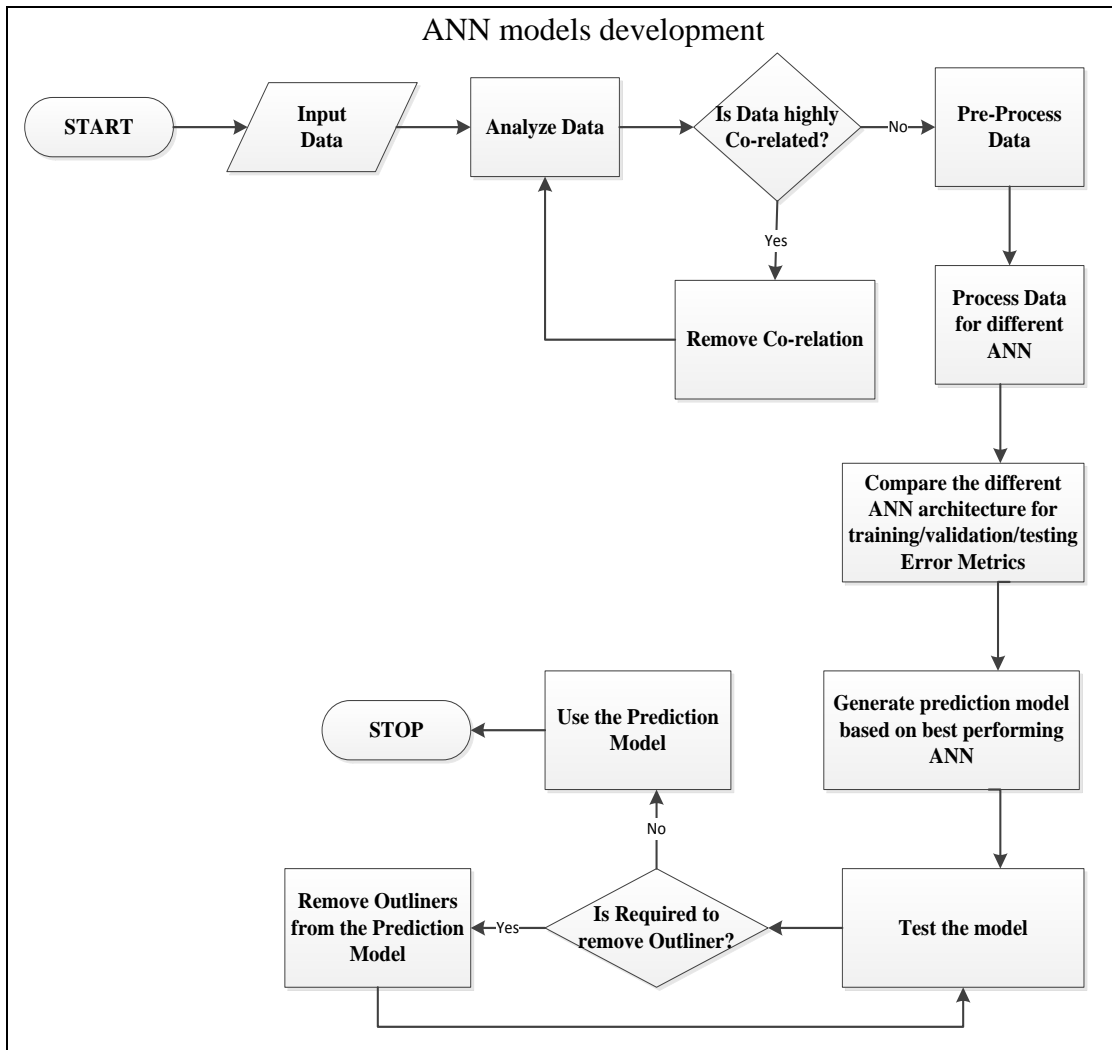


Figure 4.3 The flowchart defining the steps applied in ANN model development

performing ANN architectures in predicting the effluent quality of the GAC-MI-ME system. An additional validation was added to the predicted values to ensure that it resided within the expected range so that the model did not predict values out of range.

The study also included a sensitivity analysis for the developed models. Two different cases of sensitivity analysis were performed for GREY-ANN unit models and BOD-MP model respectively. The model output sensitivity was determined using Neuro

Solutions6 (2008) platform, where the input was varied about its mean by a fixed number of *stdev* (1) for 50 steps by keeping other input parameters fixed (Kamari, 2015).

The sensitivity about the mean was determined for water quality parameters at Treatment Train D (UF effluent) and Treatment Train E (RO effluent) with the intent of determining the impact of the pre-filtration on RO and UF membrane. The same procedure was applied for BOD-MP model sensitivity analysis.

4.4 Results & discussions

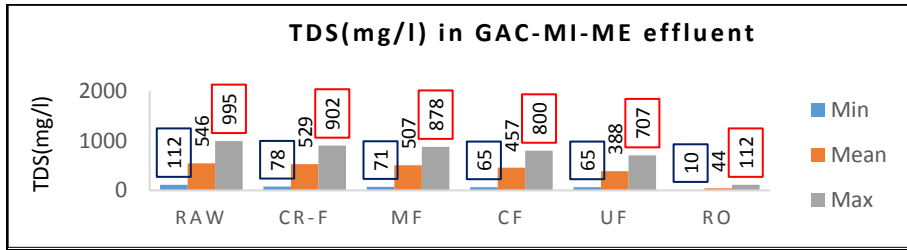
The results have been illustrated in four different sections: 1) raw and GAC-MI-ME effluents analysis, 2) GREY-ANN Unit-Models [BOD-ANN, TDS-ANN, TURBIDITY-ANN, PH-ANN, and ORP-ANN.] performance evaluation and model sensitivity analysis, 3) the multi-parameter BOD-MP model analysis, and 4) storage impacts of raw and GAC-MI-ME treated effluent.

4.4.1 Raw and GAC-MI-ME treated effluent characteristics:

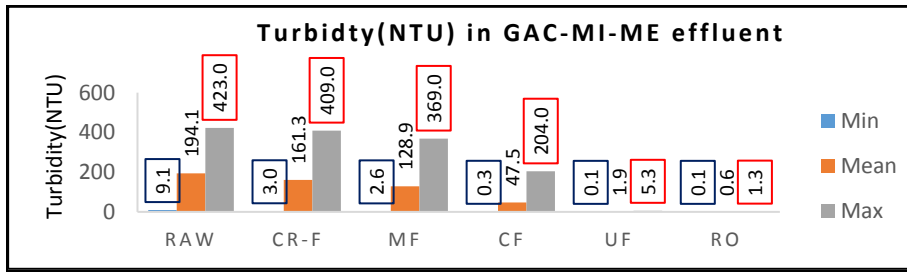
The raw and GAC-MI-ME treated greywater showed wide variability in water quality parameters (TDS, Turbidity, pH, ORP, and BOD) as shown in Figure 4.4. Regarding turbidity, the GAC-MI-ME treated effluents at RO and UF show significant turbidity reduction. The GAC along with CR-F and MF played a vital role as pre-filtration for UF and RO modules. The average turbidity reduction observed at GAC module was about 75%, where the individual contribution of GAC was 42%, and CR-F and MF contribution was 33%. The RO and UF effluent showed the turbidity range between 0.11 to 5.23NTU and 0.1 to 1.17 NTU respectively, whereas the raw greywater turbidity ranged from 9.13 to 423 NTU.

However, for the TDS removal, CR-F, MF, and GAC filtration only accounted for 16.3 % average reduction. Along with that, the UF membrane module only accounted for 12.6 % reduction. The RO module was responsible for a majority of TDS removal with the overall GAC-MI-ME terminal efficiency of 92 %. The observed TDS at UF and RO module ranged between 65 to 770, and 10 to 112 mg/l respectively compared to the raw influent range of 112 to 995 mg/l. It shows that RO is a critical part of GAC-MI-ME in dissolved solids removal.

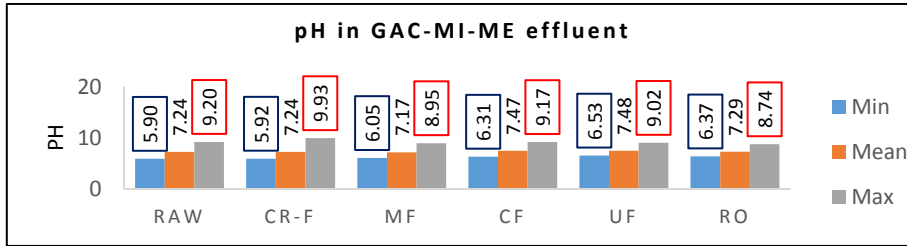
The BOD₅ values also showed wide variability in treated effluents. The GAC-MI-ME average terminal efficiency for BOD₅ removal was 99% , with the highest contribution from GAC module of about 46% average. Though the raw greywater showed BOD₅ range of 8.4 to 259 mg/l, the treated effluent at GAC, UF, and RO modules were between 0 to 34, 0 to 34, and 0 to 3.6 mg/l respectively. Comparing the pH in the effluents of GAC-MI-ME, the average value of pH does not show much variation. The average pH ranged from 7.2 to 7.5 in all the effluents. However, the raw and CR-F effluent showed a broad spectrum of the pH variation from 5.9 to 9.2 and 5.9 to 9.3, respectively. The UF and RO showed minimum pH above 6.5 (more suitable for reuse). Along with that, the ORP values also showed a consistent increase from negative to a positive potential and highest in RO effluent. The ORP signified the steady improvement in effluent quality along the treatment matrix of the GAC-MI-ME system, with improving oxidizing potential (Wareham et al., 1993).



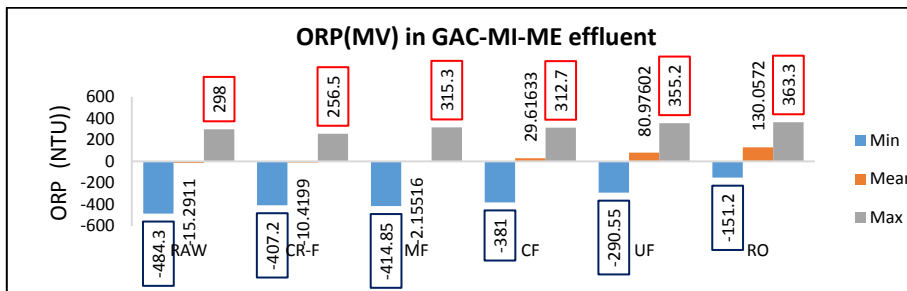
A



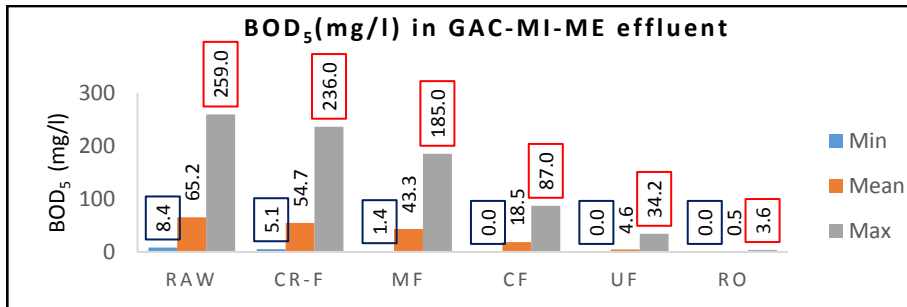
B



C



D



E

Figure 4.4 Water quality variability in raw greywater and GAC-MI-ME treated effluents

The variability in raw/treated greywater quality decreased along the treatment matrix of GAC-MI-ME. However, the stringency of water reuse regulations may not allow the selected treatment train due to the range of variability where upper limit exceeds the permissible limits. For example, the maximum limit of BOD₅ according to Asano et al.,(2007) US regulation for unrestricted and restricted urban reuse are 2 and 30 mg/l respectively. The GAC effluent of GAC-MI-ME system may not be applied, as the upper range of BOD₅ for the treated effluent (87 mg/l) exceeds the unrestricted water reuse criteria.

However, the average BOD₅ observed at the treatment train was 18mg/l, which is lower than the restricted uses. Therefore addressing the influent, effluent variability along with an appropriate treatment system selection becomes a critical task to improve water reuse potential.

4.4.2 GREY-ANN

The section demonstrates the performance evaluation of the 5 unit models of GREY-ANN including TURBIDITY-ANN, PH-ANN, ORP-ANN, BOD-ANN, and TDS-ANN, where each unit model corresponds to turbidity, pH, ORP, and BOD₅, TDS prediction at five different stages of GAC-MI-ME systems as described in section 4.3. A total of 25 sub-models were developed following the procedures in section 4.3, where optimal network selection for prediction models is based on minimum error attenuation at training, cross-validation, and testing data sets. Appendix A2 shows comparative.

Table 4.2 GREY-ANN unit models performance evaluation with best ANN architecture

GREY-ANN	ANN Model	MAE
BOD-ANN		
CR-F	MLP-PCA	8.49
MF	PNN	6.52
C-F	RBF	5.55
UF	PNN	2.84
RO	MLP	0.28
TURBIDITY-ANN		
CR-F	LR	21.69
MF	TDNN	14.01
C-F	TLRN	12.43
UF	TDNN	0.62
RO	TDNN	0.05
ORP-ANN		
CR-F	PNN	56.60
MF	MLP	32.83
C-F	PNN	41.37
UF	MLP	51.50
RO	GFF	41.74
PH-ANN		
CR-F	RBF	0.18
MF	MLP	0.11
C-F	MLP	0.28
UF	RN	0.13
RO	MLP	0.24
TDS-ANN		
CR-F	MLP	11.25
MF	MLP	19.00
C-F	MLP	34.74
UF	MLP	36.70
RO	TDNN	6.84

performance matrices of the best two ANN architectures for the training, CV, and testing data.

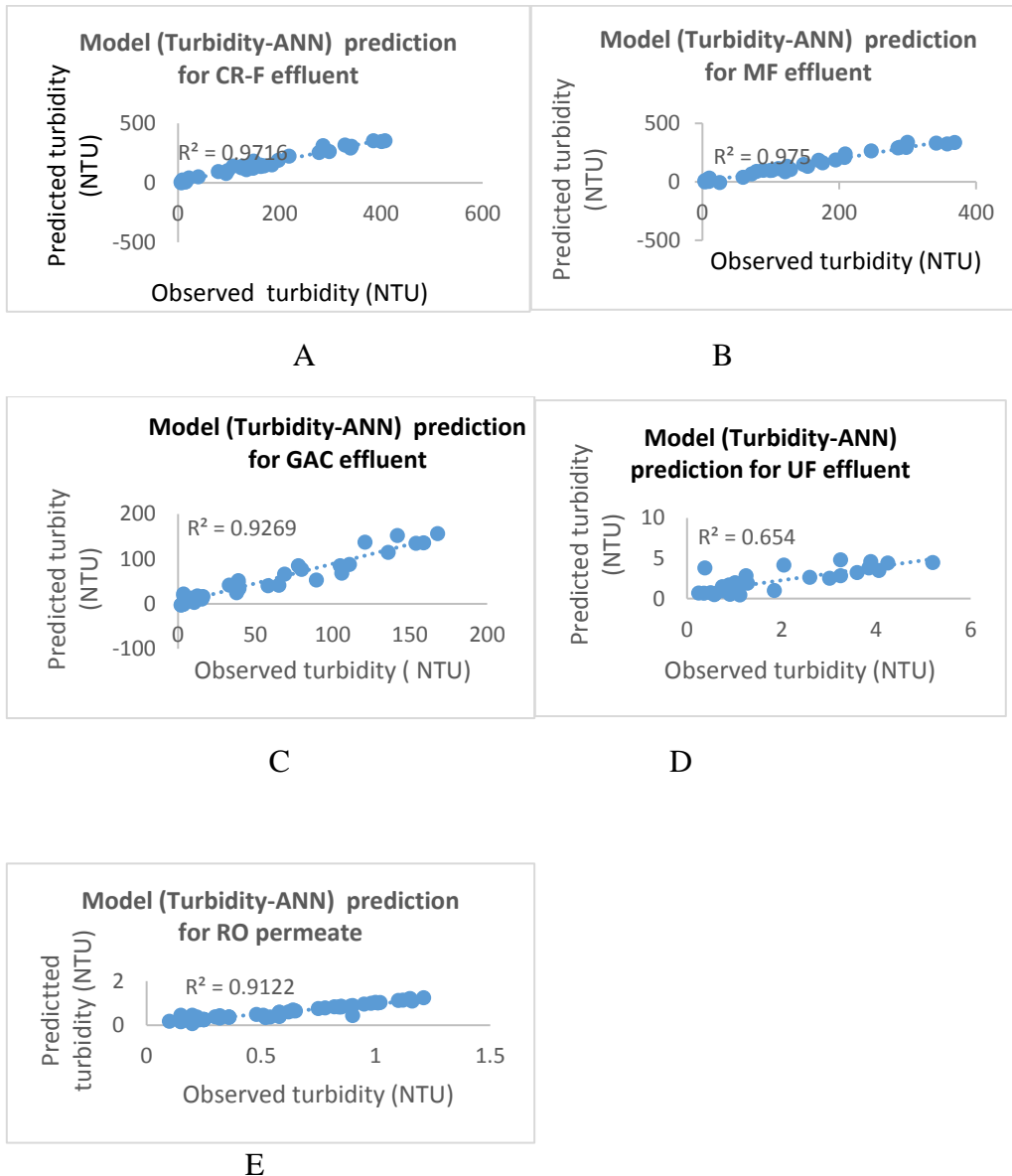


Figure 4.5 The model (Turbidity –ANN) performance in predicting the turbidity values (NTU) for CR-F (A), MF (B), and GAC (C), UF (D), and RO (E) effluents of GAC-MI-ME system

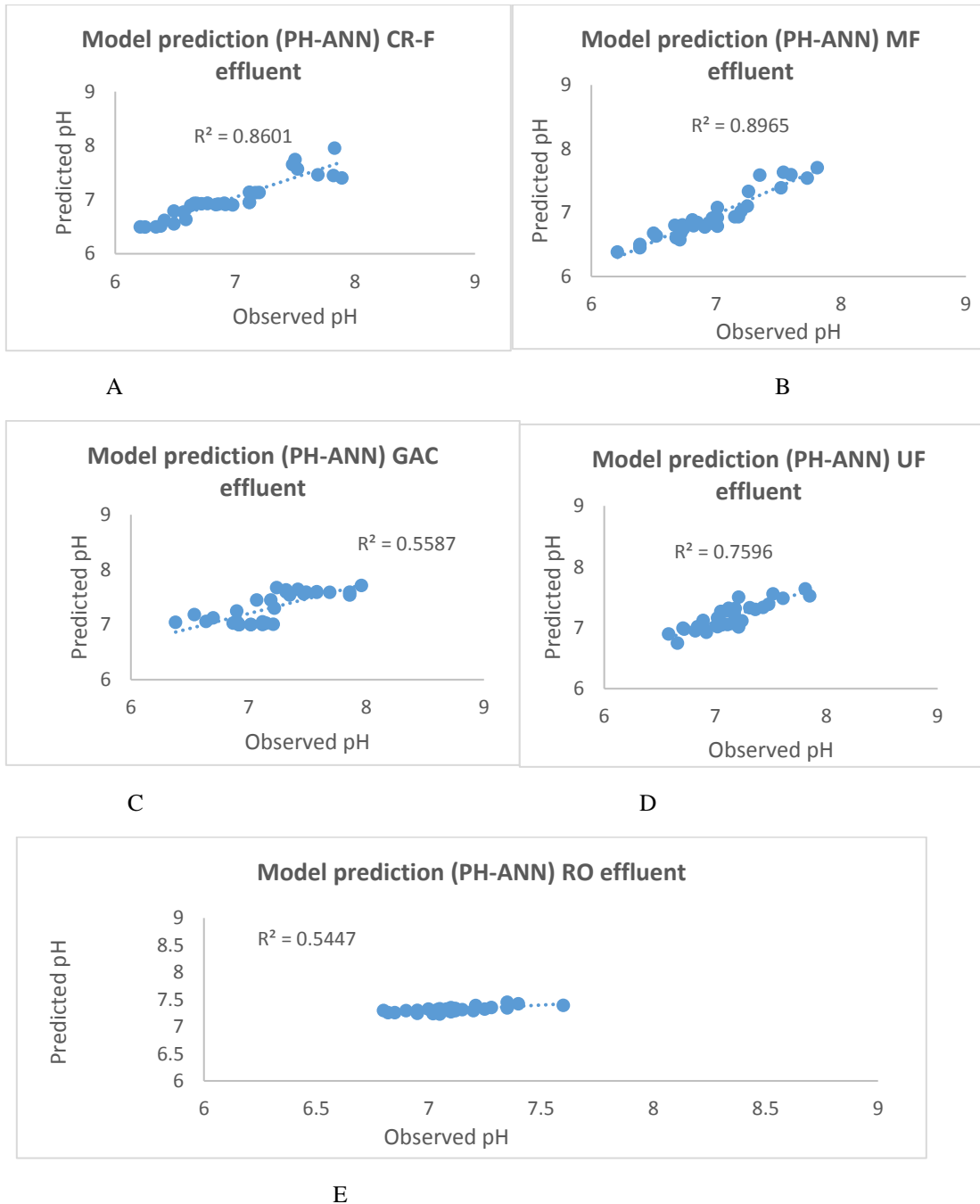
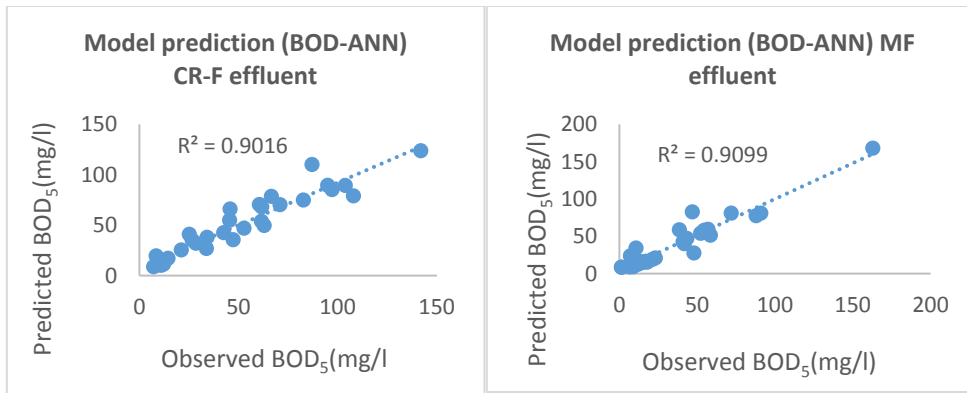


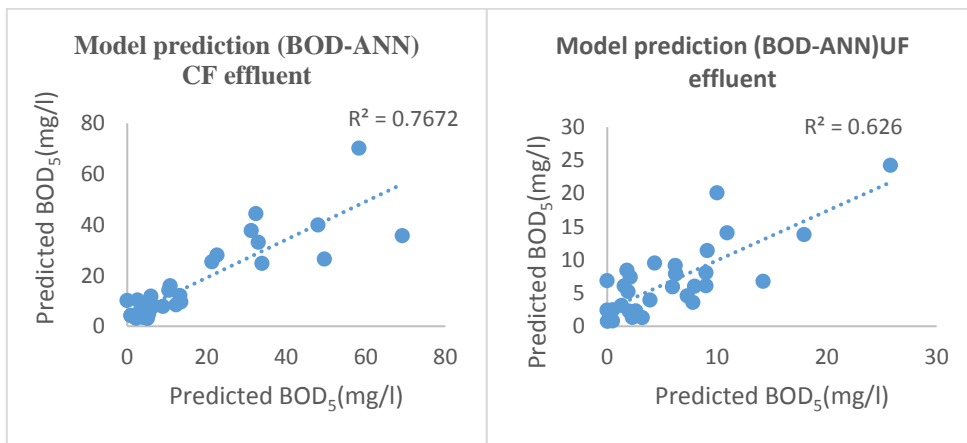
Figure 4.6 The model (PH –ANN) performance in predicting the pH values (NTU) for CR-F (A), MF (B), and GAC (C), UF (D), and RO (E) effluents of GAC-MI-ME system

The best performing networks based on least MAE criteria were appraised as the GREY-ANN unit-models. Table 4.2 shows the correspond ANN networks adapted to the unit models. Figures 4.5, 4.6, 4.7,4.8, and 4.9 shows GREY-ANN unit-models performance evaluations. It was validated using the test data, which were not part of the model development process and therefore represents unbiased results. Figure 4.8 represents TDS-ANN, where the correlations between observed and the model predicted values were made for CR-F, MF, GAC, UF, and RO effluents and corresponding R^2 values were observed as 0.99, 0.97, 0.91, 0.85, and 0.66 respectively. Although weak correlations were observed for RO effluent, the corresponding MAE values were 0.23. Figure 4.5 represents TURBIDITY-ANN, where the R^2 values were observed as 0.97. 0.98. 0.93. 0.65, and 0.91 for the corresponding effluents of the GAC-M-ME systems. In this case, most of the sub-models showed high performance in terms of coefficient of determination except for the UF, where R^2 was 0.71. In the case of ORP-ANN the R^2 values exceeded the 0.9 values in all the prediction sub-models.



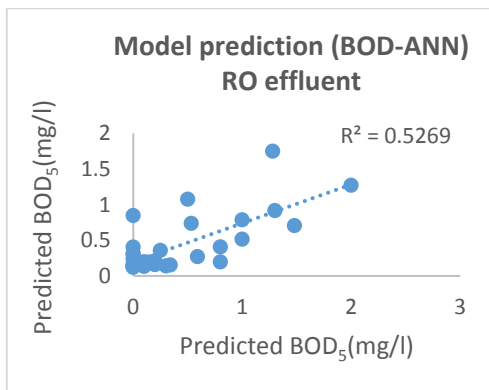
A

B



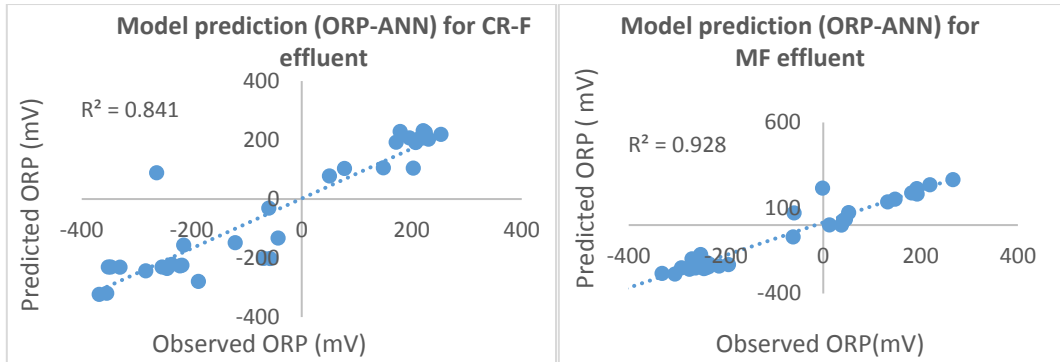
C

D



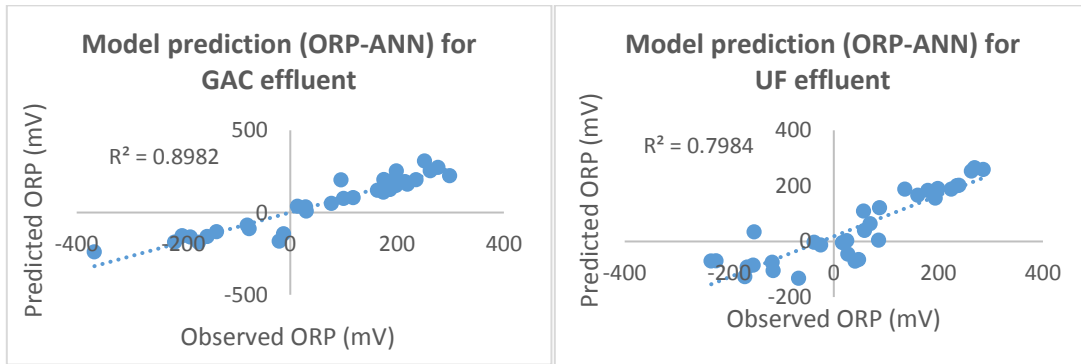
E

Figure 4.7 The model (BOD –ANN) performance in predicting the BOD₅(mg/l) values (NTU) for CR-F (A), MF (B), and GAC (C), UF (D), and RO (E) effluents of GAC-MI-ME system



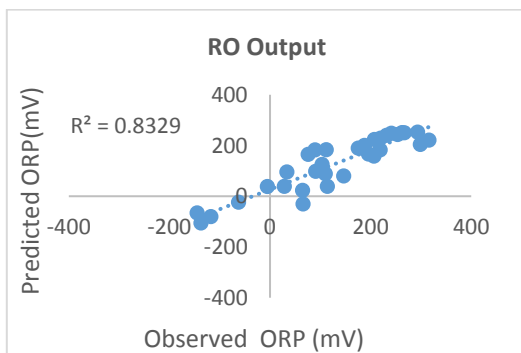
A

B



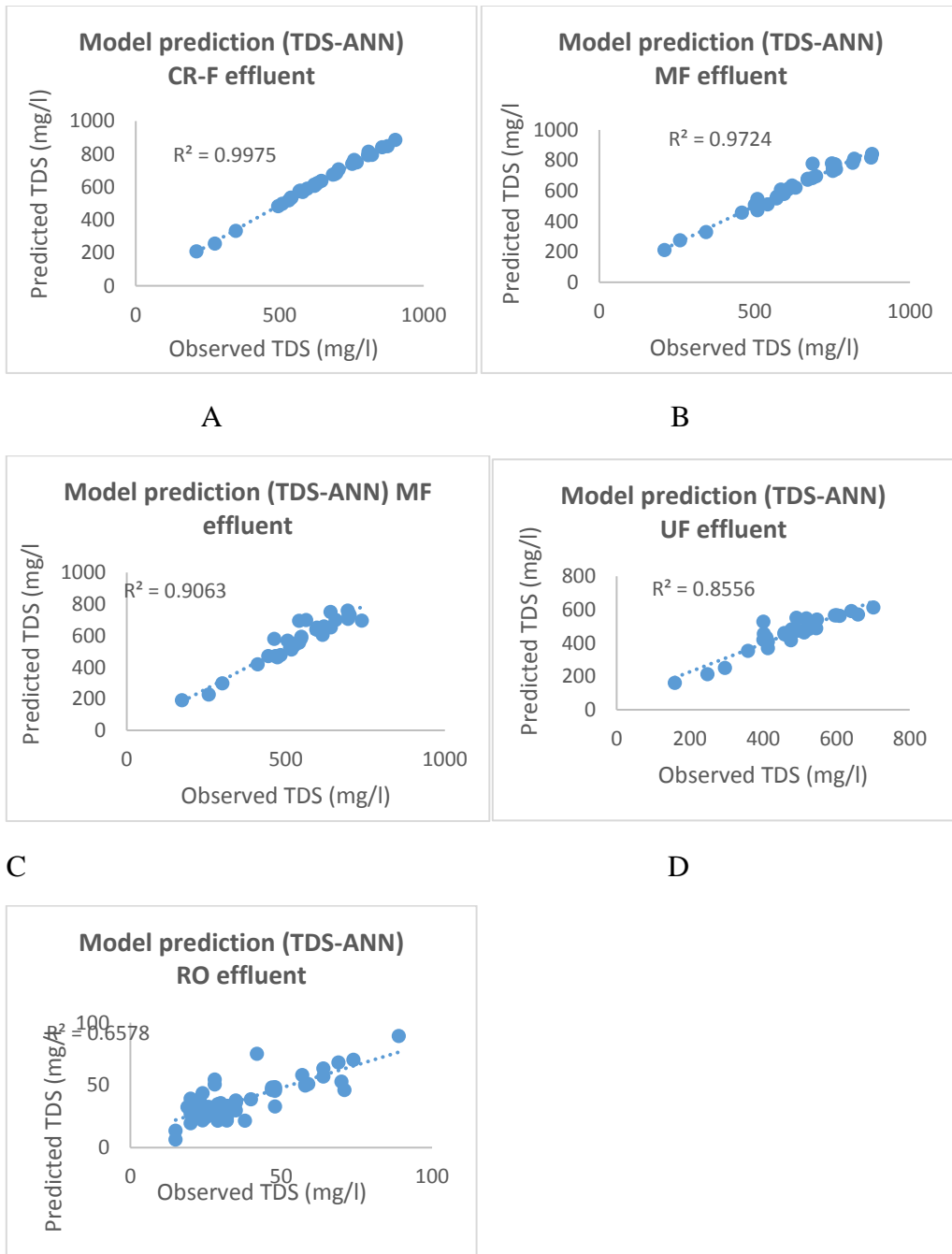
C

D



E

Figure 4.8 The model (ORP –ANN) performance in predicting the ORP values (mV) for CR-F (A), MF (B), and GAC (C), UF (D), and RO (E) effluents of GAC-MI-ME system



E
 Figure 4.9 The model (TDS –ANN) performance in predicting the TDS(mg/l) values for CR-F (A), MF (B), and GAC (C), UF (D), and RO (E) effluents of GAC-MI-ME system

the PH-ANN showed prediction performance with R^2 values under 0.7 for GAC and RO effluent with MAE of 0.28 and 0.23 respectively. At the same time, the BOD – ANN performance observed with R^2 under 0.7 and MAE of 2.8 and 0.27 for UF and RO effluent respectively.

Overall, the GREY-ANN unit-models showed high correlations between the observed and model predicted values. The decreasing trend of MAE from coarse filtration to RO signifies improving water quality along the treatment trains of the GAC-MI-MGE system. The sub-models with predictive performance of R^2 less than 0.7 were attributed mostly to the UF and RO effluent, which depends on the variability of other effluent. However the small MAE for the parameters at UF, RO, shows that the modules can be used for modeling.

Sensitivity analysis was performed for UF and RO effluents, for determining the impact of raw greywater and GAC-MI-ME effluent on the treatment. For UF effluent, the quality was considered at CR-F, MF, and C-F, and for RO effluent, CR-F, MF, and C-F, and UF were used to determine the variability of the specific water quality parameter (in this case TDS, Turbidity, pH, ORP, and BOD). UF and RO effluent sensitivity to other treatment stages (GAC, MF, and CR-F) determine the parameter if the variation in either of the effluent affects the RO water quality. Figure 4.10 and Figure 4.11 show the sensitivity about the mean for all the water quality parameters to determine the impact on UF and RO effluent water quality, respectively. Turbidity at UF was influenced by turbidity variation in CR-F, whereas as the turbidity at RO shows almost equal weight to all the effluents, even though RO turbidity is below 1 NTU in most of the cases. The least

impact was raw greywater turbidity on RO and UF effluents turbidity. TDS showed highest sensitivity at C-F for both UF and RO effluent.

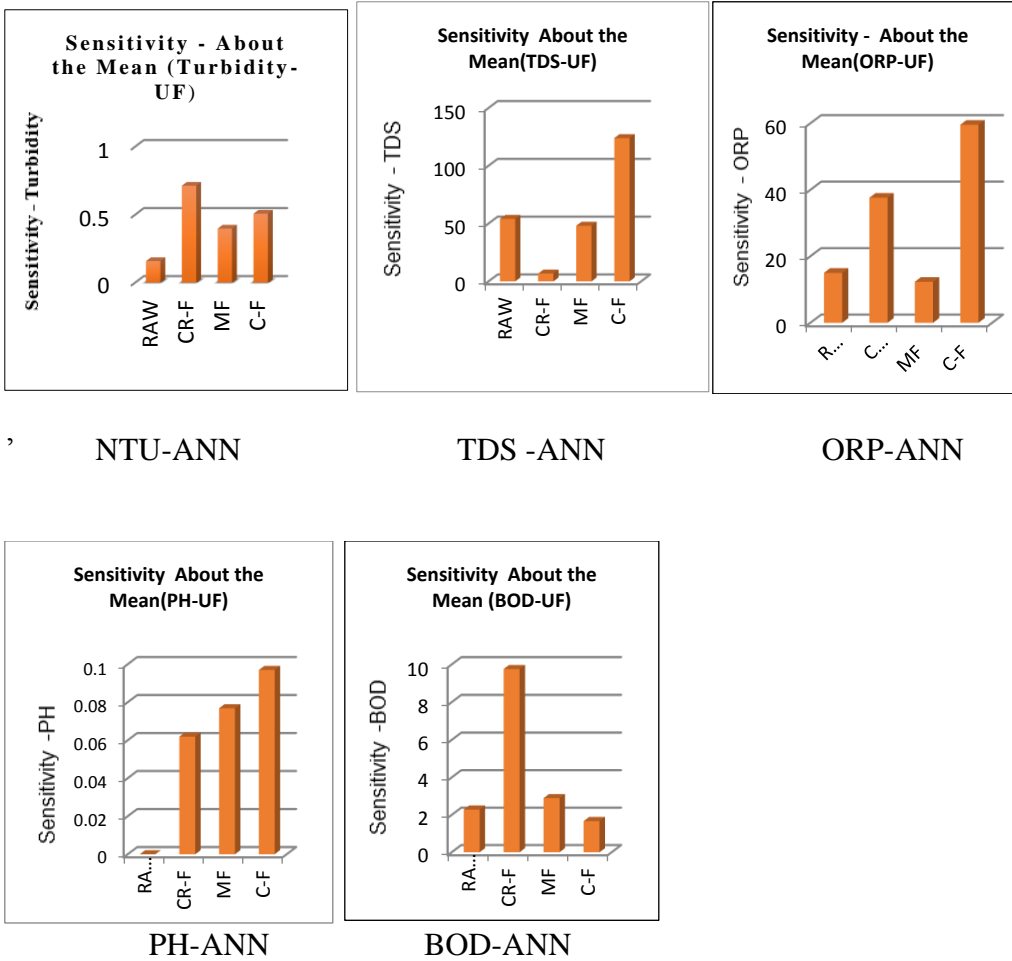


Figure 4.10 Sensitivity of GREY-ANN unit-models on UF effluents

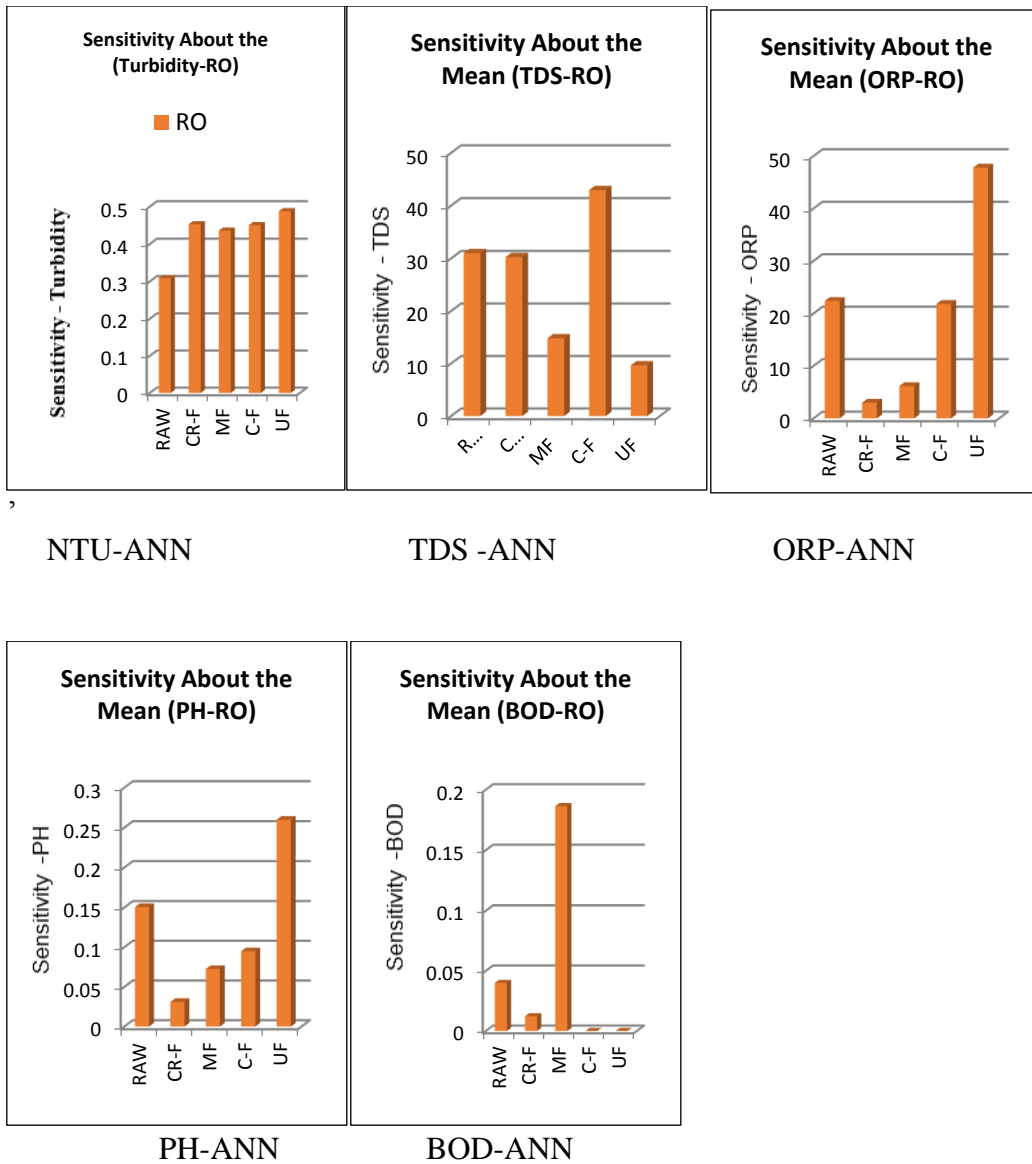


Figure 4.11 Sensitivity of GREY-ANN unit models on RO effluent

The pH and ORP showed highest sensitivity at C-F for UF. The UF effluent had the greatest impact on RO effluent. It has also been observed that the mean pH was greater in values at C-F and UF compared to raw greywater.

In a complex system such as GAC-MI-ME, where the influent quality variability along with variability in the treatment system affect the overall treatment load on the more expensive UF and RO membrane modules. The sensitivity analysis provides an understanding of load distributions and improvement potentials of the GAC-MI-ME system unique to the water quality parameters

4.4.3. BOD-MP model for predicting BOD

The multi-parameter BOD modeling was done using ANN algorithms. The corresponding input database was created for turbidity TDS, ORP, pH BOD. Outliners set between mean max values for the each of the parameters after removing the erratic or the missing data.

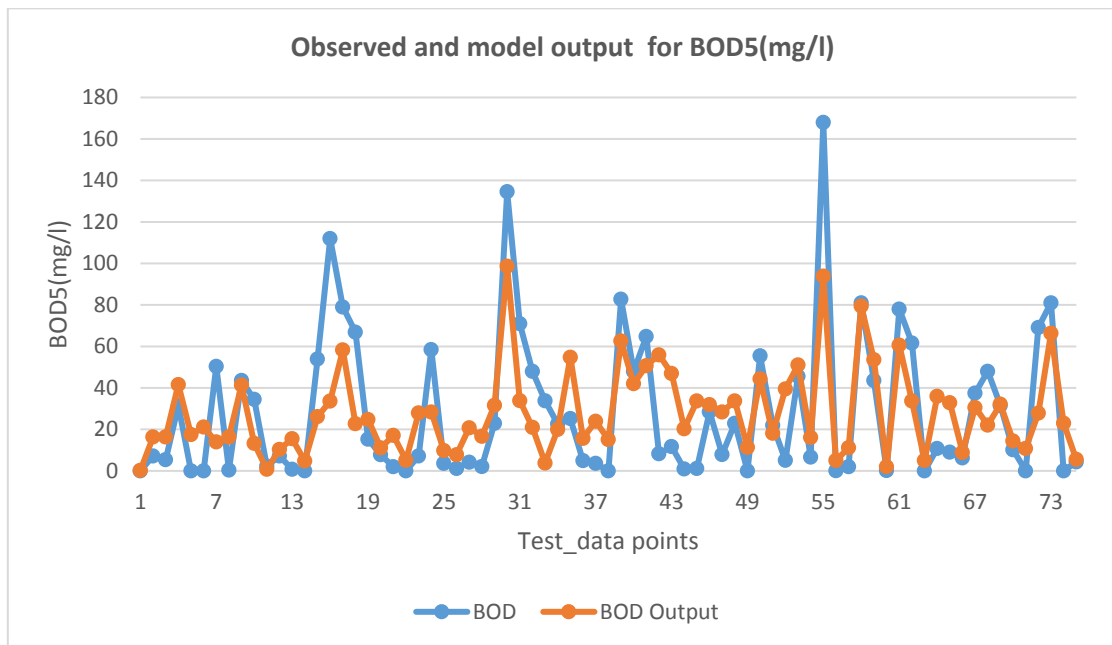


Figure 4.12 Comparison of the model simulated and observed BOD₅ values

The data were partitioned and in the best results were obtained at 60 % training and 20 % validation. The model trained through several ANN algorithms. The best performing neural network algorithm was applied to predict BOD values (Figure 4.12).

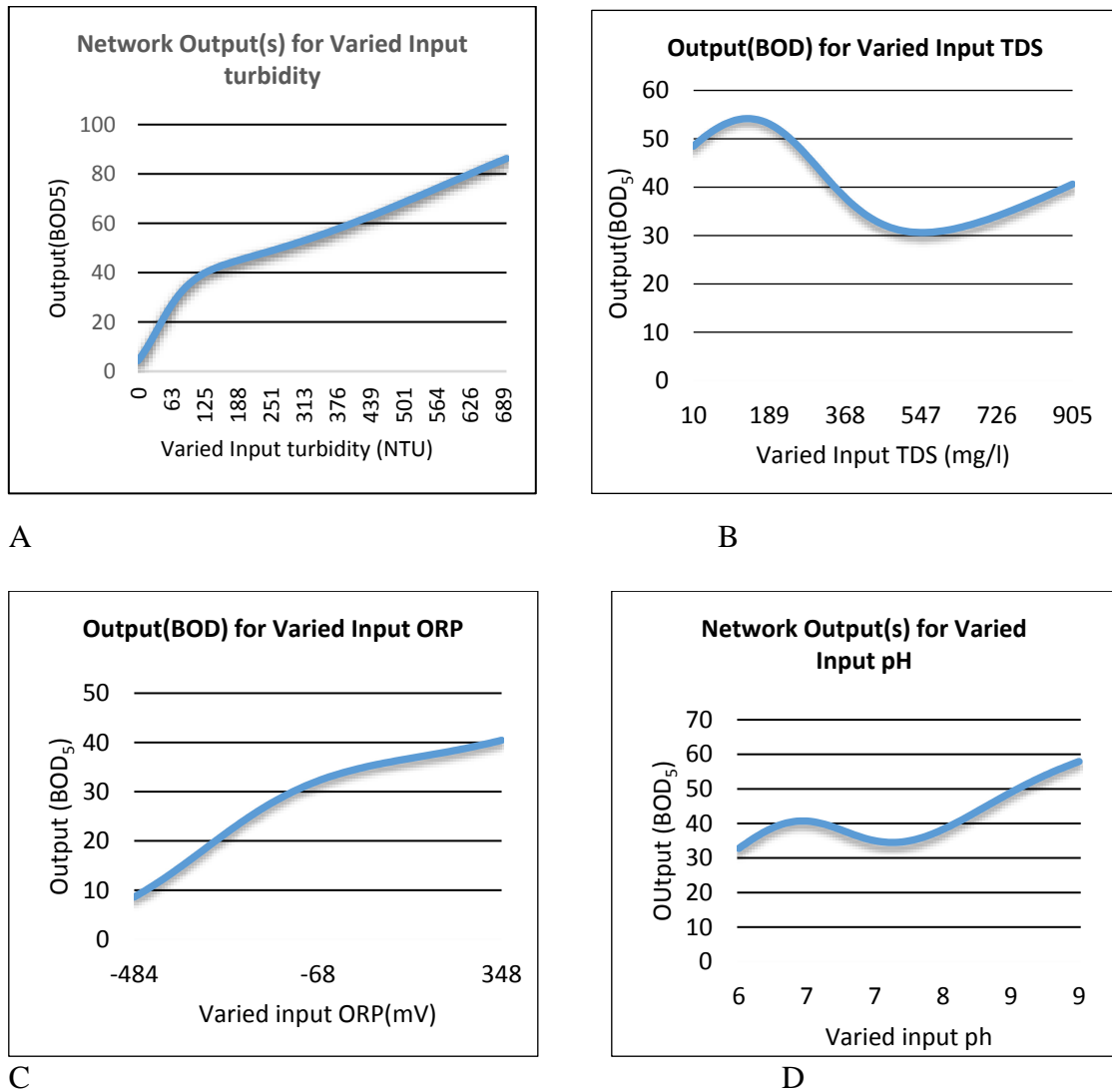


Figure 4.13 BOD (mg/l) variation in BOD-MP model with respect the independent parameters (A) turbidity (B) TDS(C) ORP and (D) pH

In this case, GFF algorithm was selected with MAE of 17 mg/l and correlation-r with (0.76) for test data. The major issues were observed with data input ranges for modeling. However, it is critical to note that the data used were varied for six different types of combination water (raw and GAC-MI-ME effluents). The primary reason for low correlation r was due to the several null values of RO and UF effluent making the data over fitted, and the model was unable to predict zero values. The error is similar to errors observed for BOD-ANN for RO and UV. Figure 4.13 shows the model prediction for a diverse input range of independent parameters.

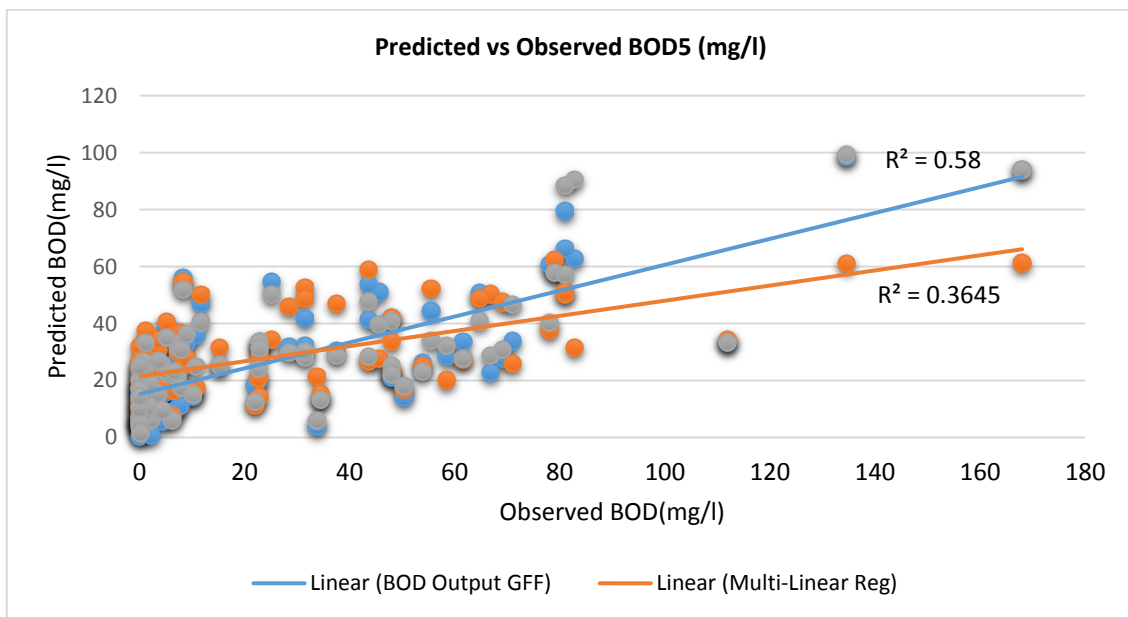


Figure 4.14 Comparison of GFF, and multilinear regression predictions for observed BOD

However, the corresponding data compared with the multiple linear regression, the coefficient of determination was equal to 0.36 as compared to 0.58 in GFF (Figure

4.14). Though, the ANN showed much better performance than the linear regression can be applied as with higher range of BOD₅

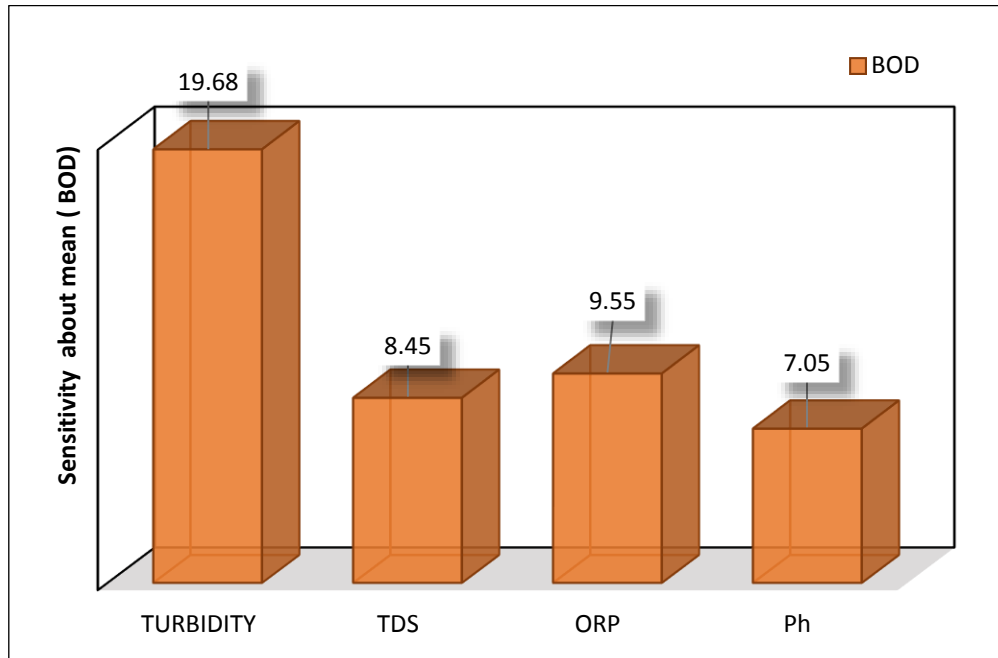


Figure 4.15 BOD sensitivity in BOD –MP model

4.4.3.1 Sensitivity analysis for BOD-MP model

The sensitivity about the mean of the BOD-MP model output (BOD₅) was determined to understand the input parameters (TDS, turbidity, pH, and ORP) influencing the BOD₅ in raw and treated greywater. The sensitivity analysis of the BOD-MP model (Figure 4.15) shows that the associated turbidity in greywater as the most sensitive parameter affecting BOD₅, which is similar to the results in GAC-MI-ME performance evaluation where GAC played a major role in turbidity as well as the BOD₅ removal. The

BOD₅ in greywater can be attributed to suspended and colloidal particles rather than dissolved substances.

4.4.4. The impact of storage on raw and “GAC-MI-ME” effluents:

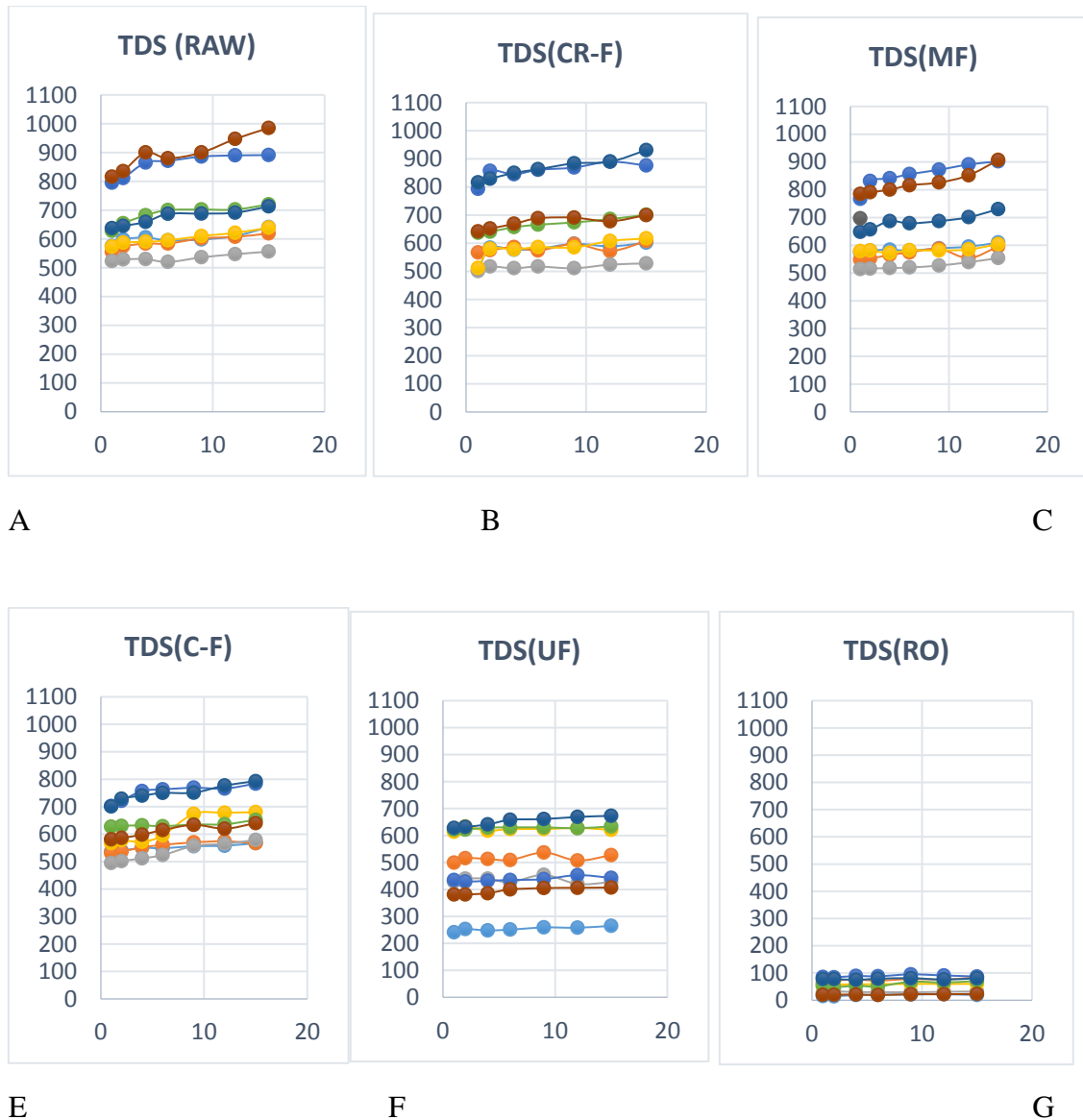


Figure 4.16 Change of TDS mg/l with storage time for raw greywater (A) and treated greywater (B, C, D, E and F) for coarse filtration (CF), microfiltration (MF), granular activated GAC), ultrafiltration (UF), and reverse osmosis (RO) respectively

Figures 4.16 to 4.19 show water quality parameter variations for the raw and GAC-MI-ME treated greywater over 15 days storage span. The corresponding statistics of the parameters variation is listed in Appendix A4.

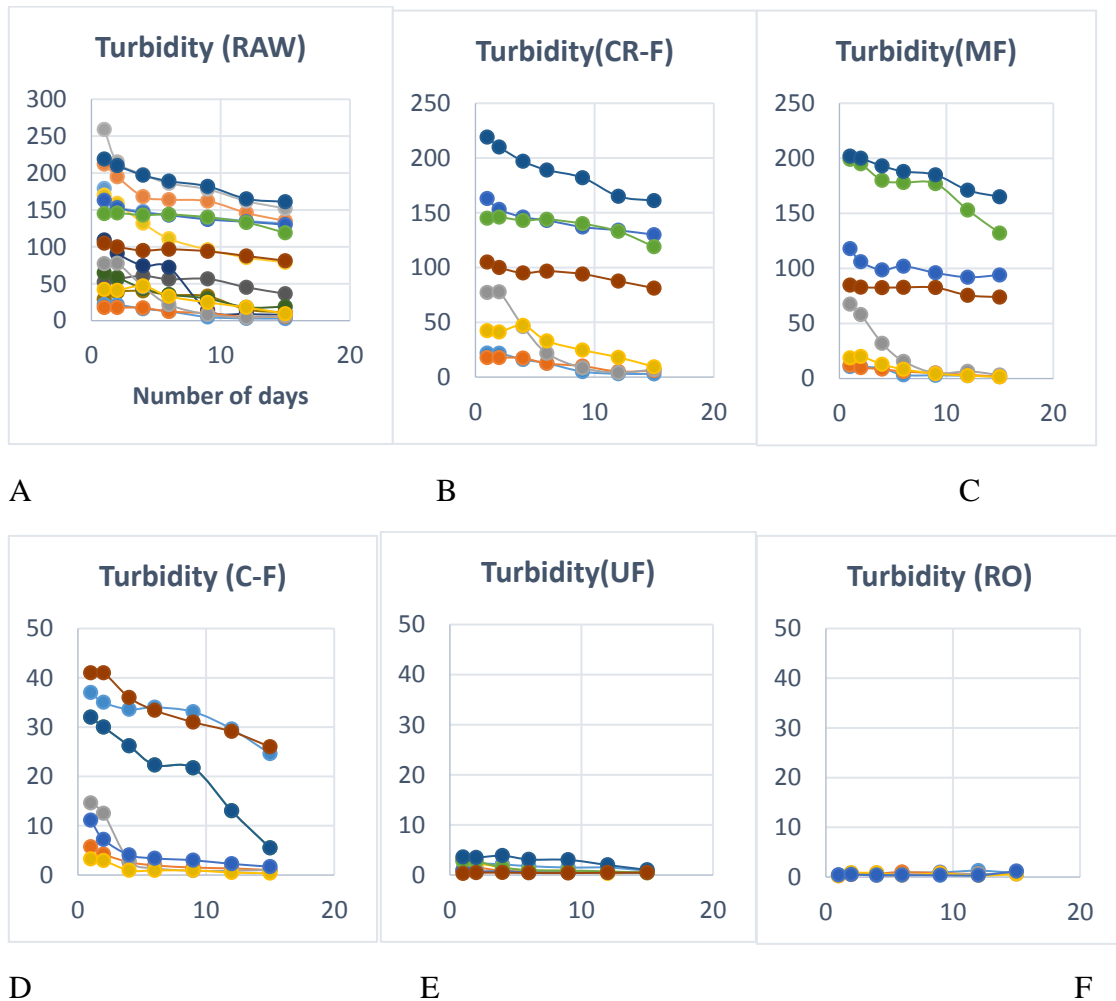


Figure 4.17 Change of turbidity (NTU) with storage time for raw greywater (A) and treated greywater (B, C, D, E, and F) for coarse filtration (CF), microfiltration (MF), granular activated GAC), ultrafiltration (UF), and reverse osmosis (RO), respectively

In raw greywater the average DO drastically changes from 6.1 to 1.6 mg/l in 24 hours and showed a further decrease during the rest of the period, reaching 1.3 mg/l on the 15th day. The pH, values kept dropping down for the entire monitoring period and

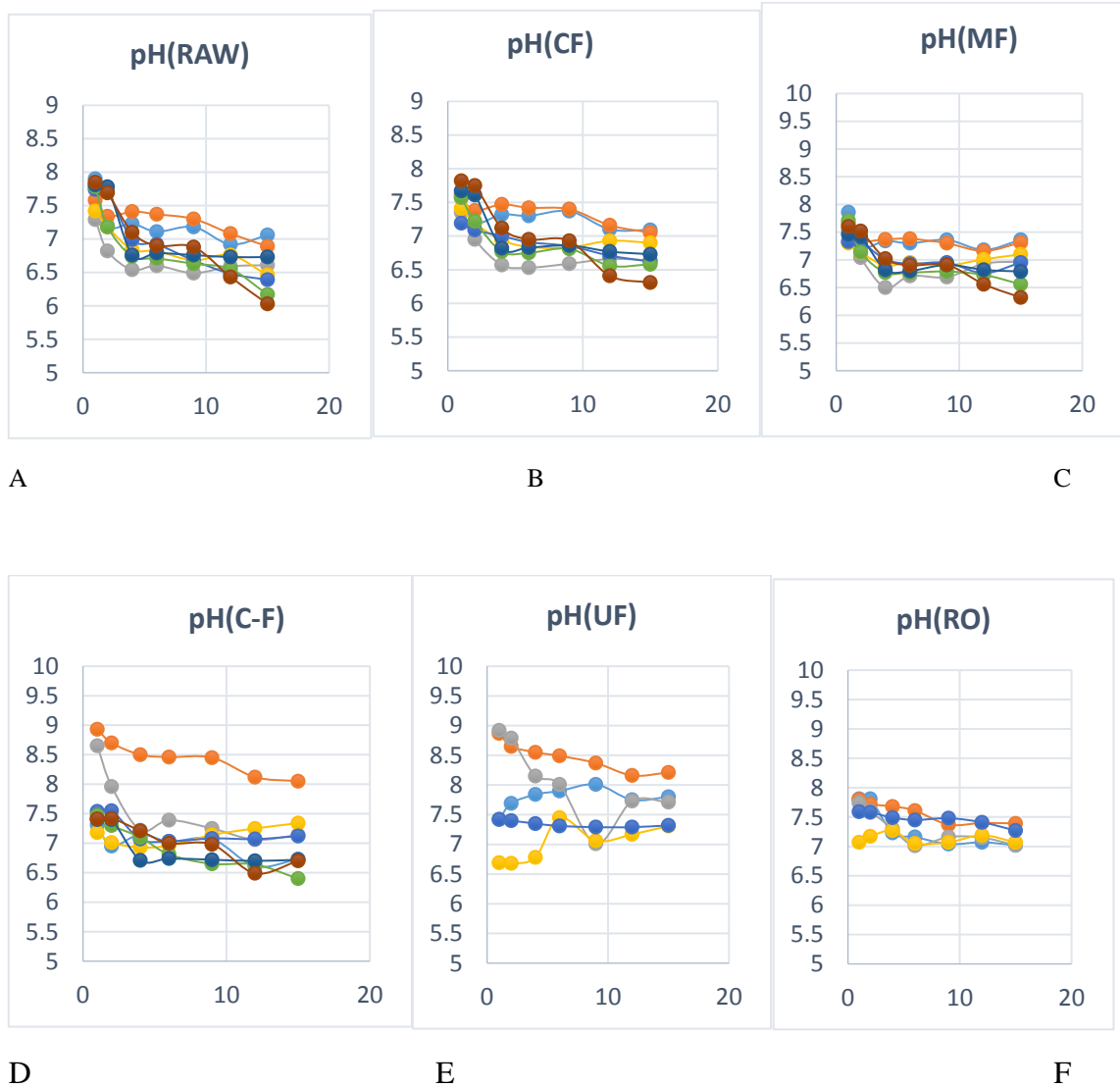


Figure 4.18 Change of pH with storage time for raw greywater (A) and treated greywater (B, C, D, E, and F) for coarse filtration (CF), microfiltration (MF), granular activated GAC), ultrafiltration (UF), and reverse osmosis (RO), respectively

reached 6.5 on the 15th day. However, some of the samples showed pH less than 6.5 as shown in Figure (4.11). The mean turbidity went down from 134 to 71.6 NTU for the storage period span (15 days). The average TDS showed a consistent increase and ranged from 637.8 to 720.5 mg/l. Overall the water quality degrades very quickly for the raw greywater and tends to be acidic over a period of 15 days.

The CR-F effluent showed a similar drift. The DO values came down to from 7.2 to 2.4 in 24 hours. It reached 1.6 mg/l in 4days and almost remained constant during the remaining days at 1.6 mg/l. The pH, values showed a decrease from 7.5 to 6.7 between the 1st and 15th day of observation. The mean turbidity decreased from 98.9 to 64.5 NTU. The TDS values showed marginal increase from 621.6 to 695.4 NTU.

For MF effluent the mean DO changed from 7.2 to 3.2 mg/l in 24 hours, which was comparatively higher than the Raw and CR-F effluents. However, within 15 days span dropped to 1.2 mg/l. The average pH fell from 7.6 to 6.9. Mean turbidity went down from 89.2 to 59.1 NTU. The TDS showed an increasing trend from 6328.9 to 699.9mg/l.

The C-F effluent showed better stability than the MF and CR-effluents. The DO values showed decrease down to 4.3 mg/l in 24 hours, at lower DO depletion rate than the previously discussed effluents, however, it attained a minimum value of 1.6 mg/l after of 15 days. The TDS showed incremental increase from 592.5 to 657.8 mg/l similar to MF effluent. However, much less turbidity was found in C-F effluent compared to MF, and it showed a slight decrease from 18.8 to 8.8 NTU. The pH also showed a marginal decrease from 7.7 to 7.

The UF effluent showed a slight increase in TDS from 481 to 499.6 mg/l. The mean turbidity went under 1 mg/l from 1.9 mg/l in 15 days. The DO showed a marginal decrease in DO from 8.1 to 7.1mg/l in 15 days, and pH showed a marginal decrease from 7.8 to 7.3.

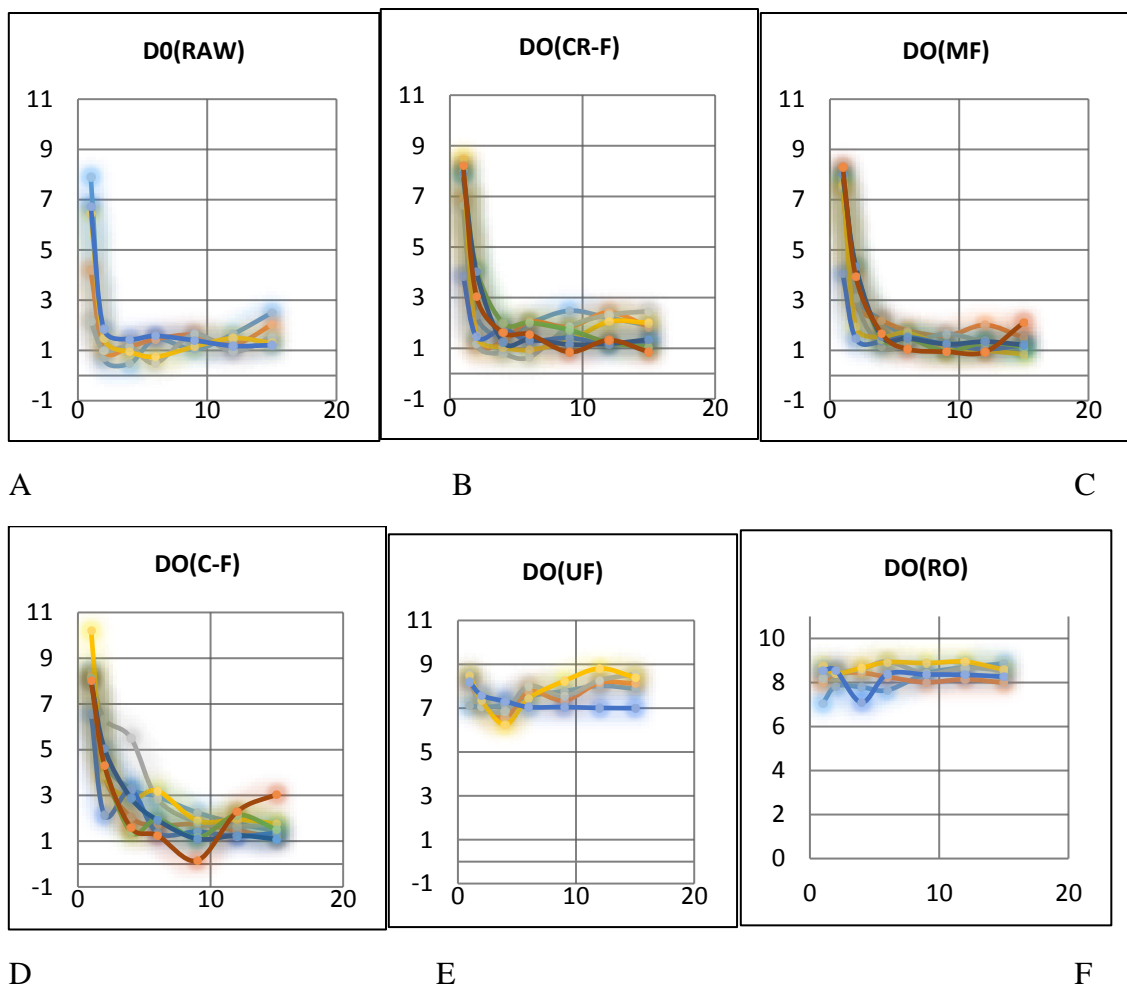


Figure 4.19 Change of dissolved Oxygen (DO) in mg/l with storage time (days) for raw greywater (A) and treated greywater (B, C, D, E and F) for coarse filtration (CF), micro filtration (MF), granular activated GAC), ultrafiltration (UF), and reverse osmosis (RO)

r

The RO water was stable in all the parameters. The DO values almost remained constant with slight fluctuation about 0.1mg/l, and turbidity was within 1 mg/l. However, it showed an increase in the average pH from 6.5 to 8.3 at the end of 15 days. However, the pH value was most stable during 5 to 10 days span with SD of 0.5 as shown in Appendix A4.

Overall, the data from Figure 4. 16 to 4.19 showed RO and UF as very stable water, which did not show much variation in DO, turbidity, and TDS. However slight upscaling in pH for some of the samples was observed. It increased in pH values in RO water averaging to about 7.1 with 0.5 SD during 5th and 10th day of storage. The effluents CR-F, MF, C-F, and RAW water showed a similar trend for all the water quality parameters with decreasing pH, DO, and Turbidity, and increasing TDS. This most likely due to anaerobic decay, where suspended COD turns to dissolved COD over time (Ward et al., 1996)

According to (Ghunmi et al., 2011), greywater excluding kitchen influent is high in COD content where 40 % of COD is dissolved, 28 % suspended, and 32 % colloidal. GAC-MI-Me treatment trains remove most of the suspended and colloidal solids up to UF. This is possibly the reason why the UF and RO effluent shows stability compared to microfiltration and other coarse filtration. However, DO depletion rate varied in all effluents. Comparing the time it took DO to reach below 2 mg/ l, it was fastest in raw water (24 hours), three days in CR-F, whereas for CF it took nine days. If a decision is to be made based on the DO depletion rate, the CF effluent is superior to the other

treatments as it can be stored up to 9 days. On the other hand, there are no restrictions on storage of UF and RO effluents.

4.5 Conclusion

GAC-MI-ME greywater treatment system is capable of improving water quality from low to high grade. The unit-models of GREY-ANN showed effective results in predicting the water quality parameter and can be applied as potential decision support tool in selections of appropriate treatment train specific to the type of greywater and treatment goal. The sensitivity analysis of the unit models determined the potential variability in treatment trains affecting the specific parameter in UF and RO effluent.

The multi- parameter model BOD-MP showed less effective results. The possible reason can be attributed to the inability of the model to predict extremely low or null values in BOD₅. At the same time, MAE was very small, which implies that BOD-MP can be applied in the prediction of higher BOD ranges. The water quality analysis also showed the BOD of the greywater selected in this study mostly associated with turbidity rather than TDS, as the BOD-MP analysis revealed that BOD is highly sensitive to the turbidity values.

Greywater storage impact of treated greywater shows longer storage potential for the GAC effluent than the MF, CR-F, and raw water. Untreated greywater has lowest storage potential due to rapid depletion of DO and increases in TDS values. Though the turbidity decreased in most of the samples, increasing TDS values may further complicate the treatment processes, and therefore it is not recommended for storage. However, RO/UF treated greywater showed unrestricted storage potentials.

This case study provided a possible solution to increase greywater reuse based on the experimental evaluations and data-driven modeling approaches. They are limited to the type of greywater applied, and the membrane modules of the GAC-MI-ME system. However, a similar approach can be implemented to develop future protocols for greywater treatment and reuse using an advanced physical filtration system.

5 AIR-CONDITIONERS (A/C) CONDENSATE MODELING USING PSYCHROMETRIC COMPUTATIONS: AN APPROACH USING MASS AND ENERGY BALANCE

5.1. Introduction

5.1.1. Background

The concept of air-conditioning (A/C) condensate collection is an emerging alternative in hot and humid climate, but it is not being widely adopted. The A/C condensate can be considered as a lucrative alternative for the regions lacking freshwater resources, which may not require additional efforts other than piping, plumbing, storage, and distribution. Conventionally, A/C condensate is drained and sometimes becomes a disposal issues by affecting sewage conveyance and volumetric load on water treatment plants (Painter et al., 2009). In this scenario, the onsite collection and use of A/C condensate will not only subside the wastewater conveyance load but also will partially offset municipal water demand, which potentially can help to promote green infrastructure for water scarce regions (Wilson et al., 2008).

The uncertainty in condensate volume with varying seasonal load was identified as a major barrier to its use as an alternative water resource (Cook et al., 2014). For a building planner to use A/C condensate, the potential drivers for condensate estimation are financial obligations and water supply strategies during low production periods (Lawrence et al., 2010). It may not be feasible with circumstances, where installation and maintenance cost exceeds the financial return. Also, the volumetric information for condensate is required for water supply management strategies. Therefore, the

condensate estimation is a critical step in improving its potential as an alternative resource.

5.1.2. Condensate

Grenard et al., (1967) proposed water recovery from a hot and humid climate of St. Croix (Caribbean island) using deep sea cold water, with an estimated recovery of 16 g of water / m³of air). ‘Heating Ventilation and Air Conditioning’ (HVAC) systems are the most common examples of cooling and dehumidification processes. The condensation occurs in HVAC systems, when hot and humid air passes through its cooling coil, and the air parcel attains the temperature below or at its dew-point (100 % moisture saturation condition). In automated temperature and humidity controlled system, where the primary function of HVACs is to offset the heat gain (cooling load) and meet indoor comfort (Alahmer et al., 2011), it’s hard to capture the system dynamics with changing cooling load.

5.1.3. Attempts made in condensate estimation

A case study in the San Antonio by Guz et al., (2005) illustrated the high potential of condensate collection in hot and humid climate (250 gallons per day from its downtown mall, and about 0.16 million gallons per month from its central library). Generalized empirical relations were developed to estimate condensate for the city of San Antonio, as shown in Equation [5.1]

$$(V)_{cond \text{ in } gph} = (tons \text{ of } capacity)(load \text{ factor})(0.2 \text{ gallons}) \quad (5.1)$$

It showed the condensate relationship with the maximum cooling capacity of HVAC system with an estimate of (0.1 to 0.3) gallon condensate per hour, per ton of cooling load.

Bryant et al., (2008) developed another case-specific set of empirical equations for condensate estimation from buildings in Qatar as shown in Equation (5.2):

$$(Mw)_{\text{condensate}} = 1.08 \text{ CFM} \frac{\Delta T}{12000} \quad (5.2)$$

Where: CFM implies for cubic feet per minute air flow, and ΔT is the temperature difference across cooling coil ($^{\circ}\text{F}$). The estimated condensate for a commercial building was proposed in this study to be around 110 gallons for per ton of cooling load, considering the dew point temperature exceeds 60°F for at least 140 days of a year.

Painter et al., (2009) estimated condensate for major cities of Texas considering energy efficient HVAC systems (enthalpy wheels as heat recovery unit). Air- psychrometric relationships were used to determine condensates shown in Equation (5.3), which considers the condensate formation as a function of humidity difference across the cooling of HVAC system i.e. between supply condition and enthalpy wheel.

$$(Y) = \Delta W_{cc} \frac{\rho_a}{1.0 \times 10^6} \quad (5.3)$$

Where: Y is condensate potential in gal/ft^3 , ΔW_{cc} is the difference of humidity ratio across cooling coil, and ρ_a stands for density of dry air (lb/ft^3). The study showed the estimated condensate volume for the cities of San Antonio, Houston, and Dallas were 6×10^{-5} , 5.6×10^{-5} , and 5.0×10^{-5} gallon per cubic feet of cooling space respectively.

Lawrence et al., (2010) developed a model for condensate estimation using air- psychrometric approach for dedicated air handling units (100% ventilation). Condensate computations in this study were based on Equation (5.4), where the volumetric condensate was considered as a function of the difference of the humidity ratio between the supply air and the outside air.

$$(Mw)_{cond} = (Airflow) (Density) 60 \frac{min}{hr} (\Delta W) \quad (5.4)$$

Where: Mw stands for mass of condensate in (kg), and ΔW is the difference of humidity ratio across cooling coil. Significant errors in the study were attributed to indirect supply-air volume measurement (logging motor current of supply fan) as well as direct measurement of temperature and humidity data of supply air. The supply flow volume resulted in 15% error, while the model simulated result was with 28% variation in condensate volume.

Cook et al., (2012) estimated condensate volume for a commercial building in Brisbane using the model developed by Lawrence et al., (2010). The study showed that the estimated condensate of 4200 l/day could meet the non-potable irrigation water demand during peak summer hours.

Most of the studies cited above were site and system specific, and models were empirical in nature. The volumetric flow rate was considered as a more conventional way to compute condensate. However, measuring volumetric flow rate is itself a challenge that could result in a significant error.

Also, predicting condensate volume at maximum cooling capacity of HVAC would be an over prediction. HVAC designs for buildings are based on the peak cooling

load (Hui et al., 1998). In real time, energy gain and loss in the system will vary with time (Al-Rabghi et al., 1999) affecting overall operation of HVAC systems and henceforth the condensate formation.

This study proposed a methodology for time-step condensate estimation by accounting for weather variability and HVAC control settings. The weather variability refers to temporal changes in temperature (T), and relative humidity (RH) of outdoor and indoor conditions. The HVAC control settings used are outdoor air ventilation (η), volumetric exchange rate (SV/hr), cooling coil temperature (T_c) and its bypass factor (f). More emphasis is given on variable cooling load for the condensate volume estimation.

5.1.4. Objective

The specific objective of the study is to develop an A/C condensate estimation tool (“ACON Model”) accounting for seasonal and HVACs operational variability.

5.2. Methods

This section presents the scientific rationale and the detailed procedures involved in developing the “ACON Model”. The “Visual Basic for Applications” (VBA) was used as a framework for the model development. The model automates the thermodynamic computations involved in cooling and dehumidification processes.

5.2.1. Model logic and assumptions

The ACON model uses mass balance and energy conservation approaches to compute condensate and considers HVAC operation under steady state conditions. It accounts for psychrometric state of different air parcels during the cooling and

dehumidification processes. The condensate formation across the cooling coil is a result of phase change of moist-air at saturation.

Figure 5.1 shows recirculating air streams for an operating HVAC system, and assumes the supply conditions in thermodynamic equilibrium with the conditioned air (?) during a given time-interval. The psychrometric states (specific enthalpy, specific humidity, relative humidity, dry bulb temperature, specific volume, dew point temperature, saturation vapor pressure and partial pressure of moist air) of air parcels continuously changes from outdoor air to supply conditions as described Figure 5.2. The node 'A' is outdoor air. The node 'B' is mixed air (the mixed condition with the return and outdoor air). The node 'C' is the point of condensation at cooling coil. The node 'D' represents air stream at the exit of the cooling coil (includes the effects of the coil-bypass factor). The node 'S' is supply air to the conditioned space at steady state, and the node 'Z' represents indoor design condition. The node 'R' is the return air stream, and the node 'E' represents the exhaust air flow. The ACON model does not account for the sensible heat gain due to fan operation, and therefore model computations consider points 'S,' 'R,' 'Z,' and 'E' at the same psychrometric state with no transition.

The following assumptions and considerations were made for "ACON model" development. (1) Cooling and dehumidification processes follow law of conservation of mass and energy. (2) HVAC systems work with constant air volume supply (CAV). (3) The moist air is an approximation of ideal gas. (5) It also assumed that the coiling-coil of HVAC system operates at constant temperature and bypass factor, but with variable volume at node 'C'. (6) The psychrometric state of supply volume at node 'S' is result

of combined thermodynamic state of mixed air stream at node 'M', and coil supply air at node 'C'. (7) The exhaust air and the return air are in the same psychrometric state as of indoor conditions. (8) The condensate temperature is the same as the cooling coil temperature. (9) There is no additional heat gain in the system due to the electric fan. (10) There were no separate considerations for enthalpy wheel, reheating coil or additional dehumidifier/humidifier in the system. (11) The model categorized the cooling load as internal cooling load and the Ventilation Load. The Ventilation Load was accounted as combined effect of outdoor air mixing as well as the room volume exchange rate. The internal cooling load was considered as all the load transitions in the conditioned space excluding Ventilation Load (building envelope, number of occupants, operating appliances, time of operation, infiltrations or any other factors affecting load gain/or loss).

5.2.2. Model input parameters

The ACON model considered thermo-hygrometric (T, RH) information as weather variant parameters. The parameters affecting HVAC operation were included as ratio of the outdoor air to the return air (η), coil temperature and coil-bypass factor (f), volumetric air exchange rate (SV/hr) for the building, duration of operation, atmospheric pressure (Pa), room volume (m^3), and time series Internal Load data (kJ).

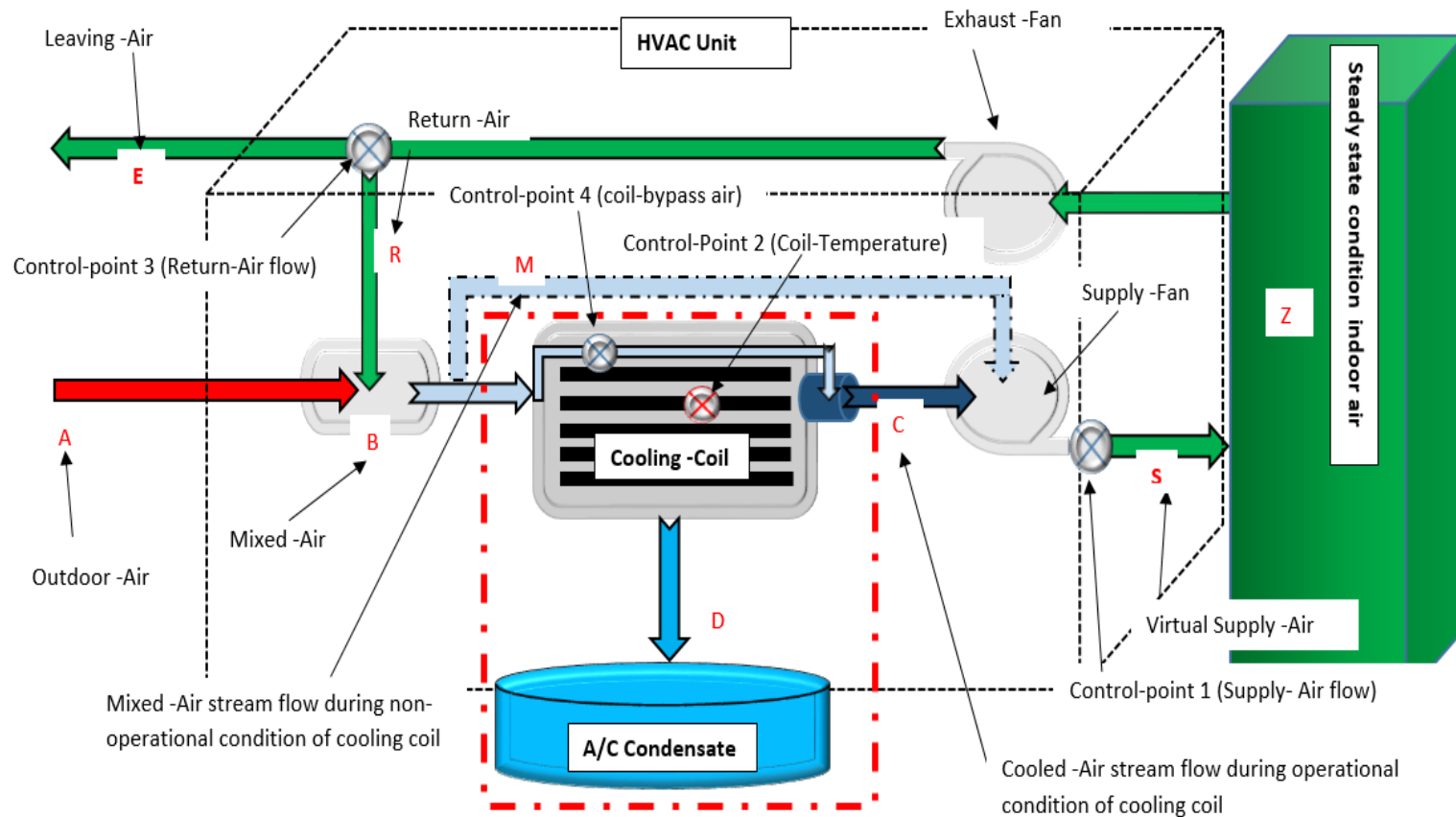


Figure 5.1 Operational details of ACON model for condensate estimation during mechanical cooling and dehumidification process, assuming steady state conditioned space and considering law of conservation and mass and energy in ideal condition

5.2.3. Model development

The model computations were based on the psychrometric chart and divided into five different sub-models: (1) “Psychrometric” module, (2) “Mixed-air” module, (3) “Condensate analysis” module, (4) “Operational HVAC module,” and (5) “Load analysis” module.”

5.2.3.1. Psychrometric module

The psychrometric module determines the thermodynamic state of air parcels from given weather variant parameters. The moist-air psychrometry is graphically represented in the psychrometric chart (Wexler et al., 1983). The module eliminates the need for manual computations, and graph-reading using the known psychrometric parameters in this case relative humidity (ϕ), and dry bulb temperature (T). It determines the following psychrometric parameters, including, dew-point temperature (T_{dew}), specific-humidity (W), specific volume (v), saturation vapor pressure (P_{ws}), and specific enthalpy (h). The following equations and derivations were applied to determine the parameters.

As, relative humidity (ϕ) is the ratio of partial pressure of moist air (P_w) to the ratio of partial pressure at saturated condition (P_{ws}) (Tsilingiris et al., 2008). Partial pressure of water vapor can be expressed in terms of relative humidity and saturation vapor pressure Equation (5.5). The partial pressure of moist air (P_w) can be determined by substituting condition (P_{ws}) from Equation (5.14) in Equation (5.5).

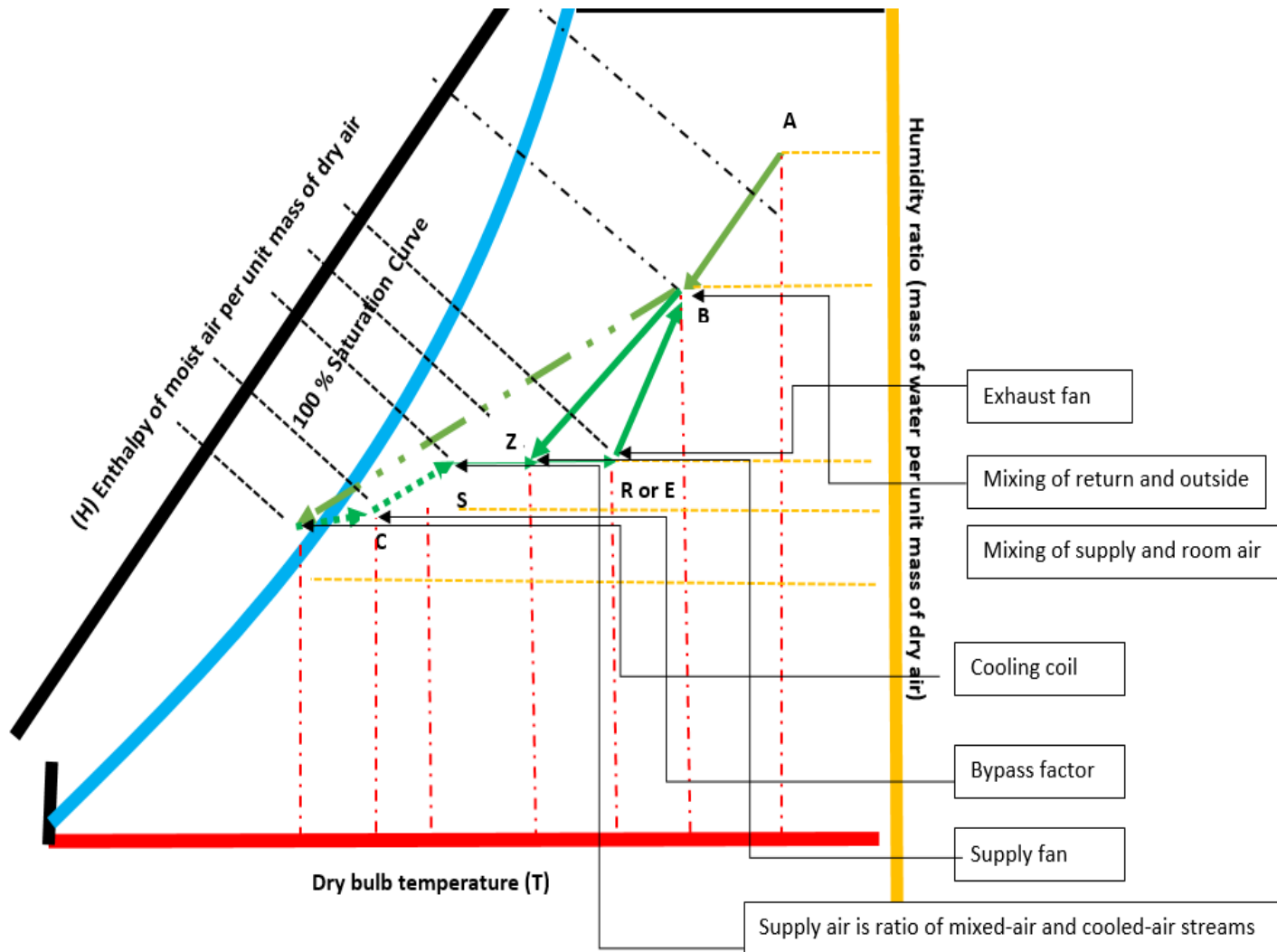


Figure 5.2 psychrometric calculations considered in “ACON” model for air parcels transition

$$P_w = \phi * P_{ws} \quad (5.5)$$

$$P_w = \phi * 610.78 \exp\left(17.269 \frac{T}{237.3+T}\right) \quad (5.6)$$

As per assumption, the moist air, dry air, and water vapor follows the ideal gas law. Using to ideal gas law in Equation 5.7, the specific volume of water in Equation 5.8 can in can be expressed in terms of dry bulb temperature and partial vapor pressure of water (P_w) in Equation 5.9.

$$P_w * v_w = R_w * T_w \quad (5.7)$$

$$v_w = V_w/M_w \quad (5.8)$$

$$v_w = R_w * \frac{T_w}{P_w} \quad (5.9)$$

So, the mass of water can be expresses in terms of ideal gas law by Equations 5.8 and 5.9 as Equation 5.10.

$$M_w = V_w * P_w / (R_w * T_w) \quad (5.10)$$

Similarly, for dry air the mass (M_a) can be expressed as in Equation (5.11)

$$M_a = V_a * P_a / (R_a * T_a) \quad (5.11)$$

The humidity ratio (W) in the psychrometric chart measures the water content of moist-air, which is the ratio of mass of water (M_w) to the mass of dry air (M_a) as expressed in Equation (5.12). The humidity ratio can be expressed as in Equation (5.13) (Alahmer et al., 2011), by substituting Equations. (5.10 and 5.11) in (5.12).

$$W = \frac{M_w}{M_a} \quad (5.12)$$

Or,
$$W = \frac{R_w}{R_a} * \frac{P_w}{P_a} \quad [V_a = V_w, \text{ And } T_a = T_w]$$

Or,

$$W = 0.622 * \frac{P_w}{P_a} \quad \left[\frac{R_w}{R_a} = 0.622 \right] \quad (5.13)$$

Saturation vapor pressure P_{ws} is as function of temperature can be obtained from the psychrometric chart. In this model, the expression for(P_{ws}) was used from Singh et al., (2002) as shown in Equation (5.14).

$$P_{ws} = 610.78 \exp\left(17.269 \frac{T}{237.3+T}\right) \quad [0^\circ \text{ C} < T < 63^\circ \text{ C}] \quad (5.14)$$

Relative humidity and dry bulb temperature are known psychrometric parameter here, so for the air-vapor mixture, humidity ratio can be written in terms of saturation pressure (P_{ws}), and relative humidity (ϕ) as Equation (5.15) by substituting Equation (5.6) in (5.13).

$$W = 0.622 * \frac{\phi * P_{ws}}{P_{atm} - \phi * P_{ws}} \quad [P_{atm} = P_w + P_a, \text{ and } P_{ws} = \phi * P_w] \quad (5.15)$$

The specific enthalpy(h) of air parcel can be obtained using the psychrometric chart from two known psychrometric parameters. The derivation [$h = f(T)$] can also be defined (Wilhelm et al., 1975) as shown in Equation (5.16).

$$H = 1.006 T + W(2501 + 1.775T) \quad [-50^\circ \text{ C} \leq T \leq 110^\circ \text{ C}] \quad (5.16)$$

The model computes the dew point temperature of air parcel using Wilhelm et al., [1975]

$$T_{dew} = 6.983 + 14.38 \ln\left(\frac{P_w}{1000}\right) + 1.079\left\{\ln\left(\frac{P_w}{1000}\right)\right\}^2$$

(5.17)

$$[0^\circ \text{ C} < T \leq 50^\circ \text{ C}]$$

5.2.3.2. Determining psychrometric transitions of airstreams due to HVAC control settings using “Mixed-air module”

The HVAC control settings in the ACON model accounts for outdoor air ventilation (η), cooling coil temperature (T_{coil}) and corresponding bypass factor (f), and room volume exchange rate (SV/hr). This section emphasizes the psychrometric state change in air parcels in cooling and dehumidification processes as a result of varying operating conditions primarily due to outside air ventilation (η), and cooling coil and associated bypass factor (f).

If η is the volumetric ratio of air streams (outside air, and total volumetric flow) with different humidity ratio and temperature, the humidity ratio and temperature of the mixed stream can be determined using mass balance for mixing two streams with no humidification (Kamm et al., 2007). The following Equation (5.18) can be written.

$$(1 - \eta)(M_a, M_w)_{Return} + \eta (M_a, M_w)_{outside} = (M_a, M_w)_{mixed}$$

(5.18)

Where, $\eta = \frac{(V)_{Outside}}{(V)_{Total}}$, and

$$1 - \eta = \frac{(V)_{Return}}{(V)_{Total}}$$

Using energy conservation, as the energy exchange between two streams as result of temperature gradient can stated below (Kamm et al., 2007).

$$\{(h)_{mixed} - (h)_{return}\}(Ma)_{return} = \{(h)_{outside} - (h)_{mixed}\}(Ma)_{outside}$$

So,

$$\begin{aligned} (h)_{mixed} &= [\{(h)_{return} (Ma)_{return} + (h)_{mixed}\}(Ma)_{outside}] / \\ & \{(Ma)_{Outside} + (Ma)_{return}\} \end{aligned} \tag{5.19}$$

$$(Ma)_{return} = (V)_{return} / (v)_{return},$$

$$(Ma)_{outside} = (V)_{outside} / (v)_{outside},$$

Hence, Equation (5.19) can be written in terms of η , and v :

$$(h)_{mixed} = \left[\frac{\left\{ \left((E)_{return} \frac{(1-\eta)}{(v)_{return}} \right) + \frac{\eta (E)_{outside}}{(v)_{outside}} \right\}}{\left\{ \frac{(1-\eta)}{(v)_{outside}} + \frac{\eta}{(v)_{return}} \right\}} \right] \tag{5.20}$$

Similarly,

$$(T)_{mixed} = \left[\frac{\left\{ \left((T)_{return} \frac{(1-\eta)}{(v)_{return}} \right) + \frac{\eta ()_{outside}}{(v)_{outside}} \right\}}{\left\{ \frac{(1-\eta)}{(v)_{outside}} + \frac{\eta}{(v)_{return}} \right\}} \right] \tag{5.21}$$

And,

$$(W)_{mixed} = \left[\frac{\left\{ \left((W)_{return} \frac{(1-\eta)}{(v)_{return}} \right) + \frac{\eta(T)_{outside}}{(v)_{outside}} \right\}}{\left\{ \frac{(1-\eta)}{(v)_{outside}} + \frac{\eta}{(v)_{return}} \right\}} \right] \quad (5.22)$$

5.2.3.3. Cooling coil temperature:

Cooling coil temperature is another parameter that determines the temperature of the air parcel passing through it. The model considers an ideal state where the air parcel exits the coil at the coil temperature and the condensation also occurs at the coil temperature which implies for air turns to 100 % saturation state. Also, the conditional statement shown below states that dehumidification only occurs if the cooling coil temperature is equal or less than the dew point of the mixed air stream:

Condition 1: (No condensate formation)

$$(T_{dew})_{mixed} > T_{coil},$$

Condition 2: (Condensate formation)

$$(T_{dew})_{mixed} \leq (T)_{coil},$$

The model accounts for the bypass factor (f) of the cooling system, which implies that a fraction of the air parcel does not come in contact with the cooling coil fins (Pita et al., 1998).

The psychrometric states of the supply air were calculated with similar analogy of mixing of two air stream with different psychrometric states without dehumidification as discussed earlier in section (5.2.3.2) and the following equations were derived, where $(h)'_{coil}$, $(T)'_{coil}$, and $(w)'_{coil}$ represents the change air parcel exiting the cooling coil

with impact of bypass factor. In this case mixing occurs in the ratio of bypass factor(f), and supply air condition is assumed to have no sensible heat gain due to operation of the fan.

$$(h)'_{coil} = \left[\frac{\left\{ \left((h)_{coil} \frac{(1-f)}{(v)_{coil}} \right) + \frac{f\eta(h)_{mixed}}{(v)_{mixed}} \right\}}{\left\{ \frac{(1-f)}{(v)_{coil}} + \frac{f\eta}{(v)_{mixed}} \right\}} \right] \quad (5.23)$$

$$(T)'_{coil} = \left[\frac{\left\{ \left((T)_{coil} \frac{(1-f)}{(v)_{coil}} \right) + \frac{f(T)_{mixed}}{(v)_{mixed}} \right\}}{\left\{ \frac{(1-f)}{(v)_{coil}} + \frac{f\eta}{(v)_{mixed}} \right\}} \right] \quad (5.24)$$

$$(w)'_{coil} = \left[\frac{\left\{ \left((w)_{coil} \frac{(1-f)}{(v)_{coil}} \right) + \frac{f(w)_{mixed}}{(v)_{mixed}} \right\}}{\left\{ \frac{(1-f)}{(v)_{coil}} + \frac{f\eta}{(v)_{mixed}} \right\}} \right] \quad (5.25)$$

5.2.4. Condensate estimation using “*condensate analysis module*”

Energy conservation and mass balance approach were used to solve the problem. The energy gain in the conditioned space due to moisture and temperature increments, results in the total cooling load, which implies that the heat is extracted from the parcel of supply air to maintain steady state at designed indoor conditions (desired humidity and temperature). Steady state equations can be determined to estimate condensate with continuous change in moisture and energy in air parcels.

Using mass balance, it can be written as follows;

$$(Ma)_{in} = (Ma)_{Out}$$

$$(Mw)_{in} = (Mw)_{out} + (Mw)_{condensate}$$

Now, writing the mass balance equation in terms of humidity-ratio using Equation (5.26).

$$(Mw)_{condensate} = (Ma)(W)_{mixed} - (Ma)(W)_{coil} \quad (5.26)$$

Using energy balance:

$$(E)_{mixed} = (E)_{coil} + (Q)_{cooling} + (E)_{condensate}$$

$$(E)_{mixed} - (E)_{coil} = (Q)_{cooling} + (E)_{condensate} \quad (5.27)$$

Considering enthalpy of dry air and water vapor in air-vapor mixture as following equations

$$(E)_{cond} = (Mw)_{cond} * (hw)_{cond} \quad (5.28)$$

The mass and energy balance equation can be written as it as Equation (5.29) (Kamm et al., 2007).

$$(h)_{mixed} - (h)_{coil} = \frac{(Q)_{cooling}}{Ma} + (W)_{mixed} - (W)_{coil} (hw)_{cond} \quad (5.29)$$

The information about cooling loads, weather data, conditioned space data, bypass factor, recirculation ratio, cooling coil temperature can be integrated together to find the condensate formation with respect to time.

However, the condensation occurs at the cooling coil. This implies that the dry mass air flow determines the condensate formation, using the energy equation

$$Ma = (Q)cooling / [(h)mixed - (h)coil - (W)mixed - (W)coil)(h)cond] \quad (5.30)$$

The above Equation (5.30) assumes a 100 % effectiveness of cooling coil. Considering the bypass factor(f), only a fraction of the total dry mass supply is effectively in condensate formation as can be written as:

$$Ma' = -(1 - f)(Q)cooling / [(h)coil - (h)mixed - (W)coil - (W)mixed)(h)cond] \quad (5.31)$$

Therefore, the condensate formation can be obtained by substituting the Equation (5.31) in Equation (5.26), and the expression of condensate formation can be written in Equation (5.32)

$$(Mw)cond = \frac{(1-f)(Q)cooling}{[(h)mixed - (h)coil - (W)mixed - (W)coil)(h)cond]} [(W)mixed - (W)coil] \quad (5.32)$$

By substituting Equations (5.20), and (5.22) in Equation (5.32), the final expression can be written as Equation (5.33).

$$(Mw)_{cond} = \frac{(1-f)(Q)_{cooling}}{\left[\frac{\left\{ \left((E)_{return} \frac{(1-\eta)}{(v)_{return}} + \frac{\eta(E)_{outside}}{(v)_{outside}} \right) \right\}}{\left\{ \frac{(1-\eta)}{(v)_{outside}} + \frac{\eta}{(v)_{return}} \right\}} - \left\{ \left((W)_{return} \frac{(1-\eta)}{(v)_{return}} + \frac{\eta(T)_{outside}}{(v)_{outside}} \right) \right\} - W_{coil} \right] (h)_{cond}}$$

$$\left[\frac{\left\{ \left((W)_{return} \frac{(1-\eta)}{(v)_{return}} + \frac{\eta(T)_{outside}}{(v)_{outside}} \right) \right\}}{\left\{ \frac{(1-\eta)}{(v)_{outside}} + \frac{\eta}{(v)_{return}} \right\}} - W_{coil} \right]$$

(5.33)

5.2.5. Determining operational duration and intensity of HVAC system using “operational HVAC module”

The “Operational HVAC module” of ACON model determines operational duration and intensity of HVAC systems for varying load conditions while meeting the thermodynamic steady state of conditioned space.

The term ‘Binary Operational Coefficients’ (€) was introduced, which represents operating/non-operating conditions of HVAC (cooling and dehumidification only). The

ACON model uses the concept to determine the time period during which the HVAC system will be operating with condensation. The ACON model determines the ambient energy with known temperature and relative humidity using Equation. 5.16, where the total ambient energy is the combined effect of sensible and latent heat energy. The term sensible heat ratio (SHR) is commonly used in HVAC design, which is the ratio of sensible load to the total load on the system (Mazzei et al., 2005). The SHR value of 1 indicates sensible cooling only (no dehumidification). The model determines the potential operating and non-operating conditions of HVAC system [ϵ (1, 0)] by considering seasonal variability, indoor design conditions along with HVAC control settings. Following conditional statements were used to determine (ϵ).

Condition 1(SHR<1):

$$(T)_{mixed} > (T)_{in}, \text{ And}$$

$$(W)_{mixed} > (W)_{coil}, \text{ Then}$$

$$\epsilon = 1$$

Condition 2 (SHR=1):

$$(T)_{mixed} > (T)_{in}, \text{ And}$$

$$(W)_{mixed} < (W)_{coil}, \text{ Then}$$

$$\epsilon = 0$$

Condition 3:

$$(T)_{mixed} < (T)_{in}, \text{ Then}$$

$$\epsilon = 0$$

The term ‘Cooling Load Index’ (ψ) was proposed in this study to represent the operational intensity of HVAC system (during cooling and dehumidification process only). The operational intensity is demonstrated in Figure 5.3 (higher cooling load implies for higher volumetric flow of mixed air stream through cooling coil to attain steady state supply conditions). The Cooling Load Index is the fraction of the coil-supply air to total supply and represents intensity of HVAC operation with cooling load on the system. The value of (ψ) Equation (5.35) increases and approaches 1 for maximum cooling load and the value is zero for non-operational conditions of HVAC system. The value of mixed flow index (∇) (Equation 5.36) decreases with increasing load, and approaches maximum (1) at non-operational condition. Equations (5.34) and (5.37) represent constant supply volume in the system.

$$V_{supply} = V_{mix} + V_{Coil} \tag{5.34}$$

$$(\psi) = \frac{V_{supply}}{V_{coil}} \tag{5.35}$$

$$(\nabla) = \frac{V_{supply}}{V_{mix}} \tag{5.36}$$

And,

$$\psi + \forall = 1$$

(5.37)

Considering that the system operates at Ventilation Load, the corresponding value of Cooling Load Index is ψv . The term Internal Load is attributed to all the heat gain and loss in the system than need to be offset by increasing the Cooling Load Index. With additional Internal Load (ψi), the total Cooling Load Index (ψ) is shown in Equation (5.38).

$$\psi v + \psi i = \psi$$

(5.38)

ACON model determines (ψ) values for time series data of temperature and relative humidity by iterating for known computed values of enthalpy (h)*supply*, mixed air (h)*mixed*, and coil supply air (h)*coil*, as shown in Equations (5.38) and (5.39).

Using conservation of the mass:

$$(Ma)_{coil} + (Ma)_{mixed} = (Ma)_{supply}$$

$$\frac{V_{coil}}{(v)_{coil}} + \frac{V_{mixed}}{(v)_{mixed}} = \frac{V_{supply}}{(v)_{supply}}$$

$$\frac{(\psi t)V_{supply}}{(v)_{coil}} + \frac{(\forall t)V_{supply}}{(v)_{mixed}} = \frac{V_{supply}}{(v)_{supply}}$$

Using conservation of energy:

$$(h)supply = \left[\frac{\{(Ma)coil(h)coil+(Ma)mixed (h)mixed\}}{\{Ma\ coil+(Ma)mixed \}} \right]$$

Or,

$$(h)supply = \frac{\left\{ \frac{(\psi t)(h)coil}{(v)coil} + \frac{(\psi t)(h)mixed}{(v)mixed} \right\}}{\left\{ \frac{(\psi t)}{(v)coil} + \frac{(\psi t)}{(v)mixed} \right\}}$$

(5.39)

$$(V)supply = (V)coolingspace \left(\frac{SV}{hr} \right) Time\ of\ operation$$

(5.40)

The ACON model determines the total supply volume time of operation, cooling space volume and volumetric exchange rate as shown in Equation (5.40). The supply condition corresponds to given indoor temperature and relative humidity. The corresponding coil-induced supply volume is determined using Equation (5.35), and the condensate is determined using Equation (5.33).

5.2.6. Determining internal load for observed condensate data using “load analysis module”

The “Load analysis module” computes the total cooling load on the system for known time series data on temperature, relative humidity, and condensate (for cooling and dehumidification cases only). The simulations include backward iterative computation of the “Condensate analysis” module by determining total coil-supply index (ψ) . It computes the Internal Load on the system by following Equation (5.41) and is used where Ventilation Load is determined.

$$\psi_i = \psi_t - \psi_v \quad (5.41)$$

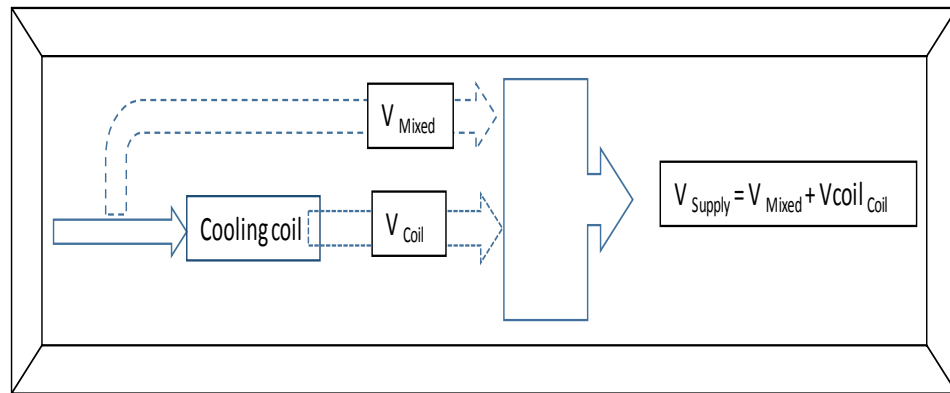


Figure 5.3 The diagram depicts variable coil supply volume and mixed air volume together for total supply volume to meet the thermodynamic steady state condition of supply volume

5.3. Conclusion

A model (ACON) was developed for condensate estimation from conventional HVAC units. Two different concepts were proposed in this study: 1) total cooling load categorized as Ventilation Load, and Internal Load, 2) “Cooling Load Index” (ratio of coil induced volume to the total supply volume) representing the intensity of system operation corresponding to cooling load on the system. The input parameters for ACON model include; (1) temperature and hygrometric data (T, and RH) for both the outdoor and indoor conditions , (2) outdoor air ventilation , (3) cooling-coil temperature and corresponding bypass factor, (4) volumetric air exchange rate for the conditioned-space,

(5) time of operation, and (6) atmospheric air pressure, (7) conditioned-space volume,(8) time series Internal Load data (condensate analysis module) or time series observed condensate data (load analysis module).

The ACON model can be used as a universal application with weather data, and Internal Load information and the HVAC settings for a given conditioned space. As outdoor air ventilation is a critical operational component affecting the total cooling load on the system and as a result condensate estimation, the ACON model facilitates user customization of ventilation and computes the condensate. The improved accuracy in condensate estimates over the conventional empirical approach will promote its use in several ways; 1) determining the financial costs and return associated with condensate collection systems and, 2) and also may help in decision making in water supply strategies during condensate recovery periods.

6 APPLICATION OF ACON MODEL SIMULATIONS IN CONDENSATE ESTIMATION USING WEATHER DATA: A CASE STUDY OF DOHA USING ANN PREDICTION TOOL

6.1. Introduction

This study determined the potential for A/C condensate use as an alternative water resource for the city of Doha using a time-step (hourly/daily) condensate-volume estimation and water quality analysis. A Hybrid modeling approach using psychrometric based ACON (air-conditioner-condensate) model, and data-driven ILAN (Internal Load analysis using neural-network) was applied semi-empirically for condensate volume estimation.

The ACON model uses the Cooling Load Index (ventilation and internal) for time-step condensate estimation using thermo-hygrometric data and HVAC control settings as described in Section 5. The model determines the Ventilation Load Index, and uses Internal Load as input. The Internal Loads are empirical in nature and vary with building type and conditions. The ILAN model was developed for the city of Doha to predict time-step Internal Load Index for variable climatic conditions (Temperature, Relative humidity). The input-output database for ILAN was derived using ACON simulations from observed condensate volume which included; 1) temperature, 2) relative humidity, 3) specific enthalpy for outdoor and indoor condition and, 4) Ventilation Load Index at 20 % for desired output of 5) Internal Load Index.

6.1.1. Background of study

The city of Doha is located in the Arabian Peninsula and is a business hub for

the State of Qatar. High economic growth, associated with its large oil and natural gas reserves, is resulting in rapid urbanization and population growth (Bryant et al., 2008). The overall impact is increasing water stress, and therefore lowering water availability per capita (UNDP, 2009). According to UNDP (2009), the country's municipal water demand will increase by five times between the years 2010 and 2060. At the same time, low freshwater availability in Qatar with annual rainfall (1.5 inch) and brackish surface water (51.4 MCM) and groundwater (15 MCM) (Abahussain et al., 2002) adds to the problem of water stress.

Desalination is the only primary means of water supply in the country, with an average production of 200 million gallons per day (MGPD) (Bryant et al., 2008). Expansions of desalination plants with increasing water demand are posing critical challenges on future water sustainability, as the desalination processes are a capital and energy intensive process that is detrimental to local marine ecosystems (Latteman et al., 2008). Therefore, a new sustainable alternative need to be found to offset dependency on desalination.

6.1.2. A/C condensate potential

There is a high potential for A/C condensate in a hot and humid climate of Doha, where most of its residential and commercial buildings are equipped with HVAC systems. The water quality evaluations and quantitative estimation will play a vital role in determining A/C condensate as an alternative resource for the city.

Water quality analysis, determines the type of water reuse that can be achieved based on, local or regional water regulations to avoid risks associated with human and

environmental safety (WHO, 2003). Table 2.3 shows water quality variations observed in A/C condensate. However the water quality of A/C condensate can be attributed to type, age, and surrounding air contamination (Loveless et al., 2013). In this scenario, a case specific study on water quality evaluations would provide a better assessment for its potential use of A/C condensate.

Information on water quantity is another critical aspect in determining supply management strategies (Abrishamchi et al., 2005). Considering A/C condensate as a potential alternative water resource, volumetric measurement is essential not only for decision making in supply strategies but also to determine its economic feasibility (Anderson et al., 2011).

6.1.3. ACON model and condensate estimation

The ACON model categories total cooling load as Ventilation Load and Internal Load. It considers indoor design conditions, weather data, HVAC operational controls, and determines Ventilation Load Index. The model uses Cooling Load Index (ventilation and internal) for time-step condensation using thermo-hygrometric data and HVAC control settings as described in Section 5. The model determines the Ventilation Load Index, and uses Internal Load as input. The Internal Load, which is completely empirical in nature, and will vary with the location and the other factors associated with building-energy-dynamics.

6.1.4. Internal load determination for ACON model

Several Building Energy Simulation Softwares (BESS) are available (Crawley et al., 2008), and can be applied to determine Internal Load for ACON model. For example, The BESS “Energy Plus” is capable of time-step cooling load simulation (Hong et al., 2009). However, the primary limitations with the BESS are their dependency on experimental data (Ben-Nakhi et al., 2004). The BESS need building information as well as exhaustive time series data log as input for thermal load simulation (Chou et al., 1986). At the same time, The ACON model (“Load Analysis Module”) can determine the cooling load using condensate data (for cooling and dehumidification cases only). Subsequently, the Internal Load can be determined as the difference between the total Load Index and the Ventilation Load Index as in Equation (5.41).

However to determine a generalized application for Internal Load as a function of weather variation, a black box modeling can be applied in lieu of non-linear data intensive complex formulation of Internal Load. The ANN can predict outputs from a complex system, and does not rely on data and time intensive process modeling approach (Ben-Nakhi et al., 2004). It is a commonly applied technique in building energy analysis either in system identification or a parameter prediction (Kreider et al., 1995). It provides a better technique in energy simulation compared to statistical tools and analyzes a complex system efficiently (Yalcintasv, 2005; Kumar et al., 2013).

6.1.5. Artificial intelligence in building energy generalization/prediction

Gouda et al., (2002) applied ANN using experimental data in the prediction of room temperature as a function of HVAC control (heating valve position) and weather data (ambient temperature for an outdoor condition, solar-irradiance). Yalcintas et al., (2005) applied ANN to determine power consumption for a chiller plant using dry bulb (Db) temperature, wet bulb (Wb)-temperature, relative humidity, dew point, and wind speed/direction. The model prediction showed the goodness of fit with 10 % error during testing and 9.7 % error during training.

Ben-Nakhi et.al, (2004) applied general regression neural networks (GRNN) to predict cooling load from outdoor ambient temperature, using a database derived from BESS (ESP-r). In this case, the BESS required a time series log for diffuse solar radiation, solar intensity, and wind speed and direction thermo-hygrometric data. In contrast, the ANN model showed high accuracy for the test data (not applied in the model building) in generalization/prediction of the cooling load by using temperature as a single dependent parameter.

6.1.6. Condensate determination for Doha using ACON model

A hybrid modeling approach (system modeling and data-driven) was proposed and applied in this case study for hourly/daily condensate simulations. The ACON model was used to determine Ventilation Load.

Whereas, the 'Internal Load Artificial Neural Network' (ILAN) model was developed using ANN to generalize/predict Internal Load using thermo-hygrometric and ACON simulated energy parameters. Accordingly, the total condensate volume can

be determined for analogous buildings of Doha using ACON simulated ventilation and ILAN simulated internal cooling load.

6.1.7. Objectives

The main objective of the Section is to determine the feasibility of condensate water collection for the city of Doha by evaluating the condensate water quality and simulating hourly/daily condensation using a hybrid modeling approach. The specific objectives for the research are as follows

- I. Develop ILAN model for internal cooling load prediction/generalization using ANN.
- II. Perform a sensitivity analysis of the ILAN model to determine the weather parameter variability in Internal Load prediction.
- III. Validate of ILAN model with real-time data.
- IV. Validate ILAN-ACON condensate estimation with real-time data
- V. Use ILAN-ACON for condensate estimation using yearlong climatic data from Doha, Qatar for a conditioned space of 100 m³.
- VI. Evaluate the water quality of A/C condensate for the city of Doha.

6.2. Methods

6.2.1. System setup and data acquisition

The data in this Section was generated from experiments conducted at Qatar University campus in Doha, Qatar.

6.2.1.1. Weather data acquisition

Temperature and relative humidity are the key psychrometric parameters used in ACON model (Section 5). The HVAC operation depends on the energy difference between the outdoor and indoor conditions (Mustafaraj et al., 2011). The outdoor conditions were used as a climate indicator, while the indoor conditions were considered to represent design conditions or thermal comfort zone (Zhang et al., 2008). Using two different installations of HOBO thermo-hydro data logger (company name, location), time series data of for temperature and relative humidity was measured for indoor and corresponding outdoor conditions for two test buildings.

6.2.1.2. Condensate data acquisition

Experimental data were acquired for continuously operating single-zone split-type HVAC units. Condensate volume was measured using ‘*WATCH DOG*’ tipping bucket rain gauge with an in-built data logger (Spectrum, Inc., Aurora, IL). Table (6.1) lists the test buildings with HVAC units used for condensate data acquisition.

Table 6.1 Test-Building specifications used in experimental data

S. No	Dimensions	Volume	Load capacity
	(L×W×H)	(m ³)	(Ton)
Test-Building-I	17×4.95×3.55	298.7	4
Test-Building-II	12×6×4m	288	4

All the data were logged at ten minute interval for different time span between January and December, and preprocessed for missing values or erratic instrumental

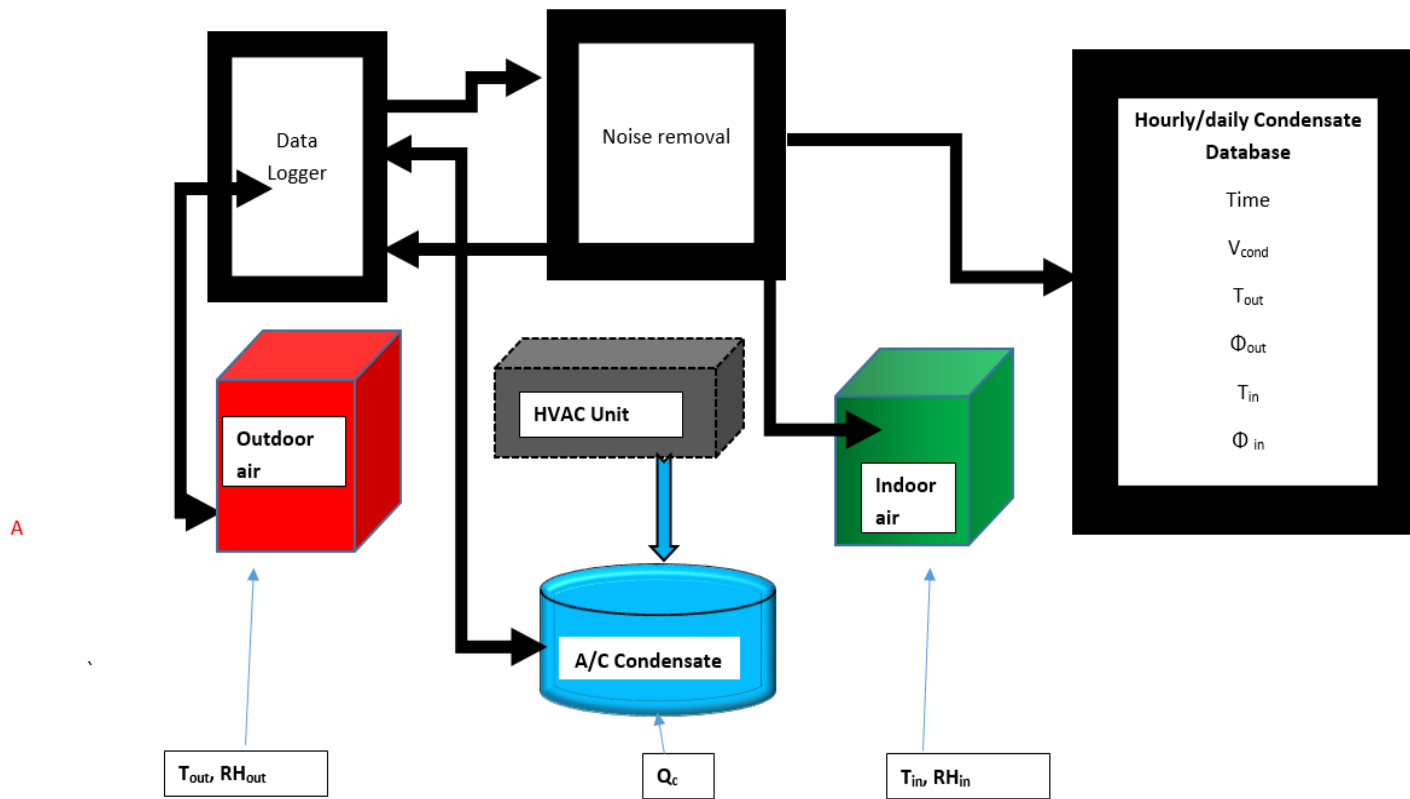


Figure 6.1 Data acquisition and processing for hourly/daily condensate data with corresponding mean outdoor/ indoor temperature and hygrometric data

reading. The databases were compiled for cumulative hourly condensate formation, and average hourly temperature and humidity variation as illustrated in Figure 6.1.

6.2.2. ILAN model development using ANN

The Internal Load represents the difference between the total load and the Ventilation Load. It represents heat gain in the system due to architectural design, construction material, operating appliances in building, human occupancy and ambient weather as well as the room temperature and relative humidity.

6.2.2.1. Input database for ILAN model using ACON simulation

The (ILAN) was developed to determine hourly Internal Load Index using experimental data from Test-Building-I. In the ACON model, the Internal Load on the system was determined as the difference between total cooling load and Ventilation Load at hourly time time-step for the operating conditions.

Table 6.2 ACON model simulation settings for case study of Doha

ACON simulation settings		
Parameters	Description	Value
P_{atm}	Atmospheric pressure , Pa	$1.031 * 10^5$
SV	Conditioned space volume, m ³	100
Ω	volumetric exchange rate, SV /hr	1
BF	Bypass factor of cooling coil	
η	Fraction of outside air,%	(1) 20
		(2) 100
Φ_{In}	Relative humidity of air, %	60
T_{in}	Indoor temperature , °C	22
T_{coil}	Coil temperature , °C	6

The ACON model was applied using simulation settings listed in Table 6.2. The Ventilation Load (ψv) was simulated using the thermo-hygrometric data for outdoor and indoor conditions and the HVAC operational controls settings. The observed condensate data along with the thermo-hygrometric data were used to derive the internal Cooling Load Index (ψi) as the difference of the total Cooling Load Index (ψt) and ventilation Cooling Load Index (ψv) using “*Load analysis module*” of ACON model. The ILAN input database was derived only for operational conditions i.e. when Binary Operational Coefficient is 1 ($\epsilon = 1$). The outliner for total load was set between 0 and 1, as the coil supply index for negative value implies for heating instead of cooling, and the values greater than one implies for under design of HVAC.

The parameters included for the ILAN model development are: (1) Weather data (T, Rh), indoor design condition (T, Rh), (2) time of operation, (3) ACON simulated energy information (enthalpy) for outdoor and indoor conditions along with, (4) Ventilation Load Index at 20 % (ψv) were considered as independent parameter, and (5) Internal Load (ψi) as dependent parameter.

6.2.2.2. ANN modeling for ILAN model development

The ANN modeling steps described in Section 4 were applied for ILAN model development. The ILAN model was developed with intent of determining internal Cooling Load Index (ψi). The parameters affecting the internal Cooling Load Index are unknown in this case. The only data available in this case were thermo-hygrometric data and time of operation. Additionally, the ACON derived parameters were considered as

independent parameters, which included indoor Cooling Load Index at 20 % ventilation, and specific enthalpy for outdoor and indoor condition.

Highly correlated input may affects the ANN model performance (Bowden et al., 2005). The independent input data correlations were determined and are shown in Table 6.3. The input parameters with correlation (r) greater than 0.85 are considered as highly correlated, and among them one of the parameters is only used in the ANN model as the training input. However, in this case, none of the independent data showed a high correlation.

Table 6.3 ILAN Input data correlation

	Time	Tout	RHOut	T In	RHIn	Eout (J/g)	Ein	(ψv)
Time	1							
Tout	0.124386	1						
RHOut	-0.17102	-0.64558	1					
T In	0.052216	0.582673	-0.0054	1				
RHIn	-0.07543	-0.4407	0.328127	-0.68325	1			
Eout (J/g)	0.027244	0.65354	0.124687	0.809668	-0.31415	1		
Ein	-0.0833	0.027476	0.017526	0.095509	-0.02007	0.058885	1	
(ψv)	-0.01461	0.376982	-0.01872	-0.0952	0.128171	0.415122	0.01595	1

6.2.2.3. ANN algorithms applied for training, cross validation and testing

The ANN model was applied for different types of network (Table 6.4). Seventy % of the data were training data, with the 15% of the data used as the cross validation, and the remaining 15 % as test data. The ANN processing were adopted in training, cross validation with activation function are described in Section 4.

6.2.3. A/C condensate water quality analysis for Doha

The preliminary water quality evaluations for A/C condensate were performed in the campus of Qatar University. Random samples from six different HVAC units were collected for water quality analysis. Because of the high ambient temperature, the sample were immediately stored at laboratory conditions. The pH measurement was done using (Hach - PHC28101-PH Electrodes). Electrical conductivity was measure using Hach HQ14d Portable Conductivity Meter. ICP-MS test methods were used to analyze Al, Ba, Cd, Co, Cr., Cu, Mn, Ni, Pb, Se, and Sr. Standard methods used to determine, Na^+ , K^+ , Ca^{++} , Mg^{++} , Cl^- , SO_4^{-2} , NO_3^{-1} , PO_4^{-3} . Microbial analysis included E.coli count using Hatch m-ColiBlue24® Prepared Agar Plate.

6.3. Results and discussion

The results are presented in three different sections: 1) Weather data and corresponding energy analysis, 2) ACON and ILAN simulation for daily condensate estimation for year-wide thermo-hygrometric data, 3) Validation of ILAN and ACON models using test data, and test building 2. ACON model was validated for Binary Coefficient of operation. ILAN model was validated for Internal Load prediction using test data. Hybrid modeling approach by integration of empirically predicted internal cooling load using ILAN and ACON simulated Ventilation Load were used to validate hourly condensate data from test building 2 (which is not part of model development). 4) The hybrid model was applied for condensate estimation for the city of Doha. 5) The A/C condensate water quality was also evaluated.

6.3.1. ILAN model analysis

The ILAN model was developed based on the performance criteria of the different ANN algorithms applied in training, cross-validation, and testing of the input database. Cross-validation (CV) were performed with several iteration, and corresponding changes for weight and bias were made in the training algorithm with the

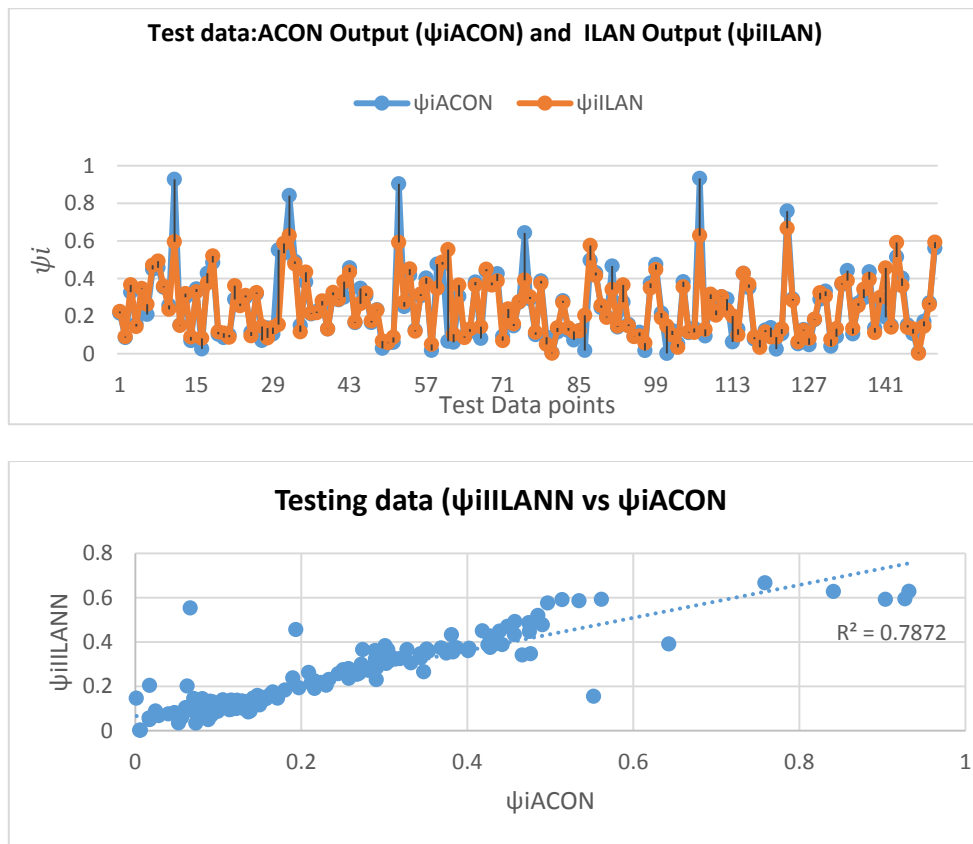


Figure 6.2 The ILAN (PNN) vs ACON estimated Cooling Load Index for Internal Load (ψ)

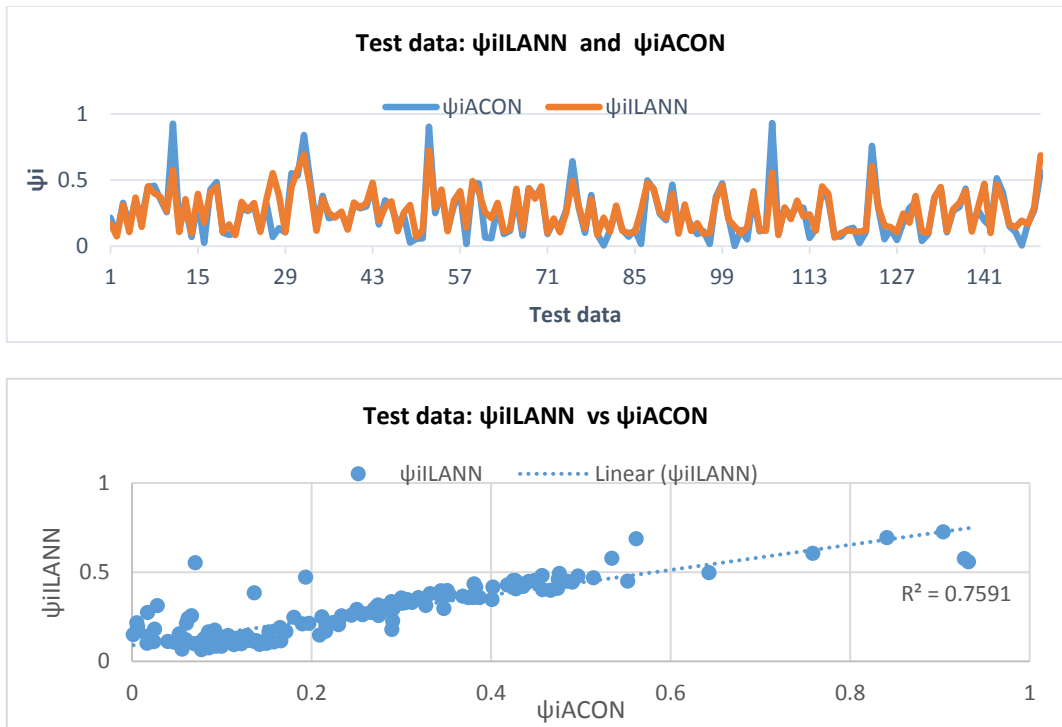


Figure 6.3 The ILAN (MLP) vs ACON estimated Cooling Load Index for Internal Load (ψ)

objective of minimizing the MSE in the CV data. The trained model applied for testing data, which are not part of training and cross validation. Different statistical performance measures including; MAE, MSE, and correlation r were used to determine the performance of the algorithms. Table 6.4 shows the performance measure for the different ANN algorithms applied for the training, CV, and testing data. The best two algorithms were PNN, and MLP with higher correlation (r) between models simulated results and test data. Figure 6.2, and Figure 6.3 show ILAN predicted and ACON derived Internal Load Index values (ψ_i) for ILAN-PNN and ILAN-MLP respectively.

Table 6.4 Performance matrix for different ANN algorithms applied in ILAN model development

ANN Model	Training			Cross Validation			Testing		
	MSE	r	MAE	MSE	r	MAE	MSE	r	MAE
MLP	0.011	0.840	0.064	0.008	0.866	0.056	0.011	0.834	0.062
PNN	0.000	0.996	0.006	0.008	0.877	0.046	0.008	0.887	0.045
RBF	0.024	0.528	0.105	0.024	0.506	0.097	0.024	0.566	0.102
GFF	0.006	0.911	0.050	0.007	0.889	0.055	0.010	0.854	0.058
TDNN	0.015	0.741	0.086	0.018	0.670	0.095	0.021	0.650	0.101

Sensitivity of the output for the given input establish how much output will be affected for a small change in the input (Loucks et al., 2005). Sensitivity analysis for the best performing ANN algorithms were performed for the independent parameters affecting Internal Load Index. The sensitivity of the input parameters is shown in Figure 6.4 and 6.5 for the corresponding PNN and MLP algorithms. The PNN shows highest sensitive index for indoor relative-humidity (0.2068) followed by indoor temperature (0.1067) while the MLP shows highest sensitive index for outdoor temperature (0.158) for Internal Load Index (ψ_i).

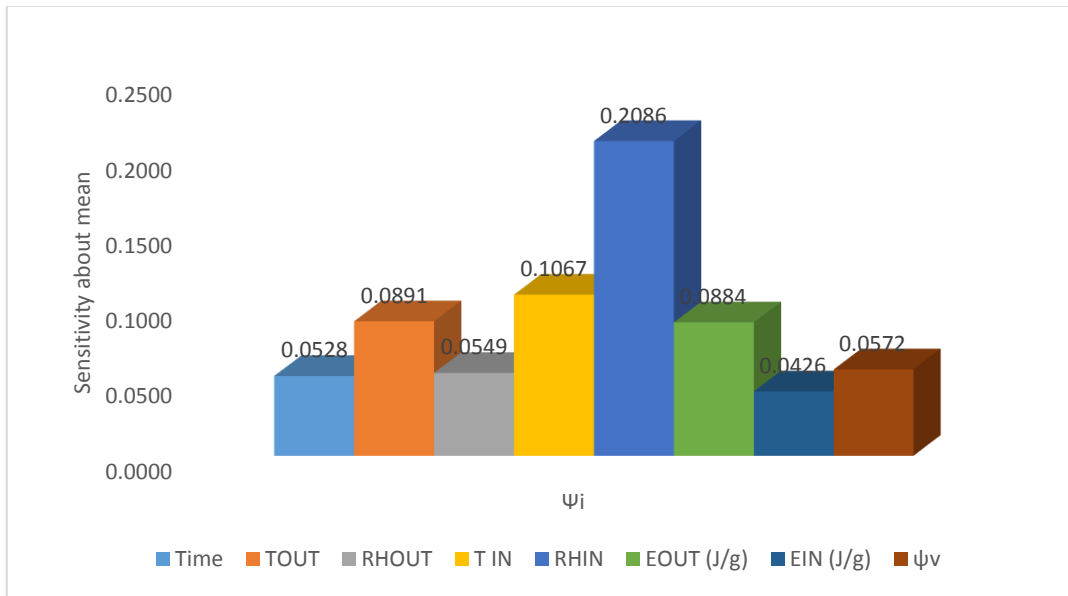


Figure 6.4 Internal Load (ψ_i) sensitivity in ILAN model for using PNN model

The essence of these two algorithms illustrated for the two different case applications 1) When the indoor temperature and relative humidity shows deviation from the design condition, 2) When thermo-hygrometric data are in accordance with the indoor design condition. The PNN can be applied for predicting Internal Loads in the initial case, and MLP can be applied in later case where outdoor temperature is more sensitive towards Internal Load Index prediction (ψ_i).

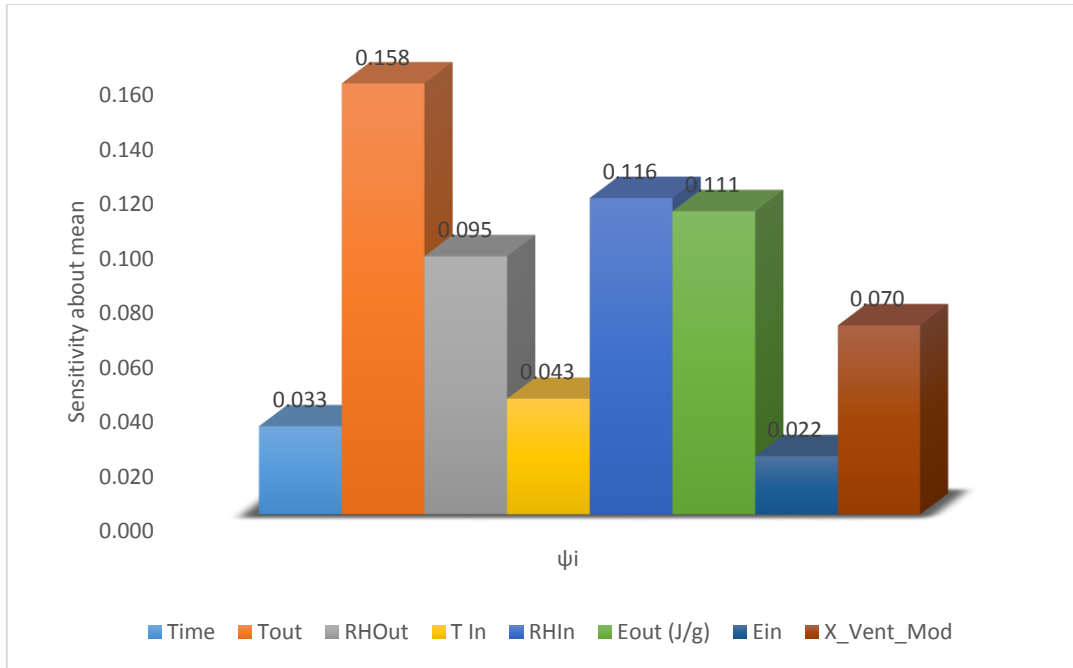


Figure 6.5 Internal Load (ψ_i) sensitivity in ILAN model for using MLP

6.3.2. ACON-ILAN model validation

The concept of hybrid-modeling applied in this case for the condensate estimation using system modeling (ACON) and data driven (ILAN) model. The hybrid model was simulated for time-step condensation and validated with the observed data from the Test-Building-II using.

Hourly simulations applied using simulation settings listed in Table 6.1 with 20 % outdoor ventilation. The validation were performed in terms of 1) Binary operating coefficient ($\epsilon = 1, 0$), and 2) time-step condensation for both the internal l, and Ventilation Load. The ACON was applied to determine Ventilation Load and Binary operating coefficient, and concurrently the ILAN was applied to estimate Internal Load Index both for PNN and MLP algorithms as discussed in previous section.

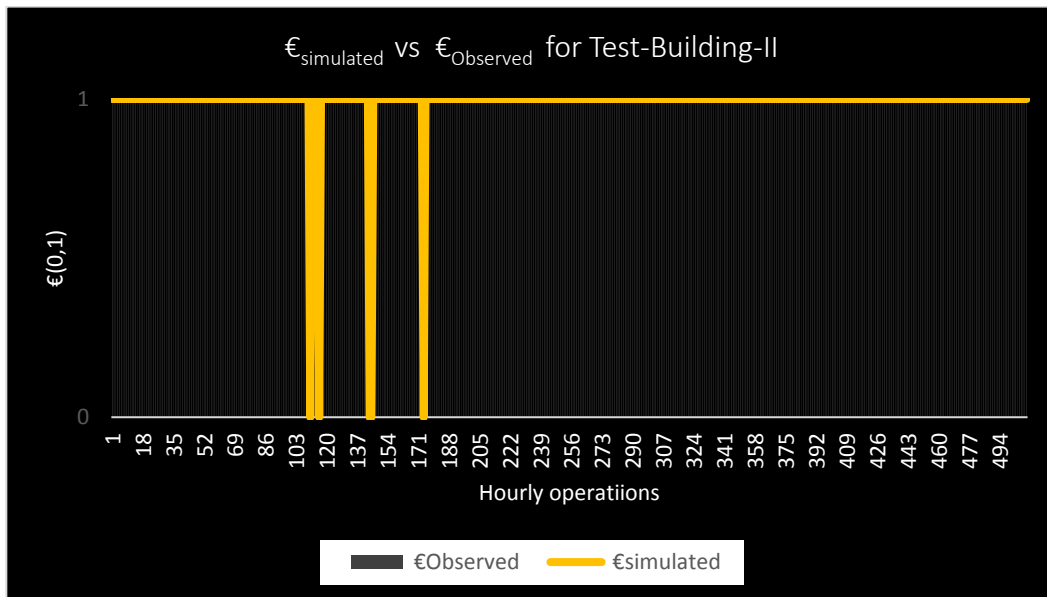


Figure 6.6 Comparison of observed and simulated Binary Operational Coefficient for Test-Building-II

As the HVAC systems operates to maintain the indoor energy by offsetting the energy gain the system, the potential operational duration of HVAC system can be determined, as discussed in Section 5. The ACON simulated Binary operating coefficients were determined for Test-Building-II for 509 hourly operating points. The real-time data shows all the 509 points as operational ($\epsilon=1$). ACON simulations for the corresponding thermo-hygro-metric conditions determined 504 cases of true-positive operating conditions ($\epsilon=1$), and 5 case

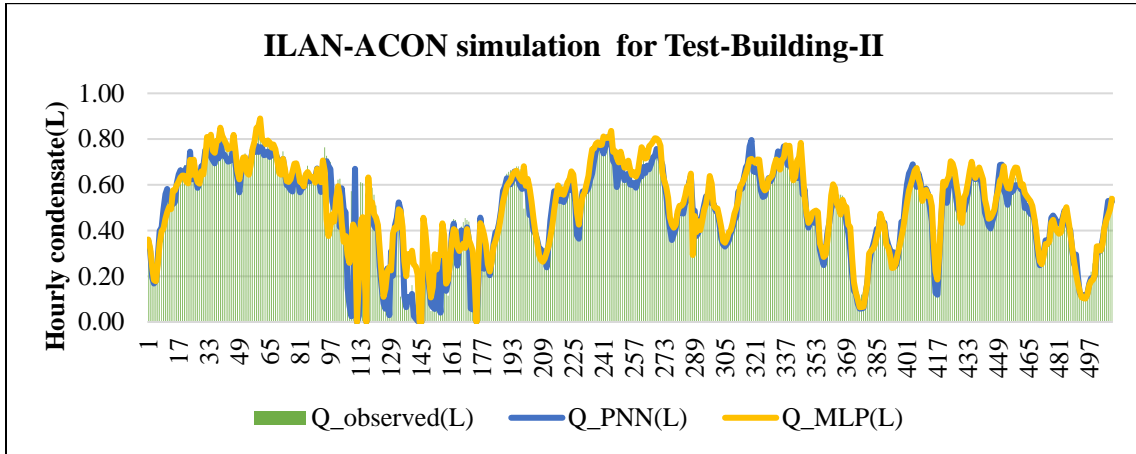


Figure 6.7 Hourly condensate simulation with ACON-ILAN for Test-Building-II

with false-negative ($\epsilon=0$), with overall accuracy of 99.1 %. The simulated and observed points for their corresponding hourly operating points are shown in Figure 6.6.

ILAN –ACON simulations for the observed thermo-hygrometric condition and the same HVAC operational settings were applied for Test-Building-II. In this case the ILAN was applied to determine Internal Load by both the algorithms; 1) PNN, and 2) MLP. The observed and simulated condensate data were shown in Figure 6.7. The corresponding scatter plots are shown in Figure 6.8, where the ILAN-ACON with PNN and MLP shows R^2 of 0.905, and 0.886 respectively.

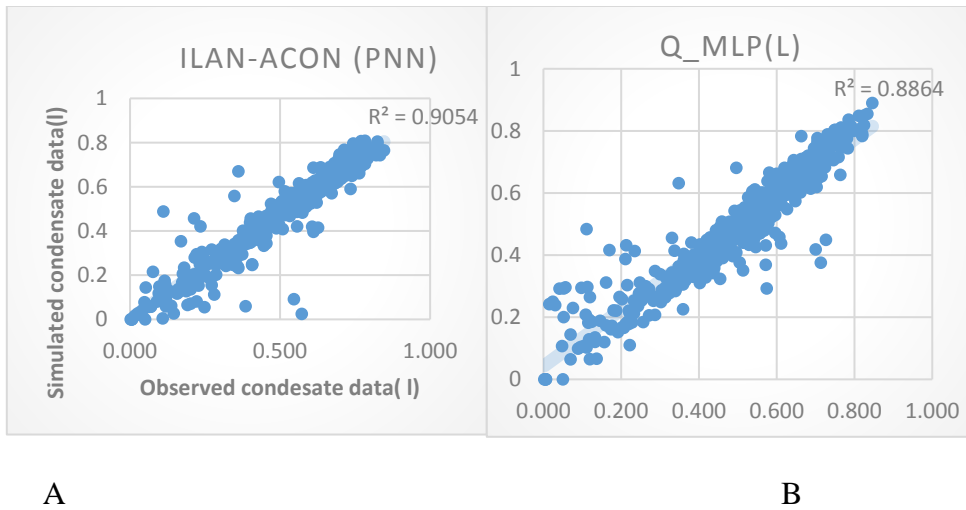


Figure 6.8 ILAN-ACON simulated condensate compared with the observed condensate applying A) PNN, B) MLP for Test-Building-II

6.4. ILAN-ACON deployment with Doha climatic data

The case study demonstrated the ILAN-ACON deployment in ideal condition; where the indoor design condition is fixed though out the year, determining condensates based on the outdoor variation in temperature and humidity data.

Variability in outdoor thermo-hygrometric conditions for the city of Doha is represented in Figure 6.9, which shows year-wide daily-mean variation of temperature, relative humidity. Indoor temperature were observed between 15 to 32 °C with most frequent operating temperature and relative humidity between 20 to 23 C and 60-65 % respectively as shown Appendix C1. Though, the conditioned space are designed to maintain specific temperature, and relative humidity, the experimental data showed significant variation in the parameters.

Considering the constant design condition of an average 22 C and relative humidity of 60 %, it shows most of the days in year particularly though April and November the daily mean the ambient temperature exceeds the indoor design conditions. The temperature and humidity data were visualized in terms of ambient energy (enthalpy), which is combined effect of sensible and latent heat energy (the temperature corresponds to the sensible heat and the moisture content as latent heat). Figure 6.10 shows the outdoor energy variation with fixed indoor energy (indoor design conditions).

The ACON model was simulated to determine the Binary-Operational Coefficient [$\epsilon (1, 0)$] HVAC operation duration corresponding to the outdoor conditions. The Figure 6.10 shows; HVAC units are operational with condensation during most part of year. In this case it determines 234 days the system will operate with condensate formation.

ILAN-ACON was applied for the 234 operating point's simulations using daily mean temperature, and the relative humidity for HVAC control setting as listed in Table 6.1 at 1 SV/hr. with cooling space of 100 m³. The ILAN was applied using MLP, in internal cooling-supply index (ψ_i) as described in section 6.3.1. In this case, the indoor design conditions are fixed, and outdoor conditions vary. Therefore MLP was applied for predicting (ψ_i), assuming the prediction will be more accurate for variable outdoor conditions than PNN (which is more sensitive towards indoor condition). The ACON model was applied with ILAN generated (ψ_i) as input, and was simulated for: 1) 20% outdoor ventilation, 2) 100 % outdoor ventilation. The ILAN-ACON daily simulation

results are shown in Figure 6.11, and monthly estimated condensate shown in Figure 6.12. The statistical analysis of simulated condensate is shown Appendix (C2) .

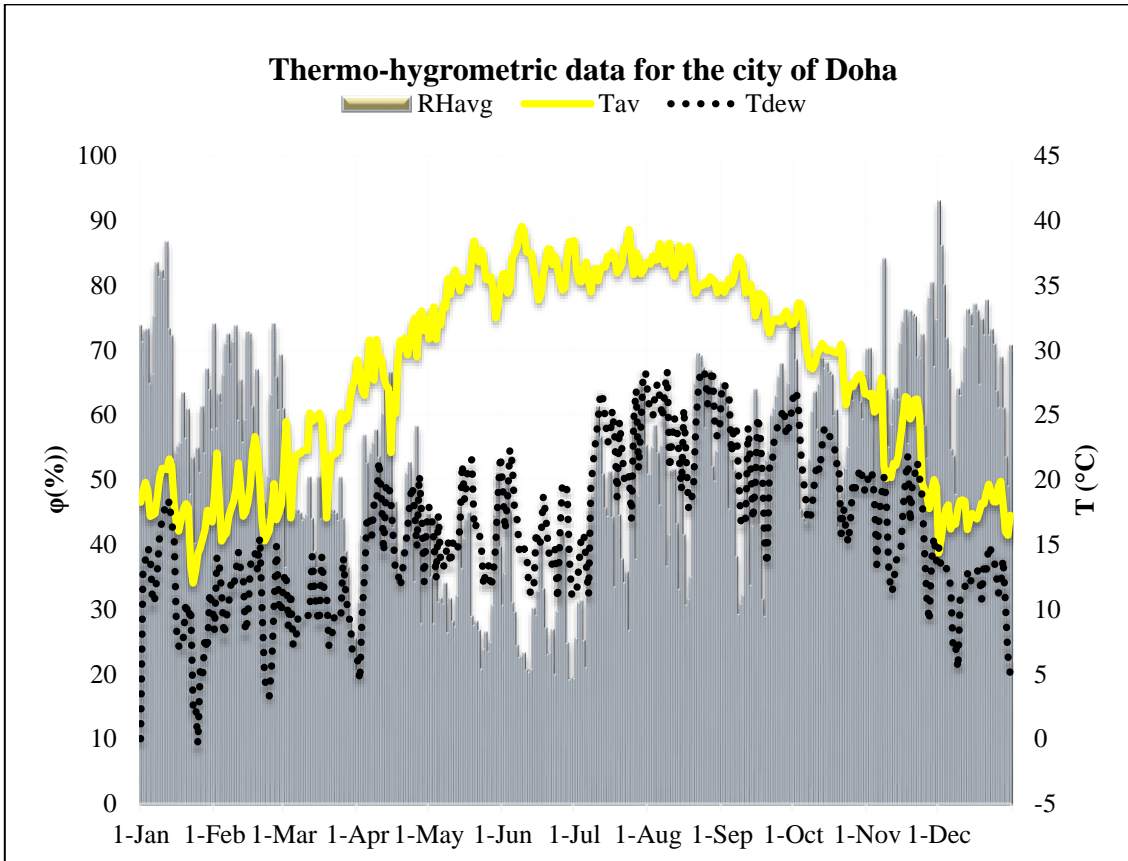


Figure 6.9 Thermo-hygrometric data variation for the city of Doha

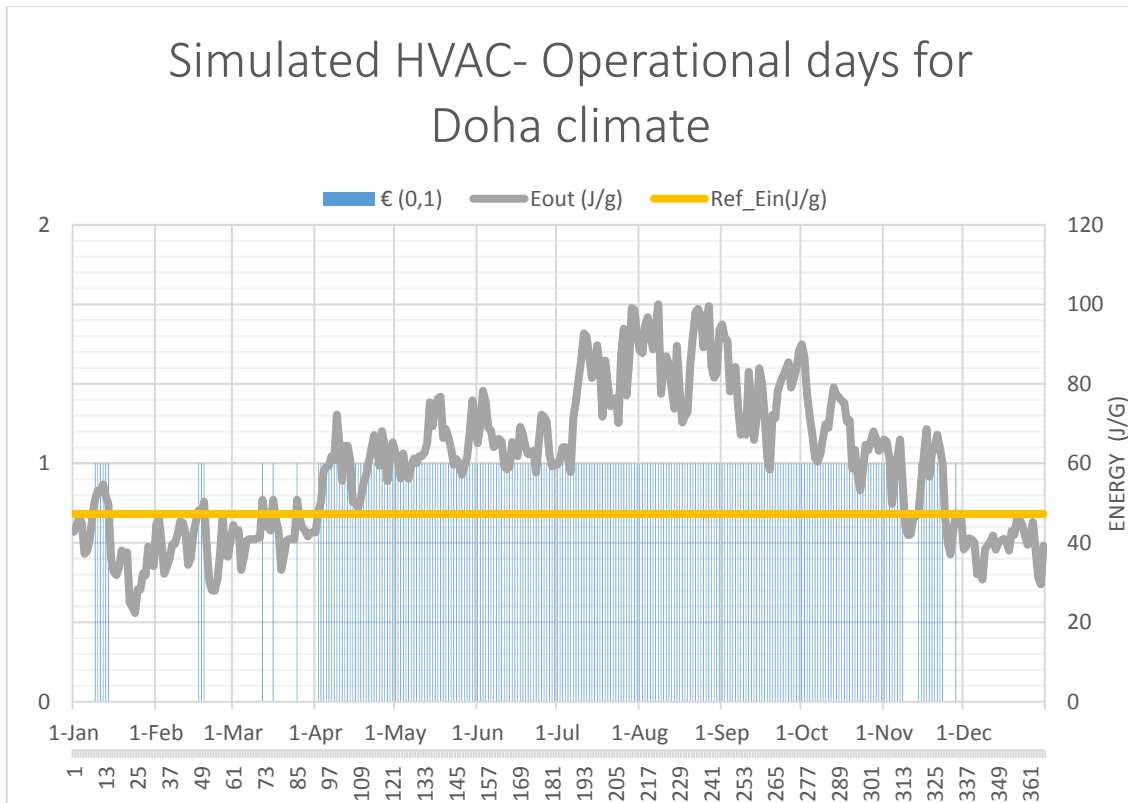


Figure 6.10 Binary Operational Coefficient with respect to outdoor energy and fixed indoor design conditions for the city of Doha

The data showed higher condensate due to higher ventilation especially during peak summer (May-September); which varied 851.4 l in August to 302.6 l in May. However ventilation has the least impact during winter or moderately warm seasons as the primary attribute to condensate is Internal Load. The HVAC system operating at lower ventilation, even during summer (May –September) the condensate is not quite significantly different, as the monthly condensate varies between 156 l in May to 221 l in August for 20 % ventilation. Overall, the total yearly condensate for 100 m³ of

cooling space is 3700 l condensate when using a 100 % ventilated HVAC system compared to 1370 l for condensate from a 20 % ventilated system.

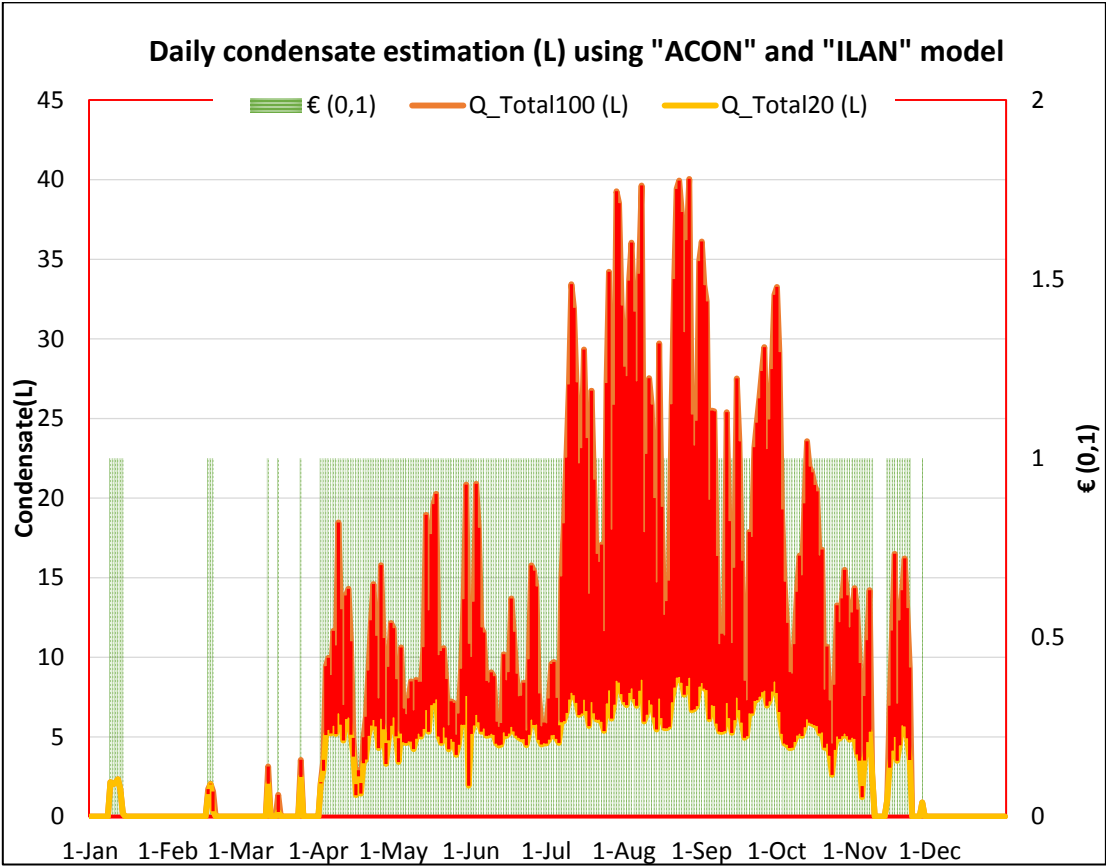


Figure 6.11 Daily condensate simulation for Doha climate at 20 and 100 % ventilation using ACON, and ILAN

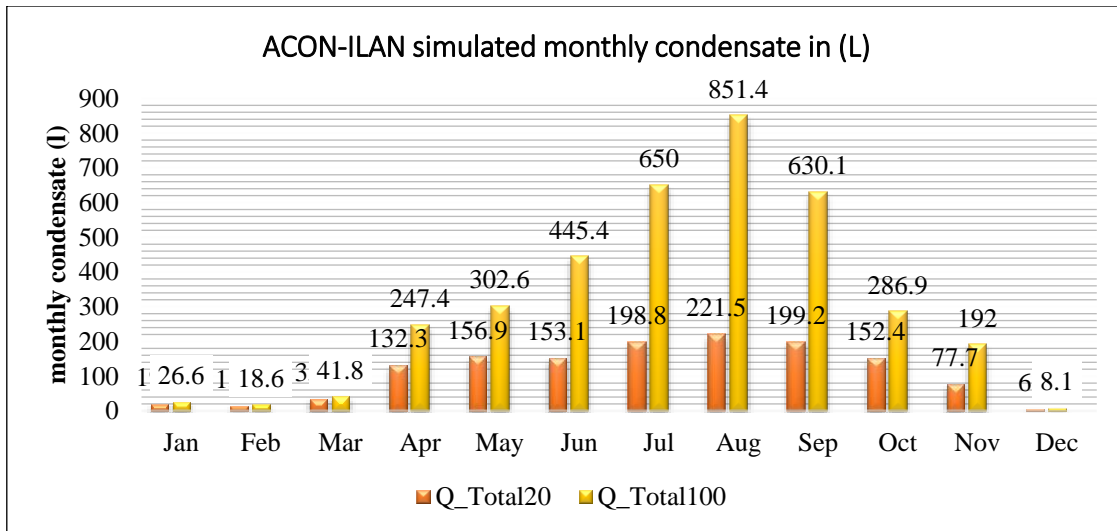


Figure 6.12 Monthly condensate estimation by ILAN-ACON

6.5. Discussion on ILAN-ACON model development and simulation

ILAN-ACON hybrid model showed an added advantage over completely empirical modeling; where the HVAC control changes and varies with the manual settings and therefore the condensate formation depends more on ventilation. Since different buildings are set at different HVAC control, the difference in the condensate is significant as observed in ILAN-ACON simulation of Qatar in Figure 6.12. Therefore the empirical modeling approach has significant disadvantage even in the same location, where it was developed

At the same time the BEES was proposed to determine the cooling load as input for ACON but the determination of the parameters needed for time-step log is quite a cumbersome process. The ILAN model was developed for Qatar using empirical data, which gives an opportunity for the building planners to design for condensate use. The

model can be applied to generalize the internal cooling load. So the total estimation may vary if the Internal Load is not analogous to the test building used in model development. However, in the ILAN-ACON simulation, it is evident that the Internal Load has comparatively lower contribution for total condensation during peak season, compared to Ventilation Load. So the variation of Internal Load is a more significant parameter for HVAC operating either at low ventilation or during moderately warm climate.

Moreover, the reliability on the ILAN model depends on the data considered during training and model development. Though the model provides prediction with correlation r of 0.88 for test data (during MLP), the overall impact on total condensate calculation was not significant. The ILAN-MLP also had similar simulation results when validated for Test-building-II.

The overall simulation result shows high potential for condensate for most of the year primarily between the months of April and November. ACON-ILAN model can be applied as a versatile condensate forecasting tool using forecasted weather data. In turn this will provide decision making strategies to the water planners for condensate use.

6.5.1. A/C condensate water quality analysis for Doha

The samples showed marginal presence of Zn, and Se, Cu, and Mn with maximum values of 0.04, 1.19, 1.63, 0.02 mg/l, respectively. However, no trace was detected for Al, Ba, Cd, Co, Cr, Ni, Pb, and Sr.

The observed pH value for condensate was between 6.5 to 7.1, which is in accordance with the Cook et al., (2014), and Bryant et al., (2008). This increases the

condensate suitability for unrestricted irrigation and livestock's, and also is within the drinking water standards, except for the observations shows pH below 6.5 (Loveless et al., 2013).

The low conductivity of the observed samples between 35.1 to 134 $\mu\text{S}/\text{cm}$ shows unrestricted water use and excellent for irrigation water. The sample showed some presence of (Na^+), (Mg^{+2}), and (Ca^{+2}) in the condensate sample with maximum value of 0.90, 8.39, and 0.31 mg/l. The drinking water not set for (Mg^{+2}), and (Ca^{+2}), but the (Na^+) concentration is below the secondary drinking water standards (20mg/l) and also suitable for irrigation, livestock and industrial uses as shown in Appendix C3.

The condensate water also showed marginal presence of (Cl^-) between 0.77 to 14.5 mg/l and (SO_4^{-2}) between 0.77 to 21.4 mg/l. Though no standards set for (Cl^-), the (SO_4^{-2}) is below the mcl of 250 mg/l for secondary drinking water standards. At the same time no presence were detected for (NO_3^-) and phosphate (PO_4^{-3}) in all the samples. A study from Cook et al., (2014) and Bryan et al., (2008) shows the marginal presence of (NO_3^-) as shown in Table 6.1.

6.5.1.1. Discussion on water quality:

The study showed the water quality of condensate equivalent to drinking water standard, and can applied for unrestricted water use beyond the conventional reuse for toilet flushing, irrigation, and industrial applications.

Latures not know to author knowledge were reported for heavy metal presence in condensate water. Parameters are under the primary and secondary drinking water standard as shown in Table 6.3 except for Cu, which exceeds the MCL (maximum

contamination limitations) for the both primary(1.3 mg/l) and secondary (1.0 mg/l) water standards as well as the irrigation, and industrial boiler standards. Though the average value of Cu was within the range, but attention may be required for Cu as limiting factor for unrestricted use of condensate water. Although, the microbial analysis showed negative results for total coliform presence, lature survey from (Alipour et al., 2013) shows substantial microbial contamination in condensate water. There could be a possible variability in condensate quality depending on the age and type of the HVAC units, corrosion of pipes or duct lines used (Diaz, 2014), and outside air quality, that require local testing before reuse..

6.6. Conclusion

6.6.1. ILAN model

The ILAN model provided a generalized solution for internal Cooling Load Index simulation primarily from time series thermo-hygrometric (T, RH) data for indoor and outdoor conditions. Different ANN algorithms and architecture were considered while developing ILAN model. PNN was applied as the best performing ANN algorithms showing the highest perdition accuracy in Cooling Load Index (ψ) with correlation r as 0.99, 0.87, and 0.88 for training, cross-validation and testing data. Sensitivity analysis showed that the Internal Load is highly correlated to indoor temperature and humidity compared to secondary parameters derived from the ACON model. The ILAN model is an added advantage to conventional BESS programs as it is less data intensive and can be used for locations where parameters are not available for

BESS simulations. However, it refers to Internal Load only simultaneous process of cooling and dehumidification.

6.6.2. ILAN-ACON hybrid model

The ILAN-ACON hybrid model provides a clear methodology in condensate estimation; which can be applied for time-step condensate simulation considering; 1) temporal, 2) geographical, and 3) climatic/seasonal variability. The ILAN-ACON model can be easily deployed with thermo-hygrometric data and is capable of determining condensate with much higher accuracy than empirical modeling for condensate estimation which are season and location specific. ILAN-ACON simulation results showed the impact of Internal Load to be higher in total condensate formation particularly during moderately warm and humid climate and also during low ventilation profile HVAC systems (e.g. 20 %). However, HVAC controls like ventilation have a significant impact on condensate formation particularly during peak summer season.

6.6.3. Impact of cooling load type on condensate formation

Internal Load is the primary factor governing condensate formation during low ventilation and moderately warm climate as the ambient and internal energy difference is much lower in these cases. The majority of condensation is a result of air ventilation in peak summer. The Internal Load shows impact during the moderately warm climate from December to March, as the simulations at 20 and 100 % ventilation do not show much difference in condensate formation. The Ventilation Load significantly varies with variable ventilation and indoor volumetric exchange rates. The model has the capability

to determine time-step Ventilation Load for varying ventilation types and room air exchange rate using the thermo-hygrometric data.

6.6.4. Potential of A/C condensate for the city of Doha

For the city of Doha with its ultramodern-urban setup, and hot-humid climate, the study showed high-quantity of condensate can be produced with potentially high water quality and can be substantially applied as alternative water resource during most part of year with significant volumetric reduction in desalinated water demand for city. ILAN-ACON can be applied as a versatile tool unlike most of condensate estimation formulations which are site-specific or completely empirical in nature (Section 5).

7 CONCLUSION AND SUMMARY

This study aims at improving potentials of greywater and Air-Conditioner (A/C) condensate reuse particularly in urban settings by providing tools to integrate emerging alternative water resources into water management plans. It addresses the water quality variability in greywater and lack of knowledge/attention in greywater treatment that is needed to make this source more widely used. It also addresses the quantification of A/C condensate in a comprehensive way that will allow builders and planners to design cost effective A/C condensate collection systems for reuse. The following specific conclusions were found:

- 1) Due to water quality variability in greywater, treatment systems were applied in series, which allows for specific treatments for the type of greywater (i.e. shower, wash basin or Washing machine), and is robust enough to produce high grade effluent good for unrestricted water use. The broad impact of this study is to reduce the cost of greywater treatment by selecting appropriate treatments to specific needs.
- 2) An advanced physical filtration like GAC-MI-ME can improve the utility of greywater in urban settings by providing ease of operation, portability, and user customized water availability. The multi-grade effluent of the treatment system provides an economic option for users by avoiding over or under treatment of greywater for a specific use and meeting local regulation on water-reuse. That will also help to determine the extent of treatment required for the specific characteristics of their greywater to meet requirements for specific uses including safe discharge into the environment to landscape and vegetable irrigation, toilet flushing, and even potable use.

- 3) The sensitivity analysis of unit-models determined the specific parameter that caused the most variability in treatment trains affecting the effluent in UF and RO effluent. This can be used to further improve the GAC-MI-ME greywater treatment system.
- 4) The ILAN-ACON model provided a methodology in condensate estimation, which can be potentially applied for time-step condensate simulation considering a) temporal, b) geographical, and c) climatic/seasonal variability.
- 5) The study also demonstrated the use of ACON model in time step condensate estimation by determining intensity and duration of HVAC operation based on the outdoor condition. This adds a strategic advantage for planners, as this tool may potentially help in water supply planning. The improved accuracy in condensate estimate over the conventional empirical approach will promote its use in several ways; a) determining the financial costs and return associated with piping and plumbing requirements of condensate collection and, b) and also may help in decision-making in water supply strategies even during low production periods.
- 6) Greywater and A/C condensate would reduce the volume of wastewater from residential and commercial buildings, and thereby reduce the municipal cost of wastewater treatment. Houses and the building can independently use their reclaimed water for lawn irrigation, toilet flushing, laundry, car wash, or other unrestricted purposes. The study may also contribute in establishing the fact that greywater reuse and A/C condensate can partially offset high-grade water supply.

- 7) This study provides planners and designers of water reuse systems with tools , which may result in a wider reuse of greywater and A/C condensate, especially in water scarce areas, thereby reducing the impact of increased water use and population growth on dwindling water resources.
- 8) The primary beneficiary would be the commercial developers and city planners working on green infrastructure.

7.1 Future work

A/C condensate and GAC-MI-ME RO effluent can be categorized as pure water. A further analysis is required to compare the condensate and RO effluent with drinking water standards.

A study on the operational performance of the GAC-MI-ME system regarding membrane fouling characteristics may help in cost & efficiency optimization.

The water quality of condensate may depend on the age and Type of A/C and the surrounding area. A thorough analysis of A/C condensate quality will improve its reuse potential primarily for direct potable use. A proper air filtration of the outdoor air duct can also improve the water quality of the condensate, as well as the quality associated with indoor air, outdoor air, and HVAC duct.

The Unit –Models for GREY-ANN can be improved with increasing the experimental data. The operational data can be applied to improve the system performance. A cost module determination based on the life of for the filter modules, energy consumption, and initial cost associated with it would be beneficial.

The study provides a method that can be applied as a micro tool for greywater reuse and water supply duration.

In addition, other factors need to be emphasized for wider application of alternative resources such as 1) improvement of water reuse regulations to be more specific to the type of alternative resource and the extent of its treatment, 2) Integration of decision support tools that determine the robustness of treatment systems specific to treatment technology for specific type of alternative resources, and will also help in providing water supply strategies for specific uses, 3) More public awareness is desired towards achieving future sustainable goals with alternative resources. That will help in increasing social acceptability and positive perception towards use the alternative resources, 4) Lifetime assessments tools are required for each of the proposed alternative resources in order to meet the overall sustainability.

REFERENCES

- Abahussain, A. A., Abdu, A. S., Al-Zubari, W. K., El-Deen, N. A., & Abdul-Raheem, M. (2002). Desertification in the arab region: Analysis of current status and trends. *Journal of Arid Environments*, 51(4), 521-545.
- Abdel-Shafy, H., El-Khateeb, M., Regelsberger, M., El-Sheikh, R., & Shehata, M. (2009). Integrated system for the treatment of blackwater and greywater via UASB and constructed wetland in egypt. *Desalination and Water Treatment*, 8(1-3), 272-278.
- Abrishamchi, A., Ebrahimian, A., Tajrishi, M., & Mariño, M. A. (2005). Case study: Application of multicriteria decision making to urban water supply. *Journal of Water Resources Planning and Management*, 131(4), 326-335.
- Aktacir, M. A., Büyükalaca, O., & Yılmaz, T. (2010). A case study for influence of building thermal insulation on cooling load and air-conditioning system in the hot and humid regions. *Applied Energy*, 87(2), 599-607.
- Alahmer, A., Omar, M., Mayyas, A., & Dongri, S. (2011). Effect of relative humidity and temperature control on in-cabin thermal comfort state: Thermodynamic and psychometric analyses. *Applied Thermal Engineering*, 31(14), 2636-2644.
- Al-Jayyousi, O. R. (2003). Greywater reuse: Towards sustainable water management. *Desalination*, 156(1), 181-192.
- Allen, L., Christian-Smith, J., & Palaniappan, M. (2010). Overview of greywater reuse: The potential of greywater systems to aid sustainable water management. *Pacific Institute*, 654.

- Al-Rabghi, O. M., Al-Beirutty, M. H., & Fathalah, K. A. (1999). Estimation and measurement of electric energy consumption due to air conditioning cooling load. *Energy Conversion and Management*, 40(14), 1527-1542.
- Al-Weshah, R. (2003). The role of UNESCO in sustainable water resources management in the arab world. *Desalination*, 152(1), 1-13.
- Anderson, D. M., & Anderson, D. E. (2011). Process for Rain Water, HVAC Condensate and Refrigeration Blowdown/Bleed Blowdown/Bleed Water Recovery, Water Quality Monitoring, Real Time Water Treatment and Utilization of Recovered Water, *U.S. Patent Application No. 12/840,894*.
- Andreadakis, A., Mamais, D., Christoulas, D., & Kabylafka, S. (1999). Ultraviolet disinfection of secondary and tertiary effluent in the mediterranean region. *Water Science and Technology*, 40(4-5), 253-260.
- Arnell, N. W. (1999). Climate change and global water resources. *Global Environmental Change*, 9, S31-S49.
- Asano, T. (2007). Milestones in the reuse of municipal wastewater. *Proceedings of Water Supply and Sanitation for all*, 295-306.
- Balaras, C. A., Dascalaki, E., & Gaglia, A. (2007). HVAC and indoor thermal conditions in hospital operating rooms. *Energy and Buildings*, 39(4), 454-470.
- Bartels, C., Franks, R., & Andes, K. (2010). Operational performance and optimization of RO wastewater treatment plants. *Singapore International Water Week, Singapore*,
- Bearg, D. W. (1993). *Indoor air quality and HVAC systems* CRC Press.

- Ben-Nakhi, A. E., & Mahmoud, M. A. (2004). Cooling load prediction for buildings using general regression neural networks. *Energy Conversion and Management*, 45(13), 2127-2141.
- Birks, R., & Hills, S. (2007). Characterisation of indicator organisms and pathogens in domestic greywater for recycling. *Environmental Monitoring and Assessment*, 129(1-3), 61-69.
- Birol, E., Koundouri, P., & Kountouris, Y. (2010). Assessing the economic viability of alternative water resources in water-scarce regions: Combining economic valuation, cost-benefit analysis and discounting. *Ecological Economics*, 69(4), 839-847.
- Boers, T. M., & Ben-Asher, J. (1982). A review of rainwater harvesting. *Agricultural Water Management*, 5(2), 145-158.
- Bowden, G. J., Dandy, G. C., & Maier, H. R. (2005). Input determination for neural network models in water resources applications. part 1—background and methodology. *Journal of Hydrology*, 301(1), 75-92.
- Boyjoo, Y., Pareek, V. K., & Ang, M. (2013). A review of greywater characteristics and treatment processes. *Water Science and Technology*, 67(7), 1403-1424.
- Bryant, J. A., & Ahmed, T. (2008). Condensate water collection for an institutional building in doha, qatar: An opportunity for water sustainability. Energy Systems Laboratory. Retrieved from <http://hdl.handle.net/1969.1/90780>
- Buratti, C., & Ricciardi, P. (2009). Adaptive analysis of thermal comfort in university classrooms: Correlation between experimental data and mathematical models. *Building and Environment*, 44(4), 674-687.

- Burton, D. J. (2008). *IAQ and HVAC workbook IVE*.
- Burton, J., DiBerardinis, L., Price, J., & Mavely, M. (2008). Standards of good practice: Overview of ANSI Z9 ventilation standards with emphasis on ANSI/AIHA Z9.2-2006: Fundamentals governing the design and operation of LEV systems. *Journal of Chemical Health and Safety*, 15(3), 4-8.
- Busch, J., Cruse, A., & Marquardt, W. (2007). Modeling submerged hollow-fiber membrane filtration for wastewater treatment. *Journal of Membrane Science*, 288(1), 94-111.
- Butler, D., & Memon, F. A. (2005). *Water demand management* Iwa Publishing.
- Chaillou, K., Gérente, C., Andrès, Y., & Wolbert, D. (2011). Bathroom greywater characterization and potential treatments for reuse. *Water, Air, & Soil Pollution*, 215(1-4), 31-42.
- Chen, R., & Wang, X. (2009). Cost–benefit evaluation of a decentralized water system for wastewater reuse and environmental protection. *Water Science and Technology*, 59(8), 1515-1522.
- Chou, S., & Wong, Y. (1986). Predicting energy performance of commercial buildings in singapore. *ASHRAE Trans.:(United States)*, 92(CONF-860106-)
- Christova-Boal, D., Eden, R. E., & McFarlane, S. (1996). An investigation into greywater reuse for urban residential properties. *Desalination*, 106(1-3), 391-397.
- Cohen, B. (2006). Urbanization in developing countries: Current trends, future projections, and key challenges for sustainability. *Technology in Society*, 28(1), 63-80.

- Cook, S., Sharma, A. K., & Gurung, T. R. (2014). Evaluation of alternative water sources for commercial buildings: A case study in brisbane, australia. *Resources, Conservation and Recycling*, 89, 86-93.
- Crawley, D. B. (2008). Estimating the impacts of climate change and urbanization on building performance. *Journal of Building Performance Simulation*, 1(2), 91-115.
- Crawley, D. B., Hand, J. W., Kummert, M., & Griffith, B. T. (2008). Contrasting the capabilities of building energy performance simulation programs. *Building and Environment*, 43(4), 661-673.
- Crittenden, J. C., Vaitheeswaran, K., Hand, D. W., Howe, E. W., Aieta, E. M., Tate, C. H., Davis, M. K. (1993). Removal of dissolved organic carbon using granular activated carbon. *Water Research*, 27(4), 715-721.
- Crittenden, J. C., Trussell, R. R., Hand, D. W., Howe, K. J., & Tchobanoglous, G. (2012). *MWH's water treatment: Principles and design* Wiley.
- De Koning, J., Bixio, D., Karabelas, A., Salgot, M., & Schäfer, A. (2008). Characterisation and assessment of water treatment technologies for reuse. *Desalination*, 218(1-3), 92-104.
- Delfani, S., Pasharshahi, H., & Karami, M. (2012). Experimental investigation of heat recovery system for building air conditioning in hot and humid areas. *Energy and Buildings*, 49, 62-68.
- Delgrange, N., Cabassud, C., Cabassud, M., Durand-Bourlier, L., & Laine, J. (1998). Neural networks for prediction of ultrafiltration transmembrane pressure—

- application to drinking water production. *Journal of Membrane Science*, 150(1), 111-123.
- Diaz, P., Isenbeck, J., & Yeh, D. H. (2014). Air conditioning condensate recovery and reuse for non-potable applications. *Alternative Water Supply Systems*, , 169.
- Dixon, A. M., Butler, D., & Fewkes, A. (1999). Guidelines for greywater Re-Use: Health issues. *Water and Environment Journal*, 13(5), 322-326.
- Dixon, A., Butler, D., Fewkes, A., & Robinson, M. (2000). Measurement and modelling of quality changes in stored untreated grey water. *Urban Water*, 1(4), 293-306.
- Duarte, R., Pinilla, V., & Serrano, A. (2014). Looking backward to look forward: Water use and economic growth from a long-term perspective. *Applied Economics*, 46(2), 212-224.
- Einav, R., & Lokiec, F. (2003). Environmental aspects of a desalination plant in ashkelon. *Desalination*, 156(1), 79-85.
- El-Din, A. G., Smith, D. W., & El-Din, M. G. (2004). Application of artificial neural networks in wastewater treatment. *Journal of Environmental Engineering and Science*, 3(S1), S81-S95.
- Elmitwalli, T. A., & Otterpohl, R. (2007). Anaerobic biodegradability and treatment of grey water in upflow anaerobic sludge blanket (UASB) reactor. *Water Research*, 41(6), 1379-1387.
- EPA. (2003). Environmental protection agency. National primary and secondary drinking water standards.
<https://www.env.nm.gov/dwb/contaminants/documents/MCLs.pdf>

EPA. (2007). Environmental protection agency.

https://www.epa.gov/sites/production/files/2015-08/documents/2007_07_10_oceans_regulatory_unds_tdddocuments_apparefriger.pdf

EPA. (2009). Environmental protection agency.

<http://www.epa.gov/sites/production/files/2015>

Eriksson, E., Auffarth, K., Henze, M., & Ledin, A. (2002). Characteristics of grey wastewater. *Urban Water*, 4(1), 85-104.

Eriksson, E., Andersen, H. R., Madsen, T. S., & Ledin, A. (2009). Greywater pollution variability and loadings. *Ecological Engineering*, 35(5), 661-669.

Evans, C., Coombes, P., & Dunstan, R. (2006). Wind, rain and bacteria: The effect of weather on the microbial composition of roof-harvested rainwater. *Water Research*, 40(1), 37-44.

Fan, L., & Boshnakov, K. (2010). Neural-network-based water quality monitoring for wastewater treatment processes. Paper presented at the *2010 Sixth International Conference on Natural Computation*, , 4 1746-1748.

Fane, S., Ashbolt, N., & White, S. (2002). Decentralised urban water reuse: The implications of system scale for cost and pathogen risk. *Water Science & Technology*, 46(6), 281-288.

Fang, L., Clausen, G., & Fanger, P. O. (1998). Impact of temperature and humidity on the perception of indoor air quality. *Indoor Air*, 8(2), 80-90.

- Fausett, L. (1994). *Fundamentals of neural networks: Architectures, algorithms, and applications* Prentice-Hall, Inc.
- Fewtrell, L., & Kay, D. (2007). Microbial quality of rainwater supplies in developed countries: A review. *Urban Water Journal*, 4(4), 253-260.
- Förster, J. (1999). Variability of roof runoff quality. *Water Science and Technology*, 39(5), 137-144.
- Friedler, E. (2004). Quality of individual domestic greywater streams and its implication for on-site treatment and reuse possibilities. *Environmental Technology*, 25(9), 997-1008.
- Friedler, E., Kovalio, R., & Galil, N. (2005). On-site greywater treatment and reuse in multi-storey buildings. *Water Science & Technology*, 51(10), 187-194.
- Gerard, R. D., & Worzel, J. L. (1967). Condensation of atmospheric moisture from tropical maritime air masses as a freshwater resource. *Science (New York, N.Y.)*, 157(3794), 1300-1302.
- Ghunmi, L. A., Zeeman, G., Fayyad, M., & van Lier, J. B. (2011). Grey water treatment systems: A review. *Critical Reviews in Environmental Science and Technology*, 41(7), 657-698.
- Gleick, P. H. (2000). A look at twenty-first century water resources development. *Water International*, 25(1), 127-138.
- Gontarski, C., Rodrigues, P., Mori, M., & Prenem, L. (2000). Simulation of an industrial wastewater treatment plant using artificial neural networks. *Computers & Chemical Engineering*, 24(2), 1719-1723.

- Gonzalez, S., Petrovic, M., & Barcelo, D. (2007). Removal of a broad range of surfactants from municipal wastewater—comparison between membrane bioreactor and conventional activated sludge treatment. *Chemosphere*, 67(2), 335-343.
- Gouda, M., Danaher, S., & Underwood, C. (2002). Application of an artificial neural network for modelling the thermal dynamics of a building's space and its heating system. *Mathematical and Computer Modelling of Dynamical Systems*, 8(3), 333-344.
- Greenlee, L. F., Lawler, D. F., Freeman, B. D., Marrot, B., & Moulin, P. (2009). Reverse osmosis desalination: Water sources, technology, and today's challenges. *Water Research*, 43(9), 2317-2348
- Gross, A., Shmueli, O., Ronen, Z., & Raveh, E. (2007). Recycled vertical flow constructed wetland (RVFCW)—a novel method of recycling greywater for irrigation in small communities and households. *Chemosphere*, 66(5), 916-923.
- Gross, A., Azulai, N., Oron, G., Ronen, Z., Arnold, M., & Nejidat, A. (2005). Environmental impact and health risks associated with greywater irrigation: A case study. *Water Science and Technology*, 52(8), 161-169.
- Guilbaud, J., Massé, A., Andrès, Y., Combe, F., & Jaouen, P. (2010). Laundry water recycling in ship by direct nanofiltration with tubular membranes. *Resources, Conservation and Recycling*, 55(2), 148-154.
- Gulyas, H. (2007). Greywater reuse—Concepts, benefits, risks and treatment technologies. Paper presented at the *International Conference on Sustainable Sanitation—Food*

and Water Security for Latin America, Fortaleza, Ceará, Brazil.

- Guo, L., & Santschi, P. H. (1996). A critical evaluation of the cross-flow ultrafiltration technique for sampling colloidal organic carbon in seawater. *Marine Chemistry*, 55(1), 113-127.
- Gur-Reznik, S., Katz, I., & Dosoretz, C. G. (2008). Removal of dissolved organic matter by granular-activated carbon adsorption as a pretreatment to reverse osmosis of membrane bioreactor effluents. *Water Research*, 42(6), 1595-1605.
- Guz, K. (2005). Condensate water recovery. *ASHRAE Journal*, 47(6), 54.
- Halalsheh, M., Dalahmeh, S., Sayed, M., Suleiman, W., Shareef, M., Mansour, M., et al., (2008). Grey water characteristics and treatment options for rural areas in Jordan. *Bioresource Technology*, 99(14), 6635-6641
- Hamed, M. M., Khalafallah, M. G., & Hassanien, E. A. (2004). Prediction of wastewater treatment plant performance using artificial neural networks. *Environmental Modelling & Software*, 19(10), 919-928.
- Hamoda, M. F., Al-Ghusain, I. A., & Hassan, A. H. (1999). Integrated wastewater treatment plant performance evaluation using artificial neural networks. *Water Science and Technology*, 40(7), 55-65.
- Handbook, A. (2009). Fundamentals atlanta: American society of heating, air-conditioning and refrigeration engineers. *Inc*,
- Harnett, L., Nicolson, J., Tennant, R., Dandy, G., & Maier, H. (2009). Sustainability trade-offs in the planning and design of cluster scale greywater reuse systems.

Paper presented at the *Proceedings of the 18th World IMACS/MODSIM Congress, Cairns, Australia, , 33363342*

- Hering, D., Borja, A., Carstensen, J., Carvalho, L., Elliott, M., Feld, C. K., . . . Pont, D. (2010). The european water framework directive at the age of 10: A critical review of the achievements with recommendations for the future. *Science of the Total Environment*, 408(19), 4007-4019.
- Hong, T. (2009). Comparisons of HVAC simulations between EnergyPlus and DOE-2.2 for data centers. *Lawrence Berkeley National Laboratory*.
- Höpner, T., & Windelberg, J. (1997). Elements of environmental impact studies on coastal desalination plants. *Desalination*, 108(1), 11-18.
- Hospodsky, D., Qian, J., Nazaroff, W. W., Yamamoto, N., Bibby, K., Rismani-Yazdi, H., & Peccia, J. (2012). Human occupancy as a source of indoor airborne bacteria. *PloS One*, 7(4), e34867.
- Hourlier, F., Masse, A., Jaouen, P., Lakel, A., Gerente, C., Faur, C., & Le Cloirec, P. (2010). Formulation of synthetic greywater as an evaluation tool for wastewater recycling technologies. *Environmental Technology*, 31(2), 215-223.
- Hui, S. C., & Cheung, K. (1998). Application of building energy simulation to air-conditioning design. Paper presented at the *Proceedings of the Mainland-Hong Kong HVAC Seminar*, 98. pp. 12-20.
- Hunter, N. (2007). Water reuse: Making use of wastewater. *Filtration & Separation*, 44(7), 24-27.

- Jain, A., & Kumar, A. M. (2007). Hybrid neural network models for hydrologic time series forecasting. *Applied Soft Computing*, 7(2), 585-592.
- Jami, M. S., Husain, I. A., Kabashi, N. A., & Abdullah, N. (2012). Multiple inputs artificial neural network model for the prediction of wastewater treatment plant performance. *Australian Journal of Basic and Applied Sciences*, 6(1), 62-69.
- Jamrah, A., Al-Futaisi, A., Prathapar, S., & Al Harrasi, A. (2008). Evaluating greywater reuse potential for sustainable water resources management in oman. *Environmental Monitoring and Assessment*, 137(1-3), 315.
- Jefferson, B., Laine, A., Parsons, S., Stephenson, T., & Judd, S. (2000). Technologies for domestic wastewater recycling. *Urban Water*, 1(4), 285-292.
- Jefferson, B., Palmer, A., Jeffrey, P., Stuetz, R., & Judd, S. (2004). Grey water characterisation and its impact on the selection and operation of technologies for urban reuse. *Water Science and Technology*, 50(2), 157-164.
- Jeppesen, B. (1996). Domestic greywater re-use: Australia's challenge for the future. *Desalination*, 106(1-3), 311-315.
- Kamari, A., Nikookar, M., Sahranavard, L., & Mohammadi, A.H. (2015).Evaluating the reservoir quality parameter (permeability) for efficient oil recovery.
- Kamm, J. (2007). *Fundamentals of psychrometrics*. Atlanta, Ga: ASHRAE.
- Kantanoleon, N., Zampetakis, L., & Manios, T. (2007). Public perspective towards wastewater reuse in a medium size, seaside, mediterranean city: A pilot survey. *Resources, Conservation and Recycling*, 50(3), 282-292.

- Karpiscak, M. M., Foster, K. E., & Schmidt, N. (1990). Residential water conservation: Casa del agua. *JAWRA Journal of the American Water Resources Association*, 26(6), 939-948.
- Kharseh, M., Altorkmany, L., Al-Khawaj, M., & Hassani, F. (2014). Warming impact on energy use of HVAC system in buildings of different thermal qualities and in different climates. *Energy Conversion and Management*, 81, 106-111.
- Kim, T., Kato, S., & Murakami, S. (2001). Indoor cooling/heating load analysis based on coupled simulation of convection, radiation and HVAC control. *Building and Environment*, 36(7), 901-908.
- Kreider, J., Claridge, D., Curtiss, P., Dodier, R., Haberl, J., & Krarti, M. (1995). Building energy use prediction and system identification using recurrent neural networks. *Journal of Solar Energy Engineering*, 117(3), 161-166.
- Kujawa-Roeleveld, K., & Zeeman, G. (2006). Anaerobic treatment in decentralised and source-separation-based sanitation concepts. *Reviews in Environmental Science and Bio/Technology*, 5(1), 115-139.
- Kumar, R., Aggarwal, R., & Sharma, J. (2013). Energy analysis of a building using artificial neural network: A review. *Energy and Buildings*, 65, 352-358.
- Lattemann, S., & Häpner, T. (2008). Environmental impact and impact assessment of seawater desalination. *Desalination*, 220(1), 1-15.
- Lawrence, P., Adham, S., & Barrott, L. (2003). Ensuring water re-use projects succeed—institutional and technical issues for treated wastewater re-use. *Desalination*, 152(1), 291-298.

Lawrence, T., Perry, J., & Dempsey, P. (2010). CONFERENCE PAPERS AB-10-C001

predicting condensate collection from HVAC air handling units. *ASHRAE Transactions*, 116(2), 3.

Lazarova, V., Levine, B., Sack, J., Cirelli, G., Jeffrey, P., Muntau, H., . . . Brissaud, F.

(2001). Role of water reuse for enhancing integrated water management in europe and mediterranean countries. *Water Science and Technology*, 43(10), 25-33.

Leal, L. H., Zeeman, G., Temmink, H., & Buisman, C. (2007). Characterisation and

biological treatment of greywater. *Water Science and Technology*, 56(5), 193-200.

Lee, D. S., Jeon, C. O., Park, J. M., & Chang, K. S. (2002). Hybrid neural network

modeling of a full-scale industrial wastewater treatment process. *Biotechnology and Bioengineering*, 78(6), 670-682.

Lee, J., Suh, C., Hong, Y. T., & Shin, H. (2011). Sequential modelling of a full-scale

wastewater treatment plant using an artificial neural network. *Bioprocess and Biosystems Engineering*, 34(8), 963-973.

Lens, P., Zeeman, G., & Lettinga, G. (2005). Decentralised sanitation and reuse:

Concepts, systems and implementation. *Water Intelligence Online*, 4, 9781780402949.

Lesjean, B., & Gnirss, R. (2006). Grey water treatment with a membrane bioreactor operated

at low SRT and low HRT. *Desalination*, 199(1-3), 432-434.

- Lewin, N., Zhang, Q., Chu, L., & Shariff, R. (2004). Predicting total trihalomethane formation in finished water using artificial neural networks. *Journal of Environmental Engineering and Science*, 3(S1), S35-S43.
- Li, F., Wichmann, K., & Otterpohl, R. (2009). Review of the technological approaches for grey water treatment and reuses. *Science of the Total Environment*, 407(11), 3439-3449.
- Li, F., Behrendt, J., Wichmann, K., & Otterpohl, R. (2008). Resources and nutrients oriented greywater treatment for non-potable reuses. *Water Science and Technology*, 57(12), 1901-1908.
- Li, Z., Boyle, F., & Reynolds, A. (2010). Rainwater harvesting and greywater treatment systems for domestic application in ireland. *Desalination*, 260(1), 1-8.
- Licina, D., & Sekhar, C. (2012). Energy and water conservation from air handling unit condensate in hot and humid climates. *Energy and Buildings*, 45, 257-263.
- Lin, Z., & Deng, S. (2004). A study on the characteristics of nighttime bedroom cooling load in tropics and subtropics. *Building and Environment*, 39(9), 1101-1114.
- Liu, R., Huang, X., Chen, L., Wen, X., & Qian, Y. (2005). Operational performance of a submerged membrane bioreactor for reclamation of bath wastewater. *Process Biochemistry*, 40(1), 125-130.
- Liu, S., Butler, D., Memon, F. A., Makropoulos, C., Avery, L., & Jefferson, B. (2010). Impacts of residence time during storage on potential of water saving for grey water recycling system. *Water Research*, 44(1), 267-277.

- Loucks, D., Van Beek, E., Stedinger, J., Dijkman, J., & Villars, M. (2005). Model sensitivity and uncertainty analysis. *Water Resources Systems Planning and Management*, , 255-290.
- Loveless, K. J., Farooq, A., & Ghaffour, N. (2013). Collection of condensate water: Global potential and water quality impacts. *Water Resources Management*, 27(5), 1351-1361.
- Lye, D. J. (2009). Rooftop runoff as a source of contamination: A review. *Science of the Total Environment*, 407(21), 5429-5434.
- Madaeni, S. S. (1999). The application of membrane technology for water disinfection. *Water Research*, 33(2), 301-308.
- Madungwe, E., & Sakuringwa, S. (2007). Greywater reuse: A strategy for water demand management in harare? *Physics and Chemistry of the Earth, Parts A/B/C*, 32(15), 1231-1236.
- Maier, H. R., & Dandy, G. C. (2000). Neural networks for the prediction and forecasting of water resources variables: A review of modelling issues and applications. *Environmental Modelling & Software*, 15(1), 101-124.
- Maimon, A., Tal, A., Friedler, E., & Gross, A. (2010). Safe on-site reuse of greywater for irrigation-a critical review of current guidelines. *Environmental Science & Technology*, 44(9), 3213-3220.
- Makropoulos, C., Natsis, K., Liu, S., Mittas, K., & Butler, D. (2008). Decision support for sustainable option selection in integrated urban water management. *Environmental Modelling & Software*, 23(12), 1448-1460.

- Mazzei, P., Minichiello, F., & Palma, D. (2005). HVAC dehumidification systems for thermal comfort: A critical review. *Applied Thermal Engineering*, 25(5), 677-707.
- Metcalf, I. (1991). EDDY. Wastewater engineering, treatment, disposal and reuse.
- Miller, G. W. (2006). Integrated concepts in water reuse: Managing global water needs. *Desalination*, 187(1), 65-75.
- Mirsepahi, A., Chen, L., & O'Neill, B. (2014). A comparative approach of inverse modelling applied to an irradiative batch dryer employing several artificial neural networks. *International Communications in Heat and Mass Transfer*, 53, 164-173.
- Mohamed, A., Maraqa, M., & Al Handhaly, J. (2005). Impact of land disposal of reject brine from desalination plants on soil and groundwater. *Desalination*, 182(1), 411-433.
- Molinos-Senante, M., Hernández-Sancho, F., & Sala-Garrido, R. (2010). Economic feasibility study for wastewater treatment: A cost-benefit analysis. *Science of the Total Environment*, 408(20), 4396-4402.
- Mustafaraj, G., Lowry, G., & Chen, J. (2011). Prediction of room temperature and relative humidity by autoregressive linear and nonlinear neural network models for an open office. *Energy and Buildings*, 43(6), 1452-1460.
- Neal, J. (1996). Wastewater reuse studies and trials in canberra. *Desalination*, 106(1), 399-405.
- NS (2008). Neuro Solutions 6. <http://www.neurosolutions.com> (2008)

- Nghiem L., Oschmann, N., and Schafer, A. (2006). Fouling in grey water recycling by direct ultrafiltration. *Desalination*, 187(1–3), 183–290.
- Nhapi, I. (2004). A framework for the decentralised management of wastewater in zimbabwe. *Physics and Chemistry of the Earth, Parts A/B/C*, 29(15), 1265-1273.
- Nielsen, T. R., Rose, J., & Kragh, J. (2009). Dynamic model of counter flow air to air heat exchanger for comfort ventilation with condensation and frost formation. *Applied Thermal Engineering*, 29(2), 462-468.
- Nolde, E. (2000). Greywater reuse systems for toilet flushing in multi-storey buildings – over ten years experience in berlin. *Urban Water*, 1(4), 275-284.
- Norton-Brandão, D., Scherrenberg, S. M., & van Lier, J. B. (2013). Reclamation of used urban waters for irrigation purposes—a review of treatment technologies. *Journal of Environmental Management*, 122, 85-98.
- Obaidat, M. S. (1998). Editorial artificial neural networks to systems, man, and cybernetics: Characteristics, structures, and applications. *IEEE Transactions on Systems, Man, and Cybernetics, Part B (Cybernetics)*, 28(4), 489-495.
- Ogwueleka, T., & Ogwueleka, F. (2009). Optimization of drinking water treatment processes using artificial neural network. *Nigerian Journal of Technology*, 28(1), 16-25.
- Okeola, O., & Sule, B. (2012). Evaluation of management alternatives for urban water supply system using multicriteria decision analysis. *Journal of King Saud University-Engineering Sciences*, 24(1), 19-24.

- Olden, J. D., & Jackson, D. A. (2002). Illuminating the “black box”: A randomization approach for understanding variable contributions in artificial neural networks. *Ecological Modelling*, 154(1), 135-150.
- Onkal Engin, G., Sinmaz Ucar, B., & Senturk, E. (2011). Reuse feasibility of pre-treated grey water and domestic wastewater with a compact household reverse osmosis system. *Desalination and Water Treatment*, 29(1-3), 103-109.
- Onkal-Engin, G., Demir, I., & Engin, S. N. (2005). Determination of the relationship between sewage odour and BOD by neural networks. *Environmental Modelling & Software*, 20(7), 843-850.
- Oron, G., Adel, M., Agmon, V., Friedler, E., Halperin, R., Leshem, E., et al., (2014). Greywater use in israel and worldwide: Standards and prospects. *Water Research*, 58, 92-101.
- Painter, F. L. (2009). Condensate harvesting from large dedicated outside air-handling units with heat recovery. *ASHRAE Transactions*, 115(2)
- Peters, N. E., & Meybeck, M. (2000). Water quality degradation effects on freshwater availability: Impacts of human activities. *Water International*, 25(2), 185-193.
- Pidou, M., Memon, F. A., Stephenson, T., Jefferson, B., & Jeffrey, P. (2007). Greywater recycling: A review of treatment options and applications.
- Pimentel, D., Berger, B., Filiberto, D., Newton, M., Wolfe, B., Karabinakis, E., . . . Nandagopal, S. (2004). Water resources: Agricultural and environmental issues. *Bioscience*, 54(10), 909-918.

- Pita, E. G., & Stevenson, S. (1998). *Air conditioning principles and systems* Prentice Hall Columbus, OH.
- Pollice, A., Lopez, A., Laera, G., Rubino, P., & Lonigro, A. (2004). Tertiary filtered municipal wastewater as alternative water source in agriculture: A field investigation in southern Italy. *Science of the Total Environment*, 324(1), 201-210.
- Prathapar, S., Ahmed, M., Al Adawi, S., & Al Sidiari, S. (2006). Design, construction and evaluation of an ablution water treatment unit in Oman: A case study. *International Journal of Environmental Studies*, 63(3), 283-292.
- Prathapar, S., Jamrah, A., Ahmed, M., Al Adawi, S., Al Sidairi, S., & Al Harassi, A. (2005). Overcoming constraints in treated greywater reuse in Oman. *Desalination*, 186(1), 177-186.
- Provin, T., & Pitt, J. (2002). Description of water analysis parameters. *Texas A&M Agrilife Extension*. Texas,
- Ramona, G., Green, M., Semiat, R., & Dosoretz, C. (2004). Low strength graywater characterization and treatment by direct membrane filtration. *Desalination*, 170(3), 241-250.
- Rietman, E., & Lory, E. R. (1993). Use of neural networks in modeling semiconductor manufacturing processes: An example for plasma etch modeling. *IEEE Transactions on Semiconductor Manufacturing*, 6(4), 343-347.

- Rodriguez, M. J., & Sérodes, J. (1998). Assessing empirical linear and non-linear modelling of residual chlorine in urban drinking water systems. *Environmental Modelling & Software*, 14(1), 93-102.
- Rose, J. B., Sun, G., Gerba, C. P., & Sinclair, N. A. (1991). Microbial quality and persistence of enteric pathogens in graywater from various household sources. *Water Research*; 25(1), 37–42.
- Rosegrant, M. W., & Cai, X. (2002). Global water demand and supply projections: Part 2. results and prospects to 2025. *Water International*, 27(2), 170-182.
- Rosegrant, M. W., Cai, X., & Cline, S. A. (2002). *World water and food to 2025: Dealing with scarcity* Intl Food Policy Res Inst.
- Scanlon, B. R., Jolly, I., Sophocleous, M., & Zhang, L. (2007). Global impacts of conversions from natural to agricultural ecosystems on water resources: Quantity versus quality. *Water Resources Research*, 43(3)
- Schaefer, K., Exall, K., & Marsalek, J. (2004). Water reuse and recycling in Canada: A status and needs assessment. *Canadian Water Resources Journal*, 29(3), 195-208.
- Schäfer, A., Ravazzini, A., Aharoni, A., Savic, D., & Thoeye, C. (2005). Municipal wastewater reclamation: Where do we stand? an overview of treatment technology and management practice. *Water Science and Technology: Water Supply*, 5(1), 77-85.

- Scheumann, R., Masi, F., El Hamouri, B., & Kraume, M. (2009). Greywater treatment as an option for effective wastewater management in small communities. *Desalination and Water Treatment*, 4(1-3), 33-39.
- Shannon, M. A., Bohn, P. W., Elimelech, M., Georgiadis, J. G., Marinas, B. J., & Mayes, A. M. (2008). Science and technology for water purification in the coming decades. *Nature*, 452(7185), 301-310.
- Sharma, A. K., Grant, A. L., Grant, T., Pamminger, F., & Opray, L. (2009). Environmental and economic assessment of urban water services for a greenfield development. *Environmental Engineering Science*, 26(5), 921-934.
- Shiklomanov, I. (1998). A summary of the monograph world water resources. *A New Appraisal and Assessment for the 21st Century. UNEP: Society and Cultural Organization*.
- Shiklomanov, I. A. (1990). Global water resources. *Nature and Resources*, 26(3), 34-43.
- Shiklomanov, I. A. (2000). Appraisal and assessment of world water resources. *Water International*, 25(1), 11-32.
- Singh, A., Singh, H., Singh, S., & Sawhney, R. (2002). Numerical calculation of psychrometric properties on a calculator. *Building and Environment*, 37(4), 415-419.
- Surendran, S., & Wheatley, A. (1998). Grey-water reclamation for non-potable re-use. *Water and Environment Journal*, 12(6), 406-413.
- TCEQ (2005). The Texas commission on environmental quality. Subsection f: use of graywater systems.

<https://www.tceq.texas.gov/assets/public/legal/rules/rules/pdflib/210f.pdf>

TCEQ. (2015). The Texas Commission on Environmental quality. Amendments to §§210.81 - 210.85.

https://www.tceq.texas.gov/assets/public/legal/rules/rule_lib/proposals/15028210_proposal.pdf

Tsilingiris, P. (2008). Thermophysical and transport properties of humid air at temperature range between 0 and 100 C. *Energy Conversion and Management*, 49(5), 1098-1110.

Tsiourtis, N. X. (2001). Desalination and the environment. *Desalination*, 141(3), 223-236.

UN. (2014). United Nations world water development report. <http://unesdoc.unesco.org/images/0022/002257/225741e.pdf>.

UNDP. (2009) United Nations development programme. Qatar's second human development report human development report office.
http://www.mdps.gov.qa/en/knowledge/Doc/HDR/Qatar_Second_National_HDR_Advancing_Sustainable_Development_2009_EN.pdf

Van Voorthuizen, E. M., Zwijnenburg, A., & Wessling, M. (2005). Nutrient removal by NF and RO membranes in a decentralized sanitation system. *Water Research*, 39(15), 3657-3667.

Vitousek, P. M., Mooney, H. A., Lubchenco, J., & Melillo, J. M. (1997). Human domination of earth's ecosystems. *Science*, 277(5325), 494-499.

- Vogel, D., Simon, A., Alturki, A. A., Bilitewski, B., Price, W. E., & Nghiem, L. D. (2010). Effects of fouling and scaling on the retention of trace organic contaminants by a nanofiltration membrane: The role of cake-enhanced concentration polarisation. *Separation and Purification Technology*, 73(2), 256-263.
- Vorosmarty, C. J., Green, P., Salisbury, J., & Lammers, R. B. (2000). Global water resources: Vulnerability from climate change and population growth. *Science (New York, N.Y.)*, 289(5477), 284-288.
- Vyas, M., Modhera, B., Vyas, V., & Sharma, A. (2011). Performance forecasting of common effluent treatment plant parameters by artificial neural network. *ARPJ Journal of Engineering and Applied Sciences*, 6(1), 38-42.
- Wang, X., & Jin, P. (2006). Water shortage and needs for wastewater re-use in the north china. *Water Science and Technology*, 53(9), 35-44.
- Ward, M., (1996). *Experiences from research at linacre college, Oxford*. Architectural Digest for the 21st Century (21 AD): Water. School of Architecture, Oxford Brookes University
- Wareham, D. G., Hall, K. J., & Mavinic, D. S. (1993). Real-time control of aerobic-anoxic sludge digestion using ORP. *Journal of Environmental Engineering*, 119(1), 120-136.
- Wexler, A., Hyland, R., & Stewart, R. (1983). *Thermodynamic properties of dry air, moist air and water and SI psychrometric charts ASHRAE.*]

- Wilhelm, L. R. (1976). Numerical calculation of psychrometric properties in SI units. *Transactions of the ASAE*, 19(2), 318-325.
- Wilson, A., & Navaro, R. (2008). Alternative water sources: Supply-side solutions for green buildings. *Environmental Building News*.
- Winward, G. P., Avery, L. M., Frazer-Williams, R., Pidou, M., Jeffrey, P., Stephenson, T. (2008). A study of the microbial quality of grey water and an evaluation of treatment technologies for reuse. *Ecological Engineering*, 32(2), 187-197.
- WHO. (2003). World health organization. Guidelines for safe recreational water environments: Coastal and fresh waters.
- WHO. (2006). World health organization. Guidelines for the safe use of wastewater, excreta and greywater. http://www.who.int/water_sanitation_health/wastewater/gsuww/en/index.html.
- Yalcintas, M., & Akkurt, S. (2005). Artificial neural networks applications in building energy predictions and a case study for tropical climates. *International Journal of Energy Research*, 29(10), 891-901.
- Yu, J., Yu, H., Fang, H., Lei, M., Li, S., & Chi, J. (2014). Pollution characteristics of lead, zinc, arsenic, and cadmium in short-term storm water roof runoff in a suburban area. *Toxicological & Environmental Chemistry*, 96(7), 1034-1046.
- Zeng, Z., Liu, J., & Savenije, H. H. (2013). A simple approach to assess water scarcity integrating water quantity and quality. *Ecological Indicators*, 34, 441-449.
- Zhang, Y., & Zhao, R. (2008). Overall thermal sensation, acceptability and comfort. *Building and Environment*, 43(1), 44-50.

APPENDIX-A1

Synthetic greywater composition used by *F. Hourlier et al.*, (2010)

Product	Function	Concentration g/L
Lactic acid	Acid produced by skin	100
Cellulose	Suspended solids	100
Sodium dodecyl sulfate	Anionic surfactants	50
Glycerol	Denaturant, solvent, moisturizer	200
Sodium hydrogen carbonate	pH buffer	70
Sodium sulphate	Viscosity control agent	50
Septic effluent	Microbial load	10

*Pollution due to (1) human body; (2) shampoo and shower gel; (3) soap; (4) deodorant; (5) tooth paste; (6) shaving and moisturizing cream; (7) make-up and make-up remover

APPENDIX-A2

Performance matrix comparison of for different ANN algorithm GREY-ANN
(MSE, r, and MAE)

BOD-ANN										
Treatment-Train	ANN Model	Training			Cross Validation			Testing		
CR-F	MLP-PCA	163.0407	0.957406	8.270496	72.49303	0.990007	6.830465	121.3311	0.949543	8.491106
	GFF	159.305	0.956939	8.421551	94.57387	0.988961	7.005295	127.4458	0.94985	8.418874
MF	PNN	117.1368	0.971077	7.25617	80.93253	0.954449	7.299573	108.2654	0.953912	6.517551
	MLP	137.8085	0.965906	8.42167	66.30956	0.955591	6.361873	127.9438	0.951997	7.53685
C-F	RBF	61.99398	0.925058	6.016926	75.7508	0.881696	6.804789	78.0886	0.875875	5.549613
	TLRN	110.6521	0.88698	8.600473	59.22789	0.918062	6.859929	95.10051	0.885764	7.421898
UF	PNN	2.680487	0.945195	1.116101	35.32057	0.638876	3.217059	13.73406	0.791202	2.840956
	GFF	6.245665	0.866653	1.707363	13.26417	0.913143	2.462126	16.06708	0.710101	2.852317
RO	MLP	0.199186	0.728093	0.318648	0.816943	0.434842	0.560622	0.128382	0.725902	0.276745
	RBF	0.243676	0.648839	0.366365	0.813939	0.464345	0.572472	0.139068	0.700527	0.29046

NTU-ANN										
Treatment-Train	ANN Model	Training			Cross Validation			Testing		
CR-F	LR	728.5997	0.960467	21.49036	1184.856	0.917132	27.26219	687.3747	0.985722	21.69077
	TLRN	719.7382	0.961528	20.44818	1216.964	0.919376	25.08707	741.0605	0.981734	22.78536
MF	TDNN	260.2402	0.985559	11.64806	465.1961	0.963375	18.54478	327.8474	0.98742	14.0062
	MLP	367.8506	0.979974	13.88661	359.741	0.977748	15.67574	493.2282	0.983754	17.14552
C-F	TLRN	127.8227	0.967828	8.875741	817.9398	0.804886	21.3379	245.9245	0.962768	12.4316
	TDNN	101.7629	0.974361	6.169544	336.8172	0.908819	14.99624	445.1437	0.924412	14.10799
UF	TDNN	0.594246	0.864247	0.565642	0.684339	0.803586	0.6684	0.858981	0.808687	0.615478
	RBF	0.980135	0.748069	0.75667	0.828356	0.685312	0.687699	0.956644	0.758405	0.713996
RO	TDNN	0.009478	0.952848	0.044673	0.016442	0.909578	0.054368	0.010637	0.955108	0.054337
	PNN	0.01704	0.915896	0.078972	0.02308	0.855396	0.069765	0.013509	0.954281	0.083466

ORP-ANN										
Treatment-Train	ANN Model	Training			Cross Validation			Testing		
CR-F	PNN	1595.787	0.979322	30.11777	7307.159	0.892228	47.24812	7668.951	0.917071	56.60446
	MLP	3252.472	0.964934	43.84158	5746.592	0.908235	49.78235	9073.073	0.901277	68.5279
MF	MLP	29128.96	0.784727	53.69305	2294.505	0.973923	33.71757	3135.139	0.963318	32.82736
	GFF	29453.08	0.785072	61.54616	1801.945	0.977347	33.51491	4793.912	0.962328	47.14845
C-F	PNN	2503.556	0.960241	32.77729	3800.721	0.947541	45.99931	3090.767	0.94776	41.3662
	RBF	5026.197	0.92466	53.73667	3296.93	0.940477	43.8984	6154.341	0.911355	59.72363
UF	MLP	5776.349	0.843972	53.52857	3992.197	0.893329	45.65589	4890.546	0.893559	51.4986
	RBF	6136.64	0.834349	57.15426	4208.323	0.897056	45.31226	6181.347	0.893696	56.79518
RO	GFF	1393.613	0.945437	28.56464	5475.183	0.692341	47.02816	2675.653	0.912659	41.7399
	MLP	725.6987	0.972777	21.27872	751.1921	0.961856	22.33813	2683.014	0.911322	36.40288

APPENDIX-A2 (Continued)

Performance matrix comparison of for different ANN algorithm GREY-ANN
(MSE, r, and MAE)

PH-ANN										
Treatment	ANN Model	Training			Cross Validation			Testing		
CR-F	RBF	0.093872	0.891098	0.184919	0.033278	0.972022	0.140082	0.26646	0.68555	0.178824
	PNN	0.08702	0.899616	0.167727	0.022932	0.979739	0.10933	0.27552	0.671212	0.183394
MF	MLP	0.138365	0.791616	0.256842	0.144891	0.869418	0.320402	0.017193	0.94683	0.113475
	RBF	0.089338	0.886316	0.220524	0.206309	0.845231	0.379189	0.043528	0.889354	0.150279
C-F	MLP	0.142669	0.841368	0.296258	0.176847	0.624256	0.315346	0.112931	0.826186	0.283133
	PNN	0.122717	0.869224	0.236567	0.125658	0.727085	0.282954	0.141517	0.778147	0.270426
UF	RN	0.149947	0.778701	0.300298	0.070505	0.741859	0.23716	0.02638	0.871561	0.13242
	MLP	0.143929	0.786584	0.292755	0.045464	0.842071	0.171196	0.045897	0.909767	0.182109
RO	MLP	0.11088	0.7314	0.245746	0.084914	0.768677	0.21212	0.081934	0.793008	0.235678
	RBF	0.12059	0.639729	0.237425	0.111258	0.702359	0.259527	0.102028	0.796337	0.249861

TDS-ANN										
Treatment	ANN Model	Training			Cross Validation			Testing		
CR-F	MLP	1918.613	0.978552	23.22757	330.3283	0.997173	11.3921	178.7989	0.998756	11.25375
	GFF	1903.853	0.978503	23.72153	320.5089	0.997148	12.8421	189.9116	0.998654	12.09193
MF	MLP	1868.568	0.977261	26.01317	316.9971	0.997294	14.33915	710.827	0.986117	18.99632
	GFF	1853.802	0.978535	26.59158	332.8003	0.996966	14.35088	747.3227	0.985441	19.61428
C-F	MLP	5751.601	0.936477	58.9484	5662.346	0.947985	61.8247	1954.252	0.939894	34.74024
	RBF	6217.354	0.926963	64.58949	8319.529	0.932981	75.92976	2911.683	0.921045	41.29594
UF	MLP	6477.048	0.894714	56.21663	1993.779	0.971227	37.42164	2177.167	0.924971	36.70187
	GFF	5433.935	0.912973	50.34618	2737.455	0.955186	43.09088	2732.402	0.923257	45.54888
RO	TDNN	96.14485	0.911061	5.738778	167.4088	0.875453	7.842843	99.68606	0.811057	6.841853
	PNN	215.6558	0.823864	11.26821	241.3501	0.817768	10.90061	162.4907	0.743727	10.33335

APPENDIX-A3

Performance matrix comparison of for different ANN algorithm including MLP, and GFF and Multi-L-Regression for BOD-MP

Model Name	MSE	r	MAE
M-L-R	785.4	0.36	22.5
MLP	686.12	0.67	17.86
GFF	532.77	0.76	17.37

APPENDIX-A4

Storage Impact of raw and treated greywater

	Days	TDS (mg/l)		Turbidity (NTU)		DO(mg/l)		.pH	
		Mean	SD	Mean	SD	Mean	SD	Mean	SD
RAW WATER	1	637.8	102.9	134.4	77.6	6.1	1.9	7.7	0.2
	2	654.1	104.4	121.1	63.9	1.6	0.9	7.4	0.3
	4	676.9	126.7	108.1	57.0	1.2	0.4	7.0	0.3
	6	679.0	125.6	100.3	55.4	1.2	0.4	6.9	0.2
	9	690.3	127.0	88.8	60.4	1.2	0.3	6.8	0.3
	12	701.9	134.0	77.0	59.5	1.2	0.3	6.7	0.2
	15	720.5	136.7	71.6	56.9	1.5	0.5	6.5	0.3
CR-F	1	621.6	117.8	98.9	67.9	7.2	1.4	7.5	0.2
	2	654.4	115.9	95.9	64.9	2.4	1.2	7.3	0.3
	4	659.1	118.2	88.5	63.2	1.4	0.4	7.0	0.3
	6	667.0	123.4	81.6	66.1	1.5	0.5	6.9	0.3
	9	676.1	126.8	75.1	67.1	1.6	0.5	7.0	0.3
	12	679.6	131.2	68.7	64.4	1.7	0.5	6.8	0.2
	15	695.4	131.7	64.5	61.7	1.6	0.5	6.7	0.2
M-F	1	628.6	93.0	89.2	73.4	7.3	1.3	7.6	0.2
	2	641.0	106.1	85.3	72.3	3.2	1.0	7.3	0.2
	4	649.8	109.4	77.1	70.7	1.6	0.4	7.0	0.3
	6	657.3	113.2	73.0	72.4	1.5	0.2	7.0	0.2
	9	668.3	115.8	69.7	73.1	1.2	0.2	7.0	0.2
	12	673.8	125.6	63.3	66.0	1.3	0.3	6.9	0.2
	15	699.9	129.5	59.1	62.2	1.3	0.4	6.9	0.3
C-F	1	592.5	72.6	18.8	14.4	8.2	0.9	7.7	0.6
	2	602.8	79.1	17.0	14.8	4.3	1.1	7.5	0.5
	4	614.1	84.4	13.7	14.4	2.9	1.2	7.2	0.5
	6	623.4	83.4	12.9	13.6	2.1	0.7	7.2	0.5
	9	643.3	78.2	12.3	13.1	1.4	0.6	7.2	0.5
	12	646.8	81.3	10.4	11.6	1.7	0.4	7.0	0.5
	15	657.8	85.0	8.4	10.0	1.6	0.6	7.0	0.5
UF	1	481.1	128.4	1.9	1.2	8.1	0.4	7.8	0.8
	2	488.3	128.9	1.8	1.0	7.5	0.4	7.7	0.7
	4	488.4	129.5	1.5	1.0	7.2	0.5	7.5	0.6
	6	491.8	131.5	1.1	0.9	7.2	0.6	7.5	0.6
	9	501.0	128.8	1.0	0.8	6.9	1.1	7.2	0.5
	12	496.0	130.9	0.8	0.6	7.1	1.6	7.3	0.5
	15	499.6	130.2	0.6	0.2	7.1	1.7	7.3	0.5
RO	1	49.3	24.6	0.3	0.1	8.4	0.3	6.5	2.3
	2	50.6	25.0	0.5	0.2	8.5	0.1	6.6	1.9
	4	52.6	25.1	0.6	0.2	8.3	0.5	6.8	1.2
	6	52.3	25.2	0.5	0.2	8.5	0.3	7.1	0.5
	9	56.8	27.1	0.6	0.2	8.4	0.2	7.5	0.6
	12	55.4	25.1	0.6	0.3	8.4	0.2	7.9	1.7
	15	57.1	26.5	0.7	0.2	8.4	0.2	8.3	2.7

APPENDIX-A5

Raw and GAC-MI-ME treated greywater (Statistics)

Turbidity (NTU)	GAC-MI-ME effluent at multiple stages of tretament					
	RAW	CR-F	MF	CF	UF	RO
Mean	194.1051	161.2855	128.8796	47.5496	1.93254	0.576349
Standard Error	9.745177	9.088553	8.810301	4.204789	0.126995	0.028937
Median	178.5	146.1	115.5	34.15	1.355	0.545
Mode	162	163	111	29.6	0.85	0.2
Standard Deviation	109.3893	102.0188	98.89538	47.19864	1.425518	0.324818
Sample Variance	11966.03	10407.83	9780.296	2227.712	2.032101	0.105507
Kurtosis	-0.68222	-0.4465	-0.67307	1.219276	-0.64408	-1.01312
Skewness	0.309484	0.442251	0.521302	1.324288	0.793876	0.424739
Range	413.87	405.99	366.44	203.7	5.23	1.17
Minimum	9.13	3.01	2.56	0.3	0.11	0.1
Maximum	423	409	369	204	5.34	1.27
Sum	24457.24	20321.97	16238.83	5991.25	243.5	72.62
Count	126	126	126	126	126	126
Largest(1)	423	409	369	204	5.34	1.27
Smallest(1)	9.13	3.01	2.56	0.3	0.11	0.1
Confidence Level(95.0%)	19.28692	17.98737	17.43668	8.321799	0.251339	0.05727

APPENDIX-A5 (Continued)

Raw and GAC-MI-ME treated greywater (Statistics)

ORP(.mV)	GAC-MI-ME effluent at multiple stages of tretament					
	RAW	CR-F	MF	CF	UF	RO
Mean	-15.2911	-10.4199	-2.15516	29.61633	80.97602	130.0572
Standard Error	18.53572	18.17134	22.26886	15.6503	12.8724	10.22227
Median	49.25	37.75	15.9	52	98.7	162.95
Mode	226.9	251.1	266.9	291.5	263.4	242.4
Standard Deviation	209.7078	205.5853	251.9434	177.063	145.6346	115.6518
Sample Variance	43977.34	42265.3	63475.49	31351.3	21209.43	13375.33
Kurtosis	-1.11652	-1.49187	11.04647	-1.07729	-0.52875	-0.21635
Skewness	-0.40813	-0.26243	1.831634	-0.28031	-0.48906	-0.56734
Range	782.3	663.7	2010.05	693.7	645.75	514.5
Minimum	-484.3	-407.2	-414.85	-381	-290.55	-151.2
Maximum	298	256.5	1595.2	312.7	355.2	363.3
Sum	-1957.26	-1333.75	-275.86	3790.89	10364.93	16647.32
Count	128	128	128	128	128	128
Largest(1)	298	256.5	1595.2	312.7	355.2	363.3
Smallest(1)	-484.3	-407.2	-414.85	-381	-290.55	-151.2
Confidence Level(95.0%)	36.67885	35.95781	44.06606	30.96913	25.47215	20.22803

BOD (mg/l)	GAC-MI-ME effluent at multiple stages of tretament					
	RAW	CR-F	MF	CF	UF	RO
Mean	65.2217	54.7392	43.27671	18.47347	4.640263	0.518033
Standard Error	4.263007	3.909047	3.554472	1.716298	0.448728	0.064504
Median	52.2	42.29	29.25	11.2	3.15	0.125714
Mode	48	28.5	18	0	0	0
Standard Deviation	48.60576	44.56999	40.52721	19.5688	5.116286	0.738285
Sample Variance	2362.52	1986.484	1642.455	382.9381	26.17638	0.545065
Kurtosis	2.559283	2.872302	1.931318	1.952179	10.07495	3.753881
Skewness	1.422079	1.522398	1.480671	1.517757	2.412801	1.83708
Range	250.6	230.9	183.6	87	34.2	3.6
Minimum	8.4	5.1	1.4	0	0	0
Maximum	259	236	185	87	34.2	3.6
Sum	8478.821	7116.096	5625.972	2401.551	603.2342	67.86238
Count	130	130	130	130	130	130
Largest(1)	259	236	185	87	34.2	3.6
Smallest(1)	8.4	5.1	1.4	0	0	0
Confidence Level(95.0%)	8.434464	7.734145	7.032609	3.395737	0.887819	0.127614

APPENDIX-A5 (Continued)

Raw and GAC-MI-ME treated greywater (Statistics)

Ph	GAC-MI-ME effluent at multiple stages of tretament					
	RAW	CR-F	MF	CF	UF	RO
Mean	7.241328	7.239922	7.166016	7.466172	7.477344	7.290859
Standard Error	0.063957	0.062559	0.052702	0.055655	0.049512	0.040173
Median	7.08	7.08	7.015	7.35	7.385	7.19
Mode	6.76	6.77	7.01	7.32	7.88	7.05
Standard Deviation	0.723586	0.707771	0.596256	0.629659	0.560161	0.454503
Sample Variance	0.523577	0.500939	0.355522	0.396471	0.31378	0.206573
Kurtosis	0.070259	1.354505	0.97647	0.463449	0.425117	0.74036
Skewness	0.668147	1.009516	0.997734	0.887475	0.744895	1.011842
Range	3.3	4.01	2.9	2.86	2.49	2.37
Minimum	5.9	5.92	6.05	6.31	6.53	6.37
Maximum	9.2	9.93	8.95	9.17	9.02	8.74
Sum	926.89	926.71	917.25	955.67	957.1	933.23
Count	128	128	128	128	128	128
Largest(1)	9.2	9.93	8.95	9.17	9.02	8.74
Smallest(1)	5.9	5.92	6.05	6.31	6.53	6.37
Confidence Level(95.0%)	0.126559	0.123792	0.104288	0.11013	0.097975	0.079495

TDS(mg/l)	GAC-MI-ME effluent at multiple stages of tretament					
	RAW	CR-F	MF	CF	UF	RO
Mean	546.3306	529.1065	507.1306	457.3629	388.3306	43.79839
Standard Error	19.31079	19.3673	19.05808	17.57145	15.54657	2.067443
Median	574.5	543.5	537.5	508	428	36.5
Mode	685	512	462	535	459	21
Standard Deviation	215.0358	215.6651	212.2218	195.6674	173.1193	23.02207
Sample Variance	46240.4	46511.45	45038.09	38285.75	29970.29	530.0159
Kurtosis	-0.70969	-0.83591	-0.95042	-0.90881	-1.03162	0.375701
Skewness	-0.35307	-0.37233	-0.33923	-0.38182	-0.269	0.983832
Range	883	824	807	735	642	102
Minimum	112	78	71	65	65	10
Maximum	995	902	878	800	707	112
Sum	67745	65609.2	62884.2	56713	48153	5431
Count	124	124	124	124	124	124
Largest(1)	995	902	878	800	707	112
Smallest(1)	112	78	71	65	65	10
Confidence Level(95.0%)	38.22452	38.33638	37.7243	34.78162	30.77348	4.092377

APPENDIX-B1

Greywater water collection scheme for the experiments



Shower water collection



Laundry water collection



Washbasin water collection

APPENDIX-B2

GAC-MI-ME greywater treatment system



APPENDIX-B3

GAC-MI-ME Components (Membrane, GAC, UV)

Membrane details:

	Membrane used in GAC-MI-ME system			
Treatment - Unit	Filter media	Manufacturer	Pore diameter	
CR-F	Ployster-Plus	HARMSCO	50	µm
	Polypropylene -Spun Bonded	3M Water Filtration	20	µm
	Ployster-Plus	HARMSCO	10	µm
	Ployster-Plus	HARMSCO	5	µm
MF	Ployster-Plus	HARMSCO	1	µm
	Pleated Polyester	Flow-Max	0.35	µm
UF	Hollow Fiber Membrane, Polyether Sulfone (PES)	Neo-Pure	0.020	µm
	Hollow Fiber Membrane, Polyether Sulfone (PES)	AquaCera	0.025	µm
RO	Polyamide Thin film composite membrane	AXEON	>98% rejection	

GAC details:

	GAC
Brand	CALGON
US sieve series	
	On 8 mesh 15% max
	On30mesh 4% max
Type	Bituminous
	12×40 mesh

UV System Details:

	UV Sytem		
Brand	Sterilight Silver		
Model	S1Q-PA		
UV Fluence	16mJ/cm ²	for 3.3 gpm	
Reactor size	39.4cm× 6.4cm		

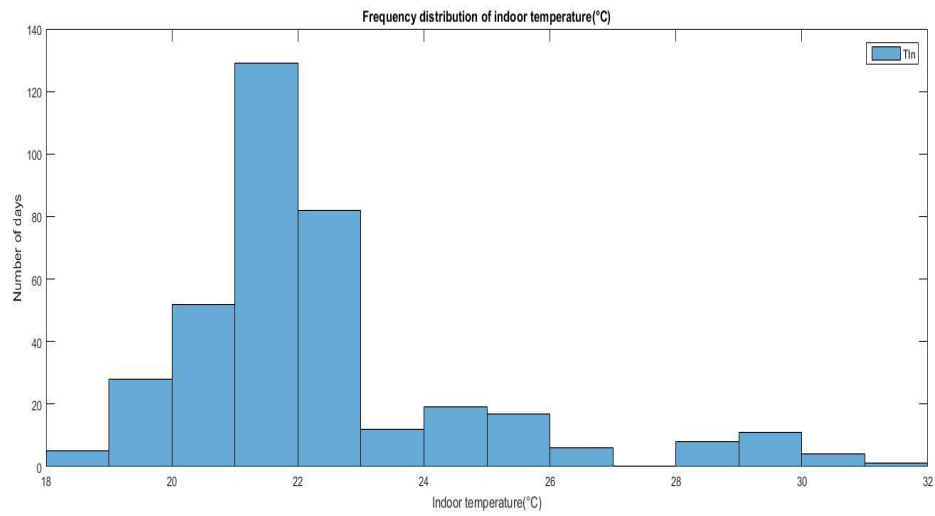
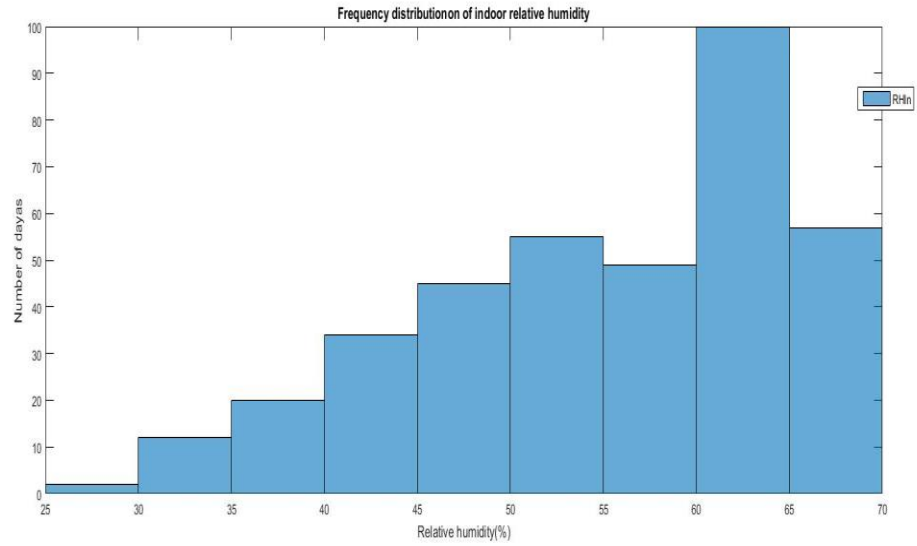
APPENDIX-B4

Instruments precision and accuracy

Instruments Name	Brand	Parameter	Accuracy
YSI 6800 XLM	YSI	pH	±0.2 unit
YSI 6800 XLM	YSI	ORP(mV)	±20 mV
YST ProBOD	YSI	DO (mg/l)	0-20 mg/L, ±0.1 mg/L
TDS-Meter	HM Digital SP2	TDS(mg/l)	± 2 %
HI88713	HANNA Instruments	Turbidity(NTU)	±2% of reading plus straylight ±5% of reading above 1000 NTU

APPENDIX C1

Histograms of indoor temperature and relative humidity



APPENDIX C2:

Yearly condensate data ILAN-ACON simulations for Doha per 100 m³ cooling space.

Month	Load_Type	Condensate (L)				
		Monthly	Daily Condensate			
		Total	Max	Average	Min	SD
January	Q_Total ₂₀	19.6	2.6	0.6	0	0.9
	Q_Total ₁₀₀	26.6	3.9	0.9	0	1.3
	IL_Qcond	18.2	2.3	0.6	0	0.9
Feb	Q_Total ₂₀	15.7	2.3	0.5	0	0.7
	Q_Total ₁₀₀	18.6	3.4	0.6	0	0.9
	IL_Qcond	15.1	2	0.5	0	0.7
March	Q_Total ₂₀	35.1	4.1	1.1	0	1.2
	Q_Total ₁₀₀	41.8	5.1	1.3	0	1.5
	IL_Qcond	32.7	3.7	1.1	0	1.1
April	Q_Total ₂₀	132.3	6.2	4.4	0.9	1.5
	Q_Total ₁₀₀	247.4	16.2	8.2	1	4.2
	IL_Qcond	106.1	4.7	3.5	0.8	1.1
May	Q_Total ₂₀	156.9	7.4	5.1	1.8	1.2
	Q_Total ₁₀₀	302.6	19.7	9.8	4.4	4.3
	IL_Qcond	118.6	5.1	3.8	0	0.9
June	Q_Total ₂₀	153.1	6.5	4.9	2.6	0.7
	Q_Total ₁₀₀	445.4	28.8	14.4	4.6	5.3
	IL_Qcond	97.6	3.5	3.1	2.1	0.3
July	Q_Total ₂₀	198.8	8.4	6.4	4.6	1.1
	Q_Total ₁₀₀	650	37.6	21	6.3	8.9
	IL_Qcond	112.4	3.9	3.6	3.3	0.2
August	Q_Total ₂₀	221.5	8.8	7.1	5.3	1
	Q_Total ₁₀₀	851.4	40.7	27.5	11.3	8.1
	IL_Qcond	109.1	3.8	3.5	3.2	0.2
September	Q_Total ₂₀	199.2	8.6	6.6	4.5	1.1
	Q_Total ₁₀₀	630.1	33.7	21	6	7.5
	IL_Qcond	119.2	4.4	4	3.4	0.3
October	Q_Total ₂₀	152.4	6.4	5.1	4.4	0.5
	Q_Total ₁₀₀	286.9	20.7	9.6	5.1	3.8
	IL_Qcond	114.3	4.1	3.8	3.5	0.1
November	Q_Total ₂₀	77.7	5.6	2.6	0	1.9
	Q_Total ₁₀₀	192	16.2	6.4	0	5.7
	IL_Qcond	56.4	4.2	1.9	0	1.3
December	Q_Total ₂₀	6.8	1.7	0.2	0	0.4
	Q_Total ₁₀₀	8.1	2.1	0.3	0	0.5
	IL_Qcond	6.5	1.6	0.2	0	0.4

Q_Total₂₀ implies for total condensate volume at 20 % outdoor ventilation, **Q_Total₁₀₀** implies for total condensate volume at 100 % outdoor ventilation, and **IL_Qcond** implies for condensate due to Internal Load'

APPENDIX C3:

Water quality of A/C condensate (For the city of Doha) compared with different water use standard [Provin et al., 2002; EPA, 2003]

Parameters	Experimental data at Qatar University, Doha					Drinking water Standards		Irrigation		Livestock	
	n	Mean	Max	Min	SD	Primary	Secondary	Recommended	potential issue	CAST	potential issue
pH	6	7.1	7.7	6.5	0.57		6.5-8.5		<5.5/>8.5		<5.5/>8.5
DO (mg/L)	-	-	-	-	-						
Turbidity (NTU)	-	-	-	-	-	<1 and not exceed 0.3 95%					
EC. µS/cm	6	83.77	134	35.1	37.92			0.0-0.25	>0.75(s)		
Cl ⁻ (mg/L)	6	3.6	14.5	0.77	4.9						
NO ₃ ⁻ (mg/L)	6	0	0	0	0				>40	300	
Coliform (Count/100 ml)	6	0	0	0		5% sample -monthly					
SO ₄ ⁻² (mg/L)	6	6.18	21.4	0.77	7.1		250				
PO ₄ ⁻³ (mg/L)	6	0	0	0	0						
Al (mg/L)	6	0	0	0	0		0.05-0.2				
Ba (mg/L)	6	0	0	0	0	2		2			>10
Cd (mg/L)	6	0	0	0	0	0.05			0.01-0.5	0.05	
Co (mg/L)	6	0	0	0	0						
Cr (mg/L)	6	0	0	0	0			0.1-1.0		1	
Cu (mg/L)	6	0.77	1.69	0	0.69	1.3	1	0.2		0.5	
Mn (mg/L)	6	0	0.02	0	0.01		0.05				
Ni (mg/L)	6	0	0	0	0			0.2		0.1	
Pb (mg/L)	6	0	0	0	0	0.015		5.0-10.0		0.1	
Se (mg/L)	6	0.01	0.04	0	0.01						
Sr (mg/L)	6	0	0	0	0						
Zn (mg/L)	6	0.52	1.19	0	0.5		5	2		25	